UNIVERSITÀ DEGLI STUDI DELL'AQUILA
DIPARTIMENTO DI SCIENZE CLINICHE APPLICATE E BIOTECNOLOGICHE

Dottorato di Ricerca in " Medicina Sperimentale"

Curriculum "Neuroscienze di base e cliniche"

XXXIII ciclo

Titolo della tesi

Towards the identification of new therapeutic targets for the treatment of sensorineural hearing loss

SSD BIO/09

Dottorando

Annamaria Tisi

Coordinatore del corso

Prof. Maria Grazia Perilli

_____

Tutor

Prof. Rita Maccarone

_____

A.A. 2019/2020

Index

Abstract

Hearing loss represents the fourth cause of disability in the world according to the Global Burden of Disease Study, and the number of affected patients is expected to increase in the next years. The absence of effective therapies for the treatment of sensorineural hearing loss leads to irreversible deafness and calls for an urgent need of new therapeutic approaches. To make improvements in the field, in this dissertation, we investigated the effects of recombinant human nerve growth factor (rhNGF) and recombinant human brain derived neurotrophic factor (rhBDNF) on sensory and non-sensory cells of the organ of Corti. To this purpose, the experiments have been conducted by three partners in the framework of the "PON ricerca e innovazione": the University of L'Aquila (L'Aquila, Italy), Dompé Farmaceutici S.p.A (Naples, Italy), and University Medical Center (UMC) Utrecht (Utrecht, The Netherlands).

The first objective of the project was the investigation of the miRNAs profiles induced by rhNGF and rhBDNF *in vitro* on murine cochlear cells derived from the organ of Corti. The subsequent *in silico* analysis allowed us to identify a wide spectrum of target genes and signalings by the modulated miRNAs. Importantly, many of the target pathways by both neurotrophins involved cell survival, proliferation, neuronal differentiation and metabolic pathways.

As a second step, we investigated the effects of rhNGF and rhBDNF on the survival of sensory and non-sensory cells of the organ of Corti of ototoxically deafened guinea pigs, and found limited effects in terms of cell number by both the treatments. At this level, we did not take into account any other aspects, such as the molecular events underlying the activity of those cells, that could affect their function.

We therefore moved to molecular investigations in the organ of Corti of deafened guinea pigs. We selected the mTOR signaling from the *in vitro* and *in silico* analysis. Since the mTOR signaling was predominantly modulated by rhBDNF, we limited our investigations to this neurotrophin. We found that the BDNF-treated organs of Corti from deafened guinea pigs presented increased levels of pmTOR compared to normal hearing ears, and increased levels of mTOR compared to both untreated and normal hearing cochleas. On this basis, it is possible that rhBDNF may exert a protective effect on the organ of Corti that is mainly associated with the molecular function of those cells and not appreciable in terms of cell number.

In conclusion, this dissertation provides a comprehensive overview over the effects of rhNGF and rhBDNF in the organ of Corti, and lays the foundation for the identification of new therapeutic targets.

CHAPTER 1

Introduction

1. Background

1.1. The organ of Corti

The organ of Corti is the sensory epithelium responsible for sound perception. It is located in the *scala media* of the cochlea and it is constituted by several cell types, which synergistically allow proper hearing. The cells of the organ of Corti can be subvided in mechano-sensory hair cells (HCs) and non-sensory supporting cells (SCs) (Figure 1).

The organ of Corti is covered by tectorial membrane and lies on a basilar membrane. The HCs are organized in one row of inner hair cells (IHC) and three rows of outer hair cells (OHC). HCs are directly responsible for the perception of the sound stimuli, thanks to the stereocilia present on their apical side. They are then innervated by cochlear nerves deriving from Spiral Ganglion cells (SGCs), which transmit the signal to the brain. In the organ of Corti, the HCs are surrounded by several types of SCs, which show peculiar structural and expression features. Five different types of SCs, organized in rows along the Organ of Corti, have been identified based on morphological, functional and expression patterns differences: (1) hensen's cells, (2) Deiters' cells, (3) pillar cells, (4) inner phalangeal cells, and (5) border cells [1].

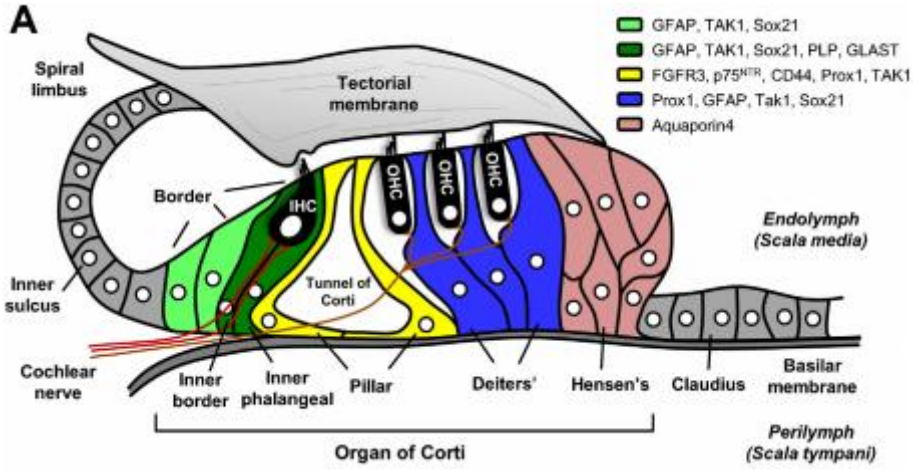

Figure 1. Schematic illustration of structural and cellular organization of the organ of Corti. The figure shows both sensory and non-sensory cells marked with different colours. The legend shows the expression of specific markers by the supporting cells. From Wan et al., 2013 [2].

The structure and function of HCs and SCs vary significantly from basal to apical cochlea [3]. Likewise, the cochlea shows a tonotopic organization, being the base responsible for high frequencies perception and the apex for that of low frequencies [4]. A recent study, based on single-cell RNA sequencing revealed that also the expression, and therefore the function of the cells in the organ of Corti, varies from base to apex. Interestingly, it has been shown that the SCs present in the apex of the cochlea show a higher expression of proliferation and

differentiation genes [3]. This is particularly important because, in addition to their "supporting" role, in recent years SCs have also been studied as a source to regenerate HCs after damage. First attempts by researchers in the field, already showed that the regeneration of HCs from SCs in the mammalian cochlea is actually possible through the targeting of specific signalings [5].

1.2. NGF and BDNF

Neurotrophic factors (NFs) are a family of proteins, which have been demonstrated to have an essential role in the development, survival, plasticity and protection of the peripheral and central nervous system [6]. Since the discovery of the nerve growth factor (NGF) by Rita Levi-Montalcini [7], several other NFs have been identified, such as brain-derived neurotrophic factor (BDNF), NT-3, neurotrophin-4/5 and others [6]. These form a subcategory of NFs named "neurotrophins".

BDNF is the most abundant neurotrophin of the brain and is essential during development in the ear, as the knock down of its receptor resulted in alterations of ear maturation in mice [8]. In the adult inner ear, the expression of BDNF by HCs and SCs has been demonstrated to be fundamental for the survival of SGCs [9]. Accordingly, the degeneration of HCs is inexorably associated with progressive secondary SGC degeneration [10] and BDNF administration resulted to be effective in preventing SGCs death following hair cell degeneration in vivo [11–15].

NGF is one of the most studied neurotrophic factors. Unlike BDNF, NGF is not essential for the development of the inner ear and several studies have demonstrated that the NGF receptor is not expressed in the ear during development. Accordingly, transgenic animals, lacking the expression of NGF receptor correctly developed the inner ear [16–18]. All these findings suggest a major role of NGF in promoting cell survival and neuroprotection in the ear once it has matured, rather than promoting its development. Nevertheless, the therapeutic efficacy of NGF as treatment of hearing loss has been sparsely investigated compared to that of BDNF [19,20].

1.3. BDNF as a therapy for hearing loss

The effects of exogenous BDNF on neuronal cochlear cells were tested in several *in vitro* and *in vivo* studies.

In vitro studies

In vitro studies demonstrated cisplantin-induced damage protection of spiral ganglion neurons and hair cells cultures by exogenous BDNF [27],[28]. Post-natal SGCs–derived neural stem cells (NSCs) differentiated in functional neurons when treated with BDNF, supporting the crucial implications of this neurotrophin in regulating ear development [29]. Some *in vitro* experiments suggest that BDNF neuroprotective effects could be synergistically enhanced by the combined treatment with other factors, such as anti-oxidant agents (D-methionine-D-Met) [27] or other neurotrophic factors [30]. Suppression of the glycine receptor by BDNF treatment in SGNs primary culture from postnatal mice was highlighted too [31]. Moreover, since a major problem of BDNF treatment is the necessity of a continuous stimulation in order to maintain its neuroprotective efficacy, nanoporous silica nanoparticles loaded with BDNF (BDNF-NPSNPs) were developed. BDNF-NPSNPs allowed constant release of BDNF over time and sustained survival of SGNs *in vitro* [32]. Remarkably, co-culture of de-afferented Organ of Corti with SGCs from embryonic mice highlighted the crucial implication of BDNF in promoting the regeneration of synapses between the hair cells and auditory neurons [33].

In vivo studies

The neuroprotective effects of exogenous BDNF in the cochlea have been demonstrated in several animal models. BDNF administration for few weeks resulted to be effective in preventing SGNs death following hair cells degeneration in guinea pigs deafened by ototoxic drugs [11],[12]. A similar study was conducted in deafened rats, which were treated with BDNF by an osmotic pump for 28 days starting 2 weeks after deafening. Also in this model the treatment was effective in promoting SGNs survival and increasing their soma dimension [13]. Recently it has been demonstrated that temporary treatment with BDNF enables a sustained protection (up to 8 weeks) of SGNs in deafened guinea pigs [14].

BDNF gene therapy

In order to improve the effects of BDNF for long-time in the cochlea lacking hair cells, BDNF gene therapy is an alternative possibility. The aim of this approach is to up-regulate the expression of BDNF endogenously in the supporting cells of the Organ of Corti, in order to compensate the deacrease of BDNF due to hair cells loss. The BDNF vector could be directly injected in the scala timpani and/or in the scala media of the cochlea. Although both sites of injections allow the protection of SGNs, some differences in the precision of fiber outgrowth

have been highlighted. In fact, the injection into the scala timpani led to an extensive and generalized expression of BDNF in the cochlea. Thus, nerve resprouting was not directed specifically into the supporting epithelium of the organ of Corti. Conversely , the injection of the adenovirus into the scala media, which is closer to the Organ of Corti, led to a more controlled sprouting of the peripheral fibers from SGNs [34]. BDNF gene therapy was first tested in guinea pigs deafened by ototoxic drugs. Recently BDNF gene therapy resulted to be neuroprotective for SGNs also in transgenic models of hearing loss, such as the Pou4f3 (POU class 4 transcription factor 3) mutant mouse [35] and the GJB2 (connexin 26) null mouse [36].

1.4. miRNAs and their role in the cochlea

miRNAs, or microRNAs, are small non-coding RNAs mainly involved in the regulation of gene expression. They can act through the degradation of target mRNA or through the block of protein translation to prevent gene expression. First, DNA polymerase II transcribes the non-coding miRNA sequence and forms the Pri-mRNAs, which are bound and then cleaved by Drosha/DGCR8 complex to form pre-MiRNAs. The pre-MiRNAs are then exported from the nucleus into the cytoplasm by the Exportin 5 – RanGTP complex. The pre-MiRNAs are then cleaved by the Drosha/DGCR8 complex to form pre-MiRNAs. The pre-MiRNAs are then exported from the nucleus into the cytoplasm by the Exportin 5 – RanGTP complex. The pre-MiRNAs are then cleaved by the and one half of them is degraded, while the other is the final miRNA. The miRNA then binds to a complex of proteins and take part to the RISC protein Complex. The RISC complex is able to bind multiple mRNA strands, enabling the silencing of gene expression [37].

The role of miRNAs has been investigated also in the cochlea and auditory function. Several miRNAs have been identified by microarrays and the specific expression pattern of miRNAs in the different inner ear locations have been identified by in situ hybridization in mice (Figure 2) [38].

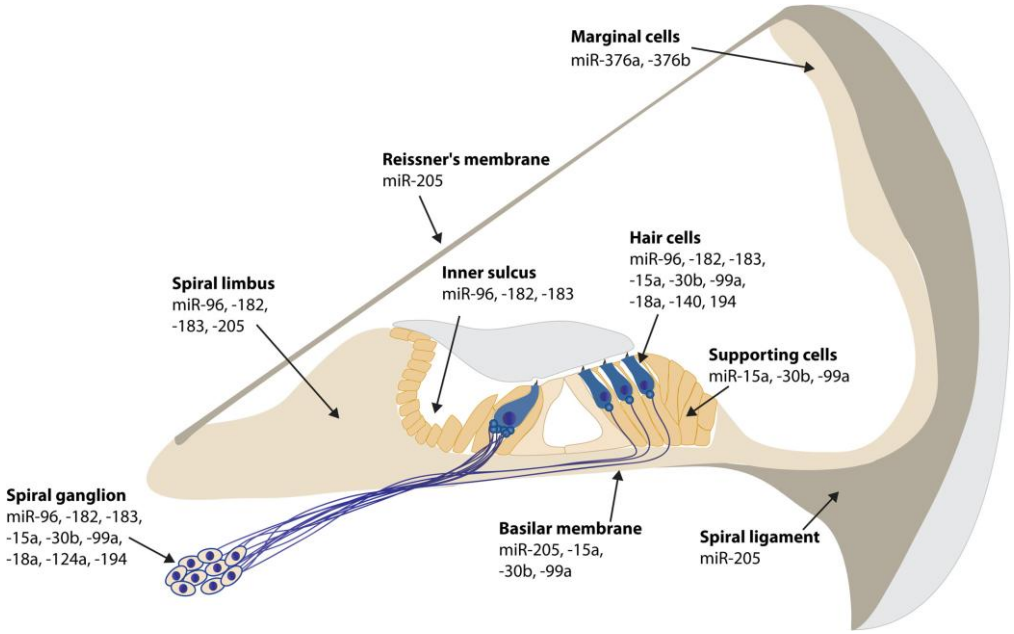

Figure 2. Schematic illustration of miRNAs expression in the cochlea of mice at P0. From: [38]

The miR-183 family is the most characterized miRNA cluster in the inner ear, that is transcribed in one plycistronic transcript and is composed by three miRNAs: miR-183, miR-182 and miR-96. The miR-183 family plays a major role for HCs and neuronal development, and has been demonstrated to be important also for other sensory systems, such as the retina [39].

Another well characterize miRNA in the nervous system is the miR-124. MiR-124 is expressed in the inner ear in neuronal cells in the spiral and vestibular ganglia. miR-124 resulted to be down regulated in aged mice compared to younger ones, suggesting a role in age-related hearing loss [39]. Moreover, several hearing loss pathologies have been associated with miRNAs mutations. The most common mutations involve miR-96, which is hence associated with familial deafness [40]. Importantly, recent studies also demonstrated that miRNAs may facilitate or prevent the sensory hair cell regeneration [40].

2. Aim of the project and development

Given the important role of neurotrophic factors in inner ear development, survival and regeneration, the aim of the present dissertation was to investigate the effects of NGF and BDNF on the cells of the organ of Corti through an *in vitro*, *in silico* and *in vivo* approach. The study was focused on the following main objectives:

1) Identification of the miRNAs profiles induced by NGF and BDNF in the cells of the organ of Corti through *in vitro* assays;
2) *In silico* study for the identification of experimentally validated target genes and pathways by the modulated miRNAs;
3) Investigation of the protective effects of NGF and BDNF on sensory and non-sensory cells of the organ of Corti of ototoxically deafened guinea pigs.
4) Validation of a selected signaling derived from the *in silico* study through *in vivo* experiments;

In order to achieve the goals of the project, the experiments have been conducted by three partners in the framework of the "PON ricerca e innovazione": the University of L'Aquila (L'Aquila, Italy), Dompé Farmaceutici S.p.A (Naples, Italy), and University Medical Center (UMC) Utrecht (Utrecht, The Netherlands). Specifically, aims 1 and 2 have been pursued at Dompé and at the University of L'Aquila (Chapter 2); aims 3 (Chapter 3) and 4 (Chapter 4) at the University of L'Aquila and at the UMC Utrecht.

3. References

1. Wan, G.; Corfas, G.; Stone, J.S. Inner ear supporting cells: Rethinking the silent majority. Semin. Cell Dev. Biol. 2013, 24, 448–459.
2. Wan, G.; Corfas, G.; Stone, J.S. Inner ear supporting cells: Rethinking the silent majority. Semin. Cell Dev. Biol. 2013, 24, 448–459.
3. Waldhaus, J.; Durruthy-Durruthy, R.; Heller, S. Quantitative High-Resolution Cellular Map of the Organ of Corti. Cell Rep. **2015**, 11, 1385–1399, doi:10.1016/j.celrep.2015.04.062.
4. Pujol, R.; Lenoir, M.; Ladrech, S.; Tribillac, F.; Rebillard, G. Correlation Between the Length of Outer Hair Cells and the Frequency Coding of the Cochlea. In Auditory Physiology and Perception; Elsevier, 1992; pp. 45–52.
5. Shu, Y.; Li, W.; Huang, M.; Quan, Y.Z.; Scheffer, D.; Tian, C.; Tao, Y.; Liu, X.; Hochedlinger, K.; Indzhykulian, A.A.; et al. Renewed proliferation in adult mouse cochlea and regeneration of hair cells. Nat. Commun. **2019**, 10, doi:10.1038/s41467-019-13157-7.
6. Skaper, S.D. Neurotrophic Factors: An Overview. In; Humana Press, New York, NY, 2018; pp. 1–17.
7. Levi-Montalcini, R.; Hamburger, V. Selective growth stimulating effects of mouse sarcoma on the sensory and sympathetic nervous system of the chick embryo. J. Exp. Zool. **1951**, 116, 321–361, doi:10.1002/jez.1401160206.
8. Schimmang, T.; Tan, J.; Müller, M.; Zimmermann, U.; Rohbock, K.; Köpschall, I.; Limberger, A.; Minichiello, L.; Knipper, M. Lack of Bdnf and TrkB signalling in the postnatal cochlea leads to a spatial reshaping of innervation along the tonotopic axis and hearing loss. Development **2003**, 130, 4741–4750, doi:10.1242/dev.00676.
9. Ylikoski, J.; Pirvola, U.; Moshnyakov, M.; Palgi, J.; Arumäe, U.; Saarma, M. Expression patterns of neurotrophin and their receptor mRNAs in the rat inner ear. Hear. Res. **1993**, 65, 69–78, doi:10.1016/0378-5955(93)90202-C.
10. Webster, M.; Webster, D.B. Spiral ganglion neuron loss following organ of corti loss: A quantitative study. Brain Res. **1981**, 212, 17–30, doi:10.1016/0006-8993(81)90028-7.
11. Gillespie, L.N.; Clark, G.M.; Marzella, P.L. Delayed neurotrophin treatment supports auditory neuron survival in deaf guinea pigs. Neuroreport **2004**, 15, 1121–1125, doi:10.1097/00001756-200405190-00008.
12. Agterberg, M.J.H.; Versnel, H.; de Groot, J.C.M.J.; Smoorenburg, G.F.; Albers, F.W.J.; Klis, S.F.L. Morphological changes in spiral ganglion cells after intracochlear application of brain-derived neurotrophic factor in deafened guinea pigs. Hear. Res. **2008**, 244, 25–34,

doi:10.1016/j.heares.2008.07.004.

13. McGuinness, S.L.; Shepherd, R.K. Exogenous BDNF rescues rat spiral ganglion neurons in vivo. Otol. Neurotol. **2005**, 26, 1064–1072, doi:10.1097/01.mao.0000185063.20081.50.
14. Ramekers, D.; Versnel, H.; Strahl, S.B.; Klis, S.F.L.; Grolman, W. Temporary neurotrophin treatment prevents deafness- induced auditory nerve degeneration and preserves function. J. Neurosci. **2015**, 35, 12331–12345, doi:10.1523/JNEUROSCI.0096-15.2015.
15. Vink, H.A.; Versnel, H.; Kroon, S.; Klis, S.F.L.; Ramekers, D. BDNF-mediated preservation of spiral ganglion cell peripheral processes and axons in comparison to that of their cell bodies. Hear. Res. **2021**, 400, 108114, doi:10.1016/j.heares.2020.108114.
16. Schimmang, T.; Alvarez-Bolado, G.; Minichiello, L.; Vazquez, E.; Giraldez, F.; Klein, R.; Represa, J. Survival of inner ear sensory neurons in trk mutant mice. Mech. Dev. **1997**, 64, 77–85, doi:10.1016/s0925-4773(97)00047-6.
17. Després, G.; Hafidi, A.; Romand, R. Immunohistochemical localization of nerve growth factor receptor in the cochlea and in the brainstem of the perinatal rat. Hear. Res. **1991**, 52, 157–65, doi:10.1016/0378-5955(91)90195-f.
18. Dai, C.F.; Steyger, P.S.; Wang, Z.M.; Vass, Z.; Nuttall, A.L. Expression of Trk A receptors in the mammalian inner ear. Hear. Res. **2004**, 187, 1–11, doi:10.1016/s0378-5955(03)00277-6.
19. Han, Z.; Wang, C.P.; Cong, N.; Gu, Y.Y.; Ma, R.; Chi, F.L. Therapeutic value of nerve growth factor in promoting neural stem cell survival and differentiation and protecting against neuronal hearing loss. Mol. Cell. Biochem. **2017**, 428, 149–159, doi:10.1007/s11010-016-2925-5.
20. Shah, S.B.; Gladstone, H.B.; Williams, H.; Hradek, G.T.; Schindler, R.A. An extended study: Protective effects of nerve growth factor in neomycin-induced auditory neural degeneration. In Proceedings of the American Journal of Otology; Am J Otol, 1995; Vol. 16, pp. 310–314.
21. Mitre, M.; Mariga, A.; Chao, M. V Neurotrophin signalling: novel insights into mechanisms and pathophysiology. Clin. Sci. (Lond). **2017**, 131, 13–23, doi:10.1042/CS20160044.
22. Benedetti, M.; Levi, A.; Chao, M. V. Differential expression of nerve growth factor receptors leads to altered binding affinity and neurotrophin responsiveness. Proc. Natl. Acad. Sci. **1993**, 90, 7859–7863, doi:10.1073/pnas.90.16.7859.
23. Geetha, T.; Jiang, J.; Wooten, M.W. Lysine 63 Polyubiquitination of the Nerve Growth

Factor Receptor TrkA Directs Internalization and Signaling. Mol. Cell **2005**, 20, 301–312, doi:10.1016/j.molcel.2005.09.014.

24. Mischel, P.S.; Smith, S.G.; Vining, E.R.; Valletta, J.S.; Mobley, W.C.; Reichardt, L.F. The Extracellular Domain of p75 ^{NTR} Is Necessary to Inhibit Neurotrophin-3 Signaling through TrkA. J. Biol. Chem. **2001**, 276, 11294–11301, doi:10.1074/jbc.M005132200.
25. Hempstead, B.L.; Martin-Zanca, D.; Kaplan, D.R.; Parada, L.F.; Chao, M. V. High-affinity NGF binding requires coexpression of the trk proto-oncogene and the low-affinity NGF receptor. Nature **1991**, 350, 678–683, doi:10.1038/350678a0.
26. Nykjaer, A.; Lee, R.; Teng, K.K.; Jansen, P.; Madsen, P.; Nielsen, M.S.; Jacobsen, C.; Kliemannel, M.; Schwarz, E.; Willnow, T.E.; et al. Sortilin is essential for proNGF-induced neuronal cell death. Nature **2004**, 427, 843–8, doi:10.1038/nature02319.
27. Gabaizadeh, R.; Staecker, H.; Liu, W.; Kopke, R.; Malgrange, B.; Lefebvre, P.P.; Van De Water, T.R. Protection of both auditory hair cells and auditory neurons from cisplatin induced damage. Acta Otolaryngol. **1997**, 117, 232–238, doi:10.3109/00016489709117778.
28. Zheng, J.L.; Stewart, R.R.; Gao, W.Q. Neurotrophin-4/5 enhances survival of cultured spiral ganglion neurons and protects them from cisplatin neurotoxicity. J. Neurosci. **1995**, 15, 5079–87.
29. Li, X.; Aleardi, A.; Wang, J.; Zhou, Y.; Andrade, R.; Hu, Z. Differentiation of Spiral Ganglion-Derived Neural Stem Cells into Functional Synaptogenetic Neurons. Stem Cells Dev. **2016**, 25, 803–813, doi:10.1089/scd.2015.0345.
30. Schwieger, J.; Warnecke, A.; Lenarz, T.; Esser, K.H.; Scheper, V.; Forsythe, J. Neuronal survival, morphology and outgrowth of spiral ganglion neurons using a defined growth factor combination. PLoS One **2015**, 10, 1–17, doi:10.1371/journal.pone.0133680.
31. Sun, W.; Salvi, R.J. Brain derived neurotrophic factor and neurotrophic factor 3 modulate neurotransmitter receptor expressions on developing spiral ganglion neurons. Neuroscience **2009**, 164, 1854–66, doi:10.1016/j.neuroscience.2009.09.037.
32. Schmidt, N.; Schulze, J.; Warwas, D.P.; Ehlert, N.; Lenarz, T.; Warnecke, A.; Behrens, P. Long-term delivery of brain-derived neurotrophic factor (BDNF) from nanoporous silica nanoparticles improves the survival of spiral ganglion neurons in vitro. PLoS One **2018**, 13, 1–23, doi:10.1371/journal.pone.0194778.
33. Tong, M.; Brugeaud, A.; Edge, A.S.B. Regenerated Synapses Between Postnatal Hair Cells and Auditory Neurons. J. Assoc. Res. Otolaryngol. **2013**, 14, 321–329, doi:10.1007/s10162-013-0374-3.

34. Wise, A.K.; Hume, C.R.; Flynn, B.O.; Jeelall, Y.S.; Suhr, C.L.; Sgro, B.E.; O'Leary, S.J.; Shepherd, R.K.; Richardson, R.T. Effects of localized neurotrophin gene expression on spiral ganglion neuron resprouting in the deafened cochlea. Mol. Ther. **2010**, 18, 1111–1122, doi:10.1038/mt.2010.28.
35. Fukui, H.; Wong, H.T.; Beyer, L.A.; Case, B.G.; Swiderski, D.L.; Di Polo, A.; Ryan, A.F.; Raphael, Y. BDNF gene therapy induces auditory nerve survival and fiber sprouting in deaf Pou4f3 mutant mice. Sci. Rep. **2012**, 2, doi:10.1038/srep00838.
36. Takada, Y.; Beyer, L.A.; Swiderski, D.L.; O'Neal, A.L.; Prieskorn, D.M.; Shivatzki, S.; Avraham, K.B.; Raphael, Y. Connexin 26 null mice exhibit spiral ganglion degeneration that can be blocked by BDNF gene therapy. Hear. Res. **2014**, 309, 124–135, doi:10.1016/j.heares.2013.11.009.
37. Bartel, D.P. MicroRNAs: Genomics, Biogenesis, Mechanism, and Function. Cell 2004, 116, 281–297.
38. Ushakov, K.; Rudnicki, A.; Avraham, K.B. MicroRNAs in sensorineural diseases of the ear. Front. Mol. Neurosci. 2013, 6.
39. Mittal, R.; Liu, G.; Polineni, S.P.; Bencie, N.; Yan, D.; Liu, X.Z. Role of microRNAs in inner ear development and hearing loss. Gene 2019, 686, 49–55.
40. Doetzlhofer, A.; Avraham, K.B. Insights into inner ear-specific gene regulation: Epigenetics and non-coding RNAs in inner ear development and regeneration. Semin. Cell Dev. Biol. 2017, 65, 69–79.

CHAPTER 2

Exploring the miRNA profiles induced by rhNGF and rhBDNF in cochlear cells: an in vitro and in silico study

1. Abstract

The present study investigated whether two major neurotrophic factors, the nerve growth factor (NGF) and the brain-derived neurotrophic factor (BDNF), have the ability to modify the miRNA profiling in cochlear cells derived from the Organ of Corti. Cochlear cells were treated with 50 ng/ml of rhNGF or rhBDNF and samples were collected after 1h, 6h and 24h of stimulation. The miRNome was investigated through microfluidic cards TaqMan array. The miRNAs target genes and pathways were then identified through Diana mirpath v.3.0. The results of this study show that both neurotrophic factors induce substantial changes of the miRNA profile, that also differs depending on the treatment duration. Through bioinformatics tools, it was possible to identify the target genes of those miRNAs and the relative target pathways. According to the well known effects that NGF and BDNF carry out in neuronal cells, pathways associated with cell cycle, differentiation, metabolism and others were predicted for the modulated miRNAs. Many of these have been never investigated in the cochlea in relationship with the neurotrophic factors. Moreover, the effects of NGF in the cochlea are poorly reported in the literature, since its role in promoting cochlear survival has only recently been considered. On this basis, the present study demonstrates that NGF and BDNF target several signalings, that were already known to be modulated by NGF and BDNF, and that this is mediated by a wide range of miRNAs. Moreover, the results of this study also show new potential pathways that, through selective miRNAs, are likely to be modulated by NGF and BDNF in the cochlea.

2. Introduction

MicroRNAs (miRNAs) are also known as small non coding RNA molecules because of their length (18-22 nucleotides). MiRNAs are encoded in intragenic or intergenic genomic sequence, as a single or multiple miRNA precursors. miRNAs then control gene expression at the post-transcriptional level. Specifically, each miRNA can bind to multiple mRNAs at their 3'-UTR region, hence reducing the expression of those genes. Thanks to their ability of targeting multiple mRNAs, each miRNA can regulate the expression of hundreds of genes, enabling a complex gene expression regulation [1].

It has been estimated that miRNAs can modulate up to 60% of protein-coding genes of the human genome. For this reason, miRNAs have been associated with several physiological functions. Likewise, their dysregulation has been implicated in several pathological conditions and have also been proposed as therapeutic agents.

In the cochlea, miRNAs have a major role in inner ear development. Specifically, a specific miRNA pattern expression has been associated with development and survival of the mechanosensory hair cells (HCs). Moreover, mutations in specific miRNAs have been related to congenital deafness [2].

In the present study, we were interested in investigating the miRNA changes upon neurotrophic factors (NFs) stimulation in cochlear cells derived from the Organ of Corti. The identification of differentially modulated miRNAs by NFs, which are known to have a protective effect for the cochlea [3–6], would enable to find new therapeutic targets for the treatment of sensorineural hearing loss. Moreover, the miRNome induced by NFs in cochlear cells has never been investigated until now and represents an important step forward for the identification of their mechanisms of action.

3. Methods

3.1. Cell culture and experimental design

Murine cochlear cells from the Organ of Corti terminally differentiated and immortalized were used to study the miRNA profiles induced by rhNGF or rhBDNF in cochlear cells. Cells were cultured at 37°C with high glucose Dulbecco's modified Eagle's medium (DMEM) containing 10% (v/v) heat-inactivated FBS. For treatments, 10^6 cells were cultured on T75 flasks and after 24h were treated with rhNGF [50 ng/ml] or rhBDNF [50ng/ml] for 1h, 6h and 24h and compared to untreated cells (CTRL).

3.2. MiRNAs profiling

Total RNAs were extracted from cochlear cells using the mirVana miRs isolation kit (Ambion, Thermo Fisher Scientific, USA) by following the manufacturer's instructions, and RNA concentrations and qualities were evaluated by NanoDrop 2000 (Thermo scientific, USA). Identical amounts of RNAs extracted were subjected (700 ng) to qRT-PCR by using the TaqMan MicroRNA reverse transcription kit (Applied Biosystems, USA). and the Megaplex RT primers murine pool (Applied Biosystems, USA)according to the manufacturer's instructions. The cDNA was then processed with microfluidic cards TaqMan array rodent microRNA A + B v3.0 (Applied Biosystems, USA, #4444909). The array is a set containing two cards with a total of 384 TaqMan MicroRNA Assays per card, and therefore enables accurate quantitation of 641 microRNAs for mouse. A detailed list of the tested miRNAs is available here: https://www.thermofisher.com /order /catalog /product/ 4444909#/4444909. Three biological replicates for each condition were performed. The expression levels of microRNAs were investigated by comparative assay on a ViiA7 (Applied Biosystems, USA). Data were processed by ViiA7 software and further analyzed by Expression Suite (v.1.0.3, Applied Biosystems, USA) through the $2^{-\Delta\Delta Ct}$ method [7]. ExpressionSuite software was also used to perform the statistical analysis. A threshold of $p < 0.05$ (p value calculation based on $2^{-\Delta\Delta Ct}$) was set to identify significant expression changes of miRNAs and the maximum CT allowed was 40.0. The U6 snRNA was used as endogenous control. The modulated miRNAs are reported in the volcano plot graphs (correlation between p value and fold change).

3.3. Pathway analysis and target gene prediction

To gain insight into the biological function of the modulated miRs, we performed an *in silico* analysis through the DIANA miRPath v.3 software (http://snf-515788.vm.okeanos.grnet.gr/). The analysis was restricted to the experimentally validated target genes of the identified

miRNAs reported in TarBase v7.0., which is a with published experimentally validated miRNA:gene interactions [8]. The results were merged as “genes unions” and only the pathways present in the Kyoto Encyclopedia of Genes and Genomes (KEGG) with a threshold of p<0,05 were identified. An FDR Correction was applied. An additional network analysis was performed for the target genes related to the mTOR signaling identified in BDNF treated cells, that is the one selected for the subsequent in vivo experiments.The GeneMANIA prediction server was used for this purpose (https://genemania.org/).

4. Results

4.1. rhNGF

Summary of the miRNAs modulated by rhNGF up to 24h of treatment in murine cochlear cells versus CTRL. The percentages of miRNAs that showed differences in expression levels were: 38,85%, 27,08% and 50% after 1h, 6h and 24h of rhNGF treatment respectively.

The following table shows the miRNAs with a p value lower or close to 0,05. For each miRNA it is indicated the nomenclature reported on Thermo Fisher (miRNA Thermo), the identification code reported on Thermo Fisher (code), the nomenclature reported on miRBase (miRBase), the p value and the relative quantification compared to the CTRL group (Fold Change).

Group	Set	miRNA Thermo	code	miRBase	p value	Fold change
NGF 1h	A	mmu-miR-196b	002215	mmu-miR-196b-5p	0,050	0.266
		rno-miR-196c	002049	rno-miR-196c-5p	0,079	0.238
NGF 1h	B	hsa-miR-183#	002270	mmu-miR-183-3p	0,025	0.374
		hsa-miR-421	002700	mmu-miR-421-3p	0,050	0.424
		hsa-miR-206	000510	mmu-miR-206-3p	0,064	0.307
NGF 6h	A	-	-	-	-	
NGF 6h	B	hsa-miR-99b#	002196	mmu-miR-99b-3p	0,062	0.243
NGF 24h	A	rno-miR-196c	002049	rno-miR-196c-5p	0,022	2.057
NGF 24h	B	mmu-miR-34c#	002584	mmu-miR-34c-3p	0,019	2.142
		mmu-mirR-466k	240990_mat	mmu-miR-466k	0,031	2.890
		rno-miR-146b	002755	mmu-miR-146b-5p	0,046	3.503
		hsa-miR-27a#	002445	mmu-miR-27a-5p	0,052	5.875
	LEGEND	up-regulated	down-regulated			

4.1.1. 1h stimulation by rhNGF

Volcano plots

Volcano Plots deriving from the analysis of the microfluidic card arrays by Expression Suite software showing the miRNAs modulated by rhNGF after 1h of treatment.

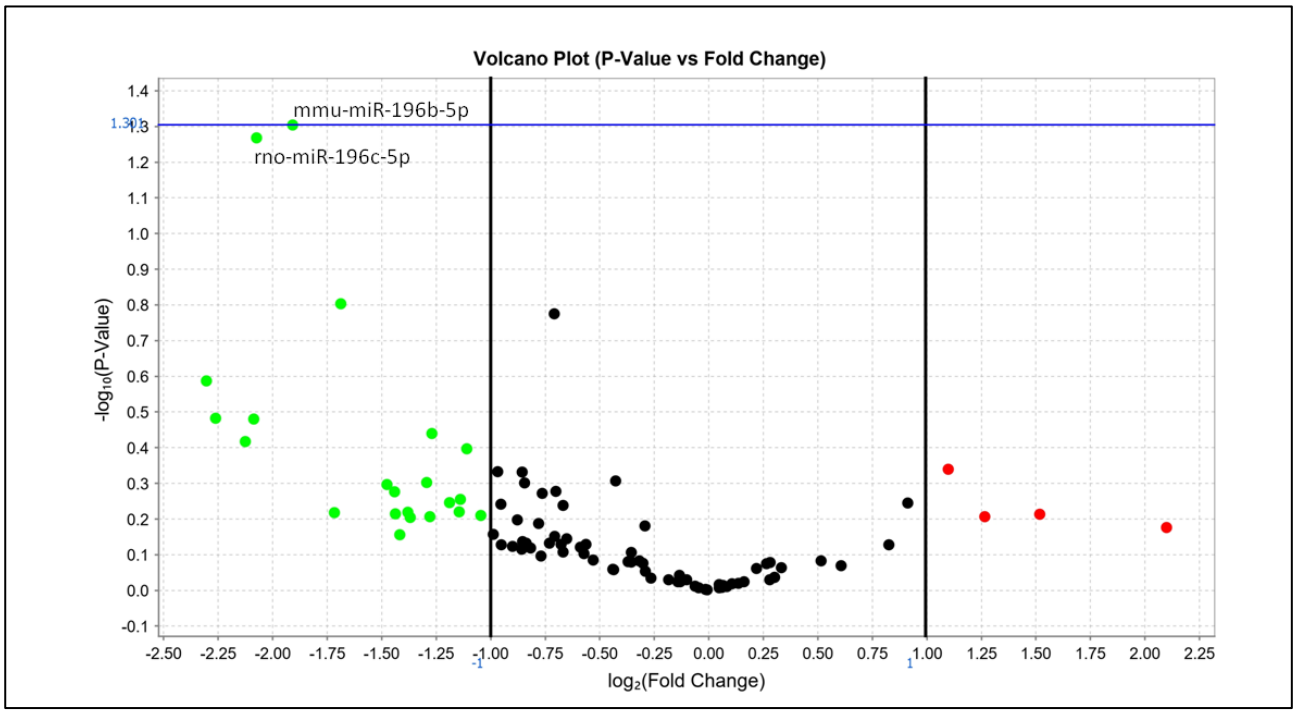

Volcano Plot – cochlea_NGF1h versus CTRL (Set A). miRNA's nomenclature refers to miRBase.

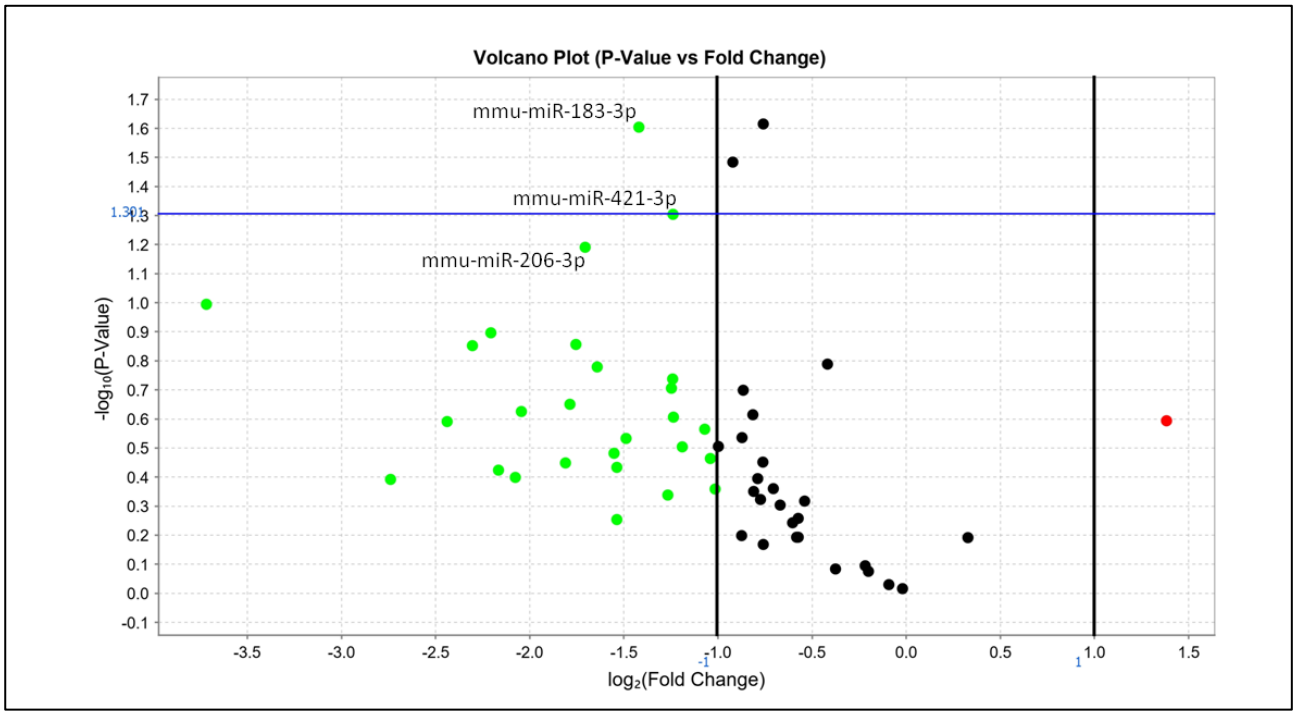

Volcano Plot – cochlea_NGF1h vs CTRL Set B. miRNA's nomenclature refers to miRBase

Target Pathways

Target pathways of the miRNAs modulated by rhNGF after 1h of treatment identified by Diana mirpath v3.0. are reported in the following table.

miRNAs	**Target genes**	**Target pathway**	**P value**
mmu-miR-196b-5p	*Igfbp1*	microRNA in cancer	0.0174918223646
mmu-miR-183-3p	*Cltc*	Synaptic vesicles cycle	0.04653825412
	Dbf4	Cell cycle	0.04945043292
	Cltc	Lysosome	0.04945043292
	Cltc	Endocrine and other factor-regulated calcium reabsorption	0.04653825412
	Mt2	Mineral absorption	0.04653825412
	Cltc	Bacterial invasion of epithelial cells	0.04653825412
mmu-miR-206-3p; mmu-miR-421-3p	*Fasn, Acadsb, Ptplb, Elovl2, Mcat, Scd1*	Fatty acid metabolism	$2.5542113015e^{-08}$
	Vav2, Cbl, Pik3r3, Tlr4, Cblb, Tlr2, Flnb, Igf1, Itgb3, Timp3, Itga5, Actb, Egfr, Ptpn11, Mapk3, Fzd7, Ccnd1, Plcg1, Ank3, Fn1, Nras, Sos1, Esr1, Elk1, Frs2, Fzd5, Cd44, Sdc2, Prkacb, Met, Cdc42, Sdc4, Cav2	Proteoglycans in cancer	$1.82894627184e^{-07}$
	Kmt2c, Nsd1, Setd2, Whsc1, Whsc1l1, Dot1l, Kmt2d	Lysine degradation	0.00412710810446
	Prkag3, Prkaa2, Pik3r3, Plk2, Foxo1, Igf1, Skp2, Nlk, Homer3, Egfr, Mapk3, Gabarapl1, Ccnd1, Nras, Sos1, Stk4, Bcl2l11, Sgk1, Homer1, Mapk8, Crebbp	FoxO signalling pathway	0.0489461775609
	Ctnna1, Ptpn1, Wasf2, Lef1, Nlk, Actb, Egfr, Mapk3, Mllt4, Vcl, Pvrl3, Baiap2, Fer, Met, Cdc42, Snai2, Crebbp	Adherens junction	0.00113703683943
	Med13, Pik3r3, Ncoa3, Foxo1, Itgb3, Rcan1, Actb, Mapk3, Dio2, Med13l, Ccnd1, Plcg1, Nras, Esr1, Slc16a2, Med27, Notch3, Prkacb, Ncoa1, Med1, Ncoa2, Crebbp	Thyroid hormone signalling pathway	0.00220376000206
	Pld1, Pld2, Map3k1, Egfr, Gnaq, Mapk3, Nras, Mmp14, Sos1, Adcy3, Calm2, Elk1, Prkacb, Pla2g4a, Cdc42, Map3k2, Mapk8	GnRH signalling pathway	0.00845820608964
	Pik3r3, Igf1, Egfr, Mapk3, Ccnd1, Plcg1, Nras, Sos1, Rb1, Calm2, E2f3	Glioma	0.0159999278218
mmu-miR-206-3p,mmu-miR-421-3p, mmu-miR-183-3p	*Cbl, Arf6, Pld1, Pld2, Cblb, Cltc, Arap2, Stambp, Chmp3, Vps37a, Arf3, Agap1, Ehd3, Cxcr4, Egfr, Pard6g, Acap2, Iqsec1, Prkci,*	Endocytosis	0.00220376000206

	Git1, Vps4b, Pdcd6ip, Met, Cdc42, Cav2, Rab5c, Dab2		
	Cbl, Pik3r3, Ctnna1, Cblb, Cltc, Wasf2, Sept2, Itga5, Actb, Fn1, Cd2ap, Vcl, Met, Cdc42, Cav2	Bacterial invasion of epithelial cells	0.0174694921069
mmu-miR-206-3p	*Fasn, Mcat*	Fatty acid biosynthesis	$1.70601029147e^{-20}$

4.1.2. 6h stimulation by rhNGF

Volcano plots

Volcano Plots deriving from the analysis of the microfluidic card arrays by Expression Suite software showing the miRNAs modulated by rhNGF after 6h of treatment.

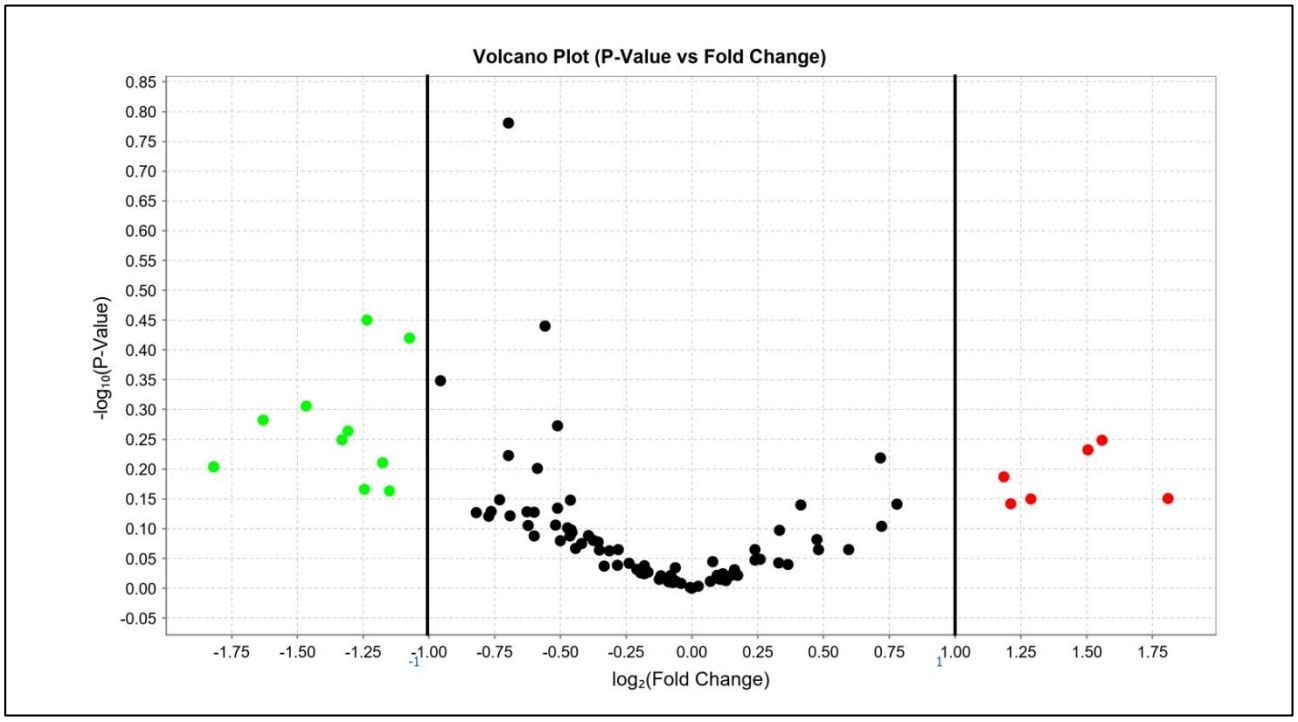

Volcano plot – cochlea_NGF6h vs CTRL Set A. miRNA's nomenclature refers to miRBase

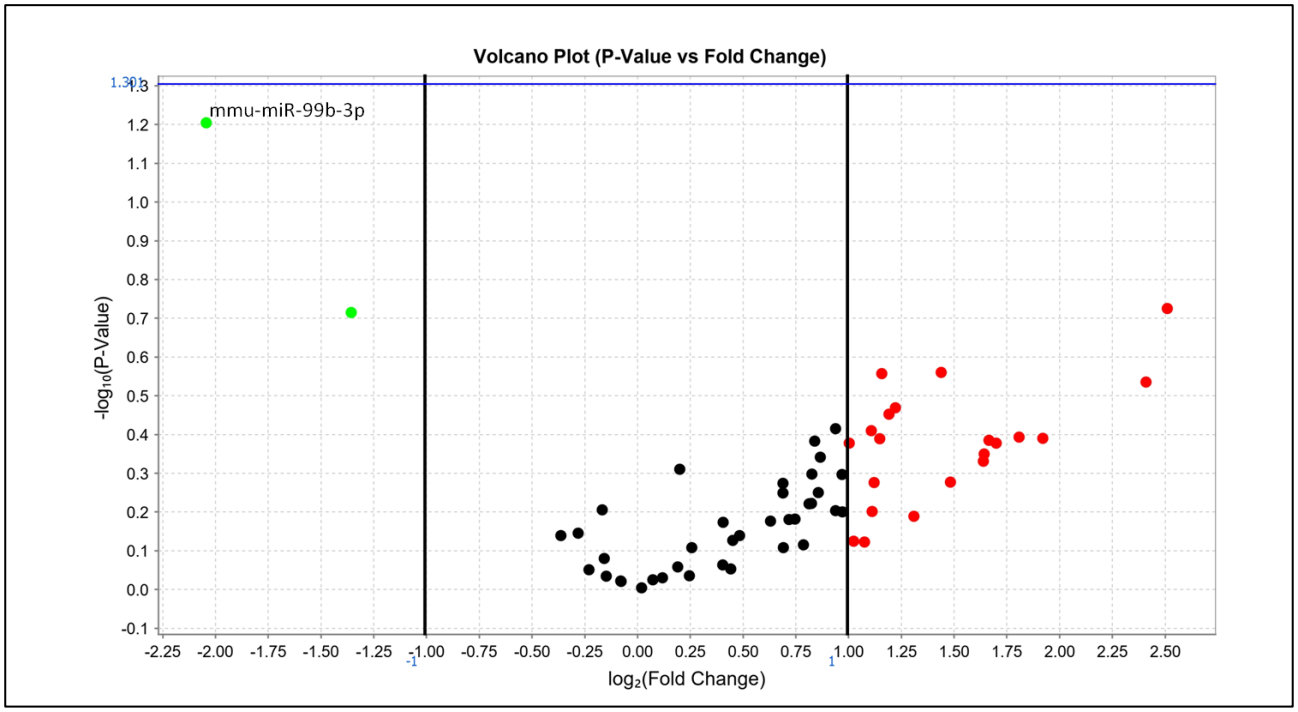

Volcano plot – cochlea_NGF6h vs CTRL Set B. miRNA's nomenclature refers to miRBase

Target pathways

Target pathways of the miRNAs modulated by rhNGF after 6h of treatment identified by Diana mirpath v3.0.

miRNAs	**Target genes**	**Target pathway**	**P value**
mmu-miR-99b-3p	*Gsk3b, Atf4*	Neurotrophin signalling pathway	0,041082542318
	Kmt2d	Lysine degradation	0,0345666942253
	Aft4	Estrogen signaling pathway	0.0225754234823

4.1.3. 24h stimulation by rhNGF

Volcano plots

Volcano Plots deriving from the analysis of the microfluidic card arrays by Expression Suite software showing the miRNAs modulated by rhNGF after 24h of treatment.

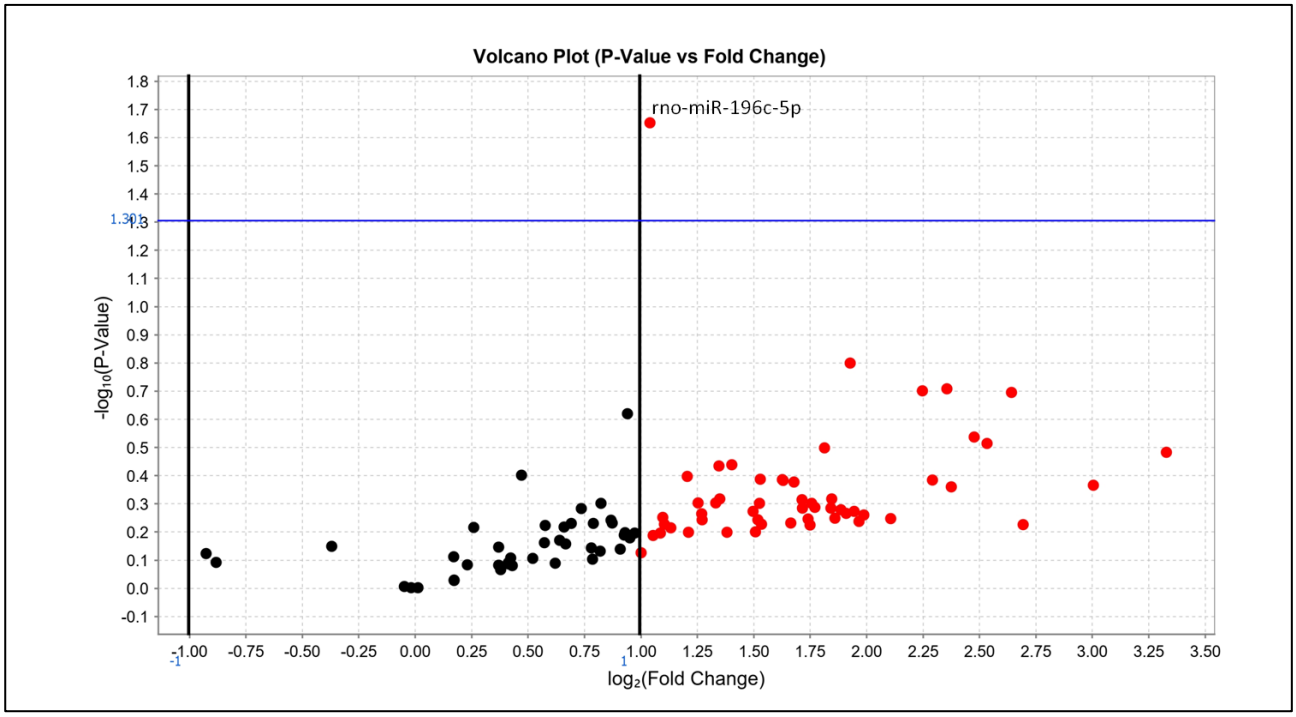

Volcano Plot – cochlea_NGF24h vs CTRL Set A. miRNA's nomenclature refers to miRBase

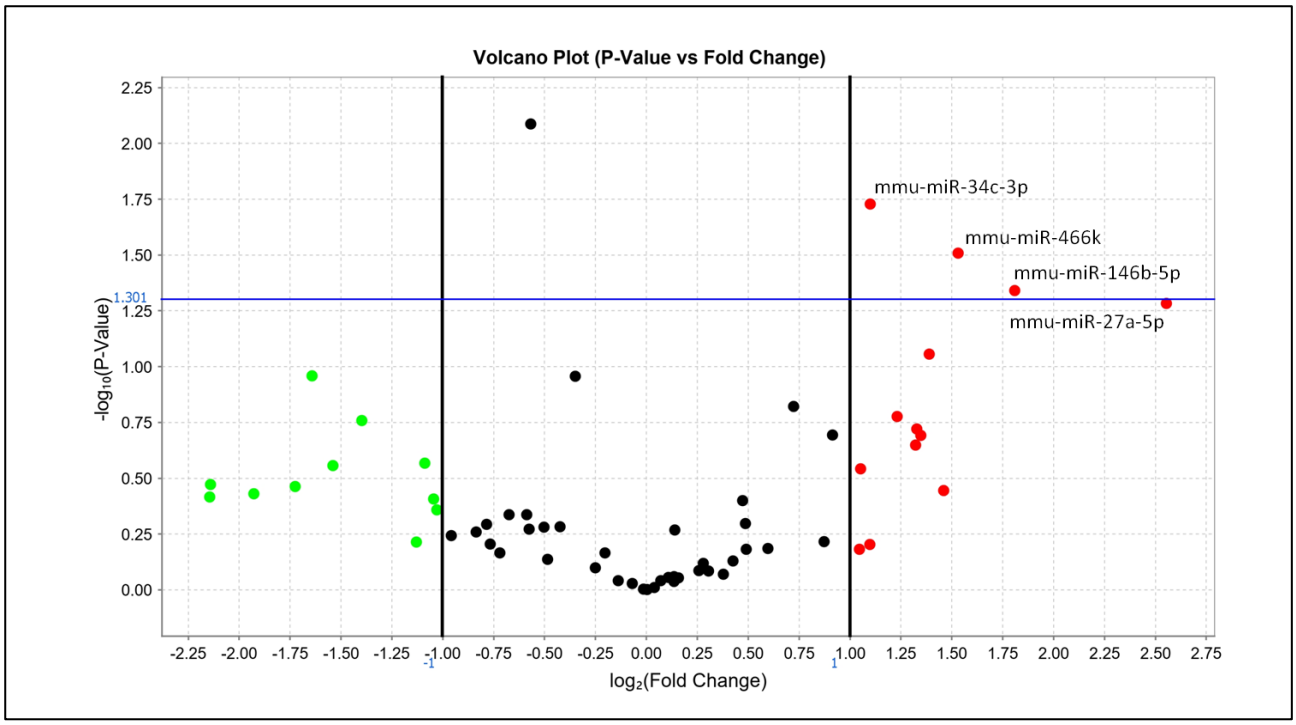

Volcano Plot – cochlea_NGF24h vs CTRL Set B. miRNA's nomenclature refers to miRBase

Target pathways

Target pathways of the miRNAs modulated by rhNGF after 24h of treatment identified by Diana mirpath v3.0.

miRNAs	**Target genes**	**Target pathway**	**P value**
mmu-miR-466k and mmu-miR-146b-5p	*Aldh2, Colgalt1, Suv39h1, Hykk, Setd1b, Suv420h1*	Lysine degradation	0,00295493704819
	Bmpr1a, Id1, Smurf2, Smad4, Sp1, Rbl1	TGF-beta signaling pathway	0.0365655633747
	Sos2, G6pc, Plk2, Foxo1, Cat, Egfr, Braf, Smad4, Ccnb2	FoxO signaling pathway	0.0198089495538
	Pank1, Pank3	Pantothenate and CoA biosynthesis	0.00452836068495
	Sos2, Egfr, Braf, Erbb3, Crk	ErbB signalling pathway	0.0365655633747
	Apob, Ppap2b, Abca1	Fat digestion and absorption	0.0175489095495
	Hif1a, Egfr, Pfkp, Slc2a2	Central carbon metabolism in cancer	0.0365655633747

4.1.4. Summary of the most relevant target pathways of rhNGF within 24h of treatment

The following table shows a summary of the pathways, that are relevant to the present study, identified within 24h of rhNGF treatment.

Time of treatment by rhNGF	Modulated miRNAs	Target genes	Target Pathways	p value
1h	mmu-miR-183-3p	*Cltc*	Synaptic vescicle cycle	0.04653825412
1h	mmu-miR-183-3p	*Dbf4*	Cell cycle	0.04945043292
1h	mmu-miR-183-3p	*Cltc*	Lysosome	0.04945043292
1h	mmu-miR-206-3p mmu-miR-421-3p	*Kmt2c, Nsd1, Setd2, Whsc1, Whsc1l1, Dot1l, Kmt2d*	Lysine degradation	0.00412710810446
1h	mmu-miR-206-3p mmu-miR-421-3p	*Fasn, Acadsb, Ptplb, Elovl2, Mcat, Scd1*	Fatty acid metabolism	$2.5542113015e^{-08}$
1h	mmu-miR-206-3p mmu-miR-421-3p	*Vav2, Cbl, Pik3r3, Tlr4, Cblb, Tlr2, Flnb, Igf1, Itgb3, Timp3, Itga5, Actb, Egfr, Ptpn11, Mapk3, Fzd7, Ccnd1, Plcg1, Ank3, Fn1, Nras, Sos1, Esr1, Elk1, Frs2, Fzd5, Cd44, Sdc2, Prkacb, Met, Cdc42, Sdc4, Cav2*	Proteoglycans in cancer	$1.82894627184e^{-07}$
1h	mmu-miR-206-3p mmu-miR-421-3p	*Prkag3,Prkaa2, Pik3r3,Plk2,Foxo1, Igf1, Skp2, Nlk, Homer3, Egfr, Mapk3,Gabarapl1, Ccnd1, Nras, Sos1, Stk4, Bcl2l11,Sgk1, Homer1, Mapk8, Crebbp*	FoxO signalling pathway	0.0489461775609
1h	mmu-miR-206-3p mmu-miR-421-3p	*Ctnna1, Ptpn1, Wasf2, Lef1, Nlk, Actb, Egfr, Mapk3, Mllt4, Vcl, Pvrl3,*	Adherens junction	0.00113703683943

		Baiap2, Fer, Met, Cdc42, Snai2, Crebbp		
1h	mmu-miR-206-3p mmu-miR-421-3p mmu-miR-183-3p	*Cbl, Arf6, Pld1, Pld2, Cblb, Cltc, Arap2, Stambp, Chmp3, Vps37a, Arf3, Agap1, Ehd3, Cxcr4, Egfr, Pard6g, Acap2, Iqsec1, Prkci, Git1, Vps4b, Pdcd6ip, Met, Cdc42, Cav2, Rab5c, Dab2*	Endocytosis	0.00220376000206
1h	mmu-miR-206-3p	*Fasn, Mcat*	Fatty acid biosynthesis	$1.70601029147e^{-20}$
6h	mmu-miR-99b-3p	*Gsk3b, Atf4*	Neurotrophin signalling pathway	0,041082542318
6h	mmu-miR-99b-3p	*Kmt2*	Lysine degradation	0,0345666942253
24h	mmu-miR-466k mmu-miR-146b-5p	*Bmpr1a, Id1, Smurf2, Smad4, Sp1, Rbl1*	TGF-β signalling pathway	0.0365655633747
24h	mmu-miR-466k mmu-miR-146b-5p	*Sos2, G6pc, Plk2, Foxo1, Cat, Egfr, Braf, Smad4, Ccnb2*	Foxo signalling pathway	0.0198089495538
24h	mmu-miR-466k mmu-miR-146b-5p	*Aldh2, Colgalt1, Suv39h1, Hykk, Setd1b, Suv420h1*	Lysine degradation	0,00295493704819
24h	mmu-miR-466k mmu-miR-146b-5p	*Pank1, Pank3*	Pantothenate and CoA biosynthesis	0.00452836068495
24h	mmu-miR-466k mmu-miR-146b-5p	*Sos2, Egfr, Braf, Erbb3, Crk*	ErbB signalling pathway	0.0365655633747

4.1.5. Target pathways of the overall miRNA profile induced by rhNGF

The following table shows the target pathways identified by Diana mirpath v3.0. for all the miRNAs modulated by rhNGF within 24h of treatment. The most relevant pathways for this study are highlighted in the red frames.

KEGG Pathway	p value	Target genes	microRNAs
Fatty acid biosynthesis	<0,001	3	466k, 206-3p
Lysine degradation	<0,001	13	466k,206-3p, 146b-5p, 421-3p,99b-3p
Proteoglycans in cancer	<0,001	40	206-3p, 421-3p, 466k,146b-5p
Fatty acid metabolism	<0,001	9	206-3p, 421-3p, 466k,146b-5p
Adherens Junction	<0,001	22	206-3p, 421-3p, 466k,146b-5p,34c-3p
Endocytosis	<0,001	36	466k, 146b-5p,206-3p, 183-3p,99b-3p,27a-5p,421-3p
Thyroide hormone signalling pathway	<0,001	27	206-3p, 146b-5p, 466k, 99b-3p, 421-3p
Bacterial invasion of epithelial cells	0.0031	18	206-3p, 183-3p, 99b-3p, 421-3p, 146b-5p
Pantothenate and CoA biosynthesis	0.0058	4	206-3p, 466k, 146b-5p
FoxO signalling pathway	0.0067	27	206-3p, 421-3p, 466k, 146b-5p
Protein processing in endoplasmic reticulum	0.0081	30	421-3p, 146b-5p, 206-3p, 99b-3p, 466k
Estrogen signalling pathway	0.0081	16	206-3p, 421-3p, 146b-5p, 466k, 99b-3p
Endometrial cancer	0.0081	15	421-3p, 206-3p, 99b-3p, 146b-5p, 466k
Glioma	0.0093	13	206-3p, 146b-5p, 421-3p, 466k
Dorso-ventral axis formation	0.0093	9	206-3p, 421-3p, 466k, 146b-5p
GnRH signalling pathway	0.0106	19	206-3p, 146b-5p, 421-3p, 466k, 99b-3p
Prostate cancer	0.0134	20	99b-3p, 206-3p, 466k, 421-3p, 146b-5p
Regulation of actin cytoskeleton	0.0153	36	146b-5p, 206-3p, 466k, 421-3p
Chronic myeloid leukemia	0.0155	16	146b-5p, 206-3p
Choline metabolism in cancer	0.0155	19	206-3p, 421-3p, 466k, 146b-5p
ErbB signalling pathway	0.0155	16	206-3p, 146b-5p, 99b-3p, 466k, 421-3p
Thyroid cancer	0.0165	7	146b-5p, 206-3p
Huntington's disease	0.0289	22	146b-5p, 206-3p, 183-3p, 99b-3p, 466k
Colorectal cancer	0.0366	12	99b-3p, 206-3p, 146b-5p
Non-small cell lung cancer	0.0444	13	206-3p, 146b-5p, 421-3p, 466k

Hippo signalling pathway	0.0488	26	206-3p, 421-3p, 146b-5p, 99b-3p, 466k

4.1.6. Analysis of selected miRNAs for each time point

For each time point the following table shows the relative quantification (RQ) (with respect to the CTRL) of the miRNAs found to be significantly modulated - or close to the statistical significance - by rhNGF, together with the p values. The data showing a statistical significance (or close to 0,05) are reported in bold. Non significant data are reported as "n.s." Intriguingly, some of the differentially modulated miRNAs, such as rno-miR-196c and mmu-miR-421-3p, showed an opposite expression trend, being down-regulated 1h after rhNGF administration and up-regulated 24h thereafter. This specific time-dependent modulation could be a retroactive effect due to NGF stimulation and could suggest a fast and transient effect of signaling activation that needs to be suppressed after a longer time.

	1h		**6h**		**24h**	
miRNA	**RQ**	**pvalue vs CTRL**	**RQ**	**pvalue vs CTRL**	**RQ**	**pvalue vs CTRL**
rno-miR-196c	**0.238**	**0,079**	0.958	n.s.	**2.057**	**0,022**
mmu-miR-196b-5p	**0.266**	**0,050**	0.679	n.s.	1.386	n.s.
mmu-miR-183-3p	**0.374**	**0,025**	0.896	n.s.	1.101	n.s.
mmu-miR-421-3p	**0.424**	**0,050**	1.79	n.s.	**2.618**	**0.088**
mmu-miR-206-3p	**0.307**	**0,064**	0.823	n.s.	0.869	n.s.
mmu-miR-99b-3p	**0.528**	**0.033**	**0.243**	**0,062**	1.387	n.s.
mmu-miR-34c-3p	0.987	n.s.	2.005	n.s.	**2.142**	**0,019**
mmu-miR-466k	0.591	n.s.	3.174	n.s.	**2.890**	**0,031**
mmu-miR-146b-5p	0.549	n.s.	2.229	n.s.	**3.503**	**0,046**
mmu-miR-27a-5p	2.608	n.s.	5.697	n.s.	**5.875**	**0,052**

Comparison between groups

The following tables show the **p values** deriving from the comparison of the expression levels of the miRNAs resulted to be significantly modulated - or close to the statistical significance - by rhNGF between the different time points. The data with p<0,05 are highlighted in green; the data close to 0,05 are highlighted in yellow. Non significant data are reported as "n.s."

rno-miR-196c-5p

	1h	6h	24h
1h		0.062	0.025
6h	0.062		n.s.
24h	0.025	n.s.	

mmu-miR-196b-5p

	1h	6h	24h
1h		n.s.	0.021
6h	n.s.		n.s.
24h	0.021	n.s.	

mmu-miR-183-3p

	1h	6h	24h
1h		n.s.	0.015
6h	n.s.		n.s.
24h	0.015	n.s.	

mmu-miR-421-3p

	1h	6h	24h
1h		n.s.	0.014
6h	n.s.		n.s.
24h	0.014	n.s.	

mmu-miR-206-3p

	1h	6h	24h
1h		n.s.	n.s.
6h	n.s.		n.s.
24h	n.s.	n.s.	

mmu-miR-99b-3p

	1h	6h	24h
1h		0.043	n.s.
6h	0.043		0.018
24h	n.s.	0.018	

mmu-miR-34c-3p

	1h	6h	24h
1h		n.s.	0.068
6h	n.s.		n.s.
24h	0.068	n.s.	

mmu-miR-466k

	1h	6h	24h
1h		n.s.	n.s.
6h	n.s.		n.s.
24h	n.s.	n.s.	

mmu-miR-146b-5p

	1h	6h	24h
1h		n.s.	0.014
6h	n.s.		n.s.
24h	0.014	n.s.	

mmu-miR-27a-5p

	1h	6h	24h
1h		n.s.	n.s.
6h	n.s.		n.s.
24h	n.s.	n.s.	

4.2. rhBDNF

Summary of the miRNAs modulated by BDNF up to 24h of treatment in murine cochlear cells versus CTRL. The percentages of miRNAs that showed differences in expression levels were: 31,25%, 18,06% and 39,46% after 1h, 6h and 24h of rhBDNF treatment respectively.

The following table shows the miRNAs with a p value lower or close to 0,050. For each miRNA it is indicated the nomenclature reported on Thermo Fisher (miRNA Thermo), the identification code reported on Thermo Fisher (code), the nomenclature reported on miRBase (miRBase), the p value and the relative quantification compared to the CTRL group (Fold Change).

Group	Set	miRNA Thermo	code	miRBase	p value	Fold change
BDNF 1h	A	rno-miR-196c	002049	rno-miR-196c-5p	0,006	0.411
		mmu-miR-196b	002215	mmu-miR-196b-5p	0,082	0.325
	B	mmu-miR-1274a	121150_mat	-	0,072	0.273
		mmu-miR-1839-3p	121203_mat	mmu-miR-1839-3p	0,077	4.257
		mmu-miR-696	001628	mmu-miR-696	0,089	2.882
BDNF 6h	A	-	-	-	-	
	B	mmu-miR-1937c	241011_mat	-	0,015	0.453
		mmu-miR-1937b	241023_mat	-	0,005	0.450
		hsa-miR-27a#	002445	mmu-miR-27a-5p	0,029	4.879
		rno-miR-146b	002755	mmu-miR-146b-5p	0,056	2.326
BDNF 24h	A	-	-	-	-	
	B	hsa-miR-196a	241070_mat	mmu-miR-196a-5p	0,049	2.615
		mmu-miR-1839-3p	121203_mat	mmu-miR-1839-3p	0,068	5.660
		mmu-miR-696	001628	mmu-miR-696	0,066	2.156
		hsa-miR-206	000510	mmu-miR-206-3p	0,064	2.380
		mmu-miR-466k	240990_mat	mmu-miR-466k	0,062	4.312
	LEGEND	up-regulated	down-regulated			

4.2.1. 1h stimulation by BDNF

Volcano plots

Volcano Plots deriving from the analysis of the microfluidic card arrays by Expression Suite software showing the miRNAs modulated by BDNF after 1h of treatment.

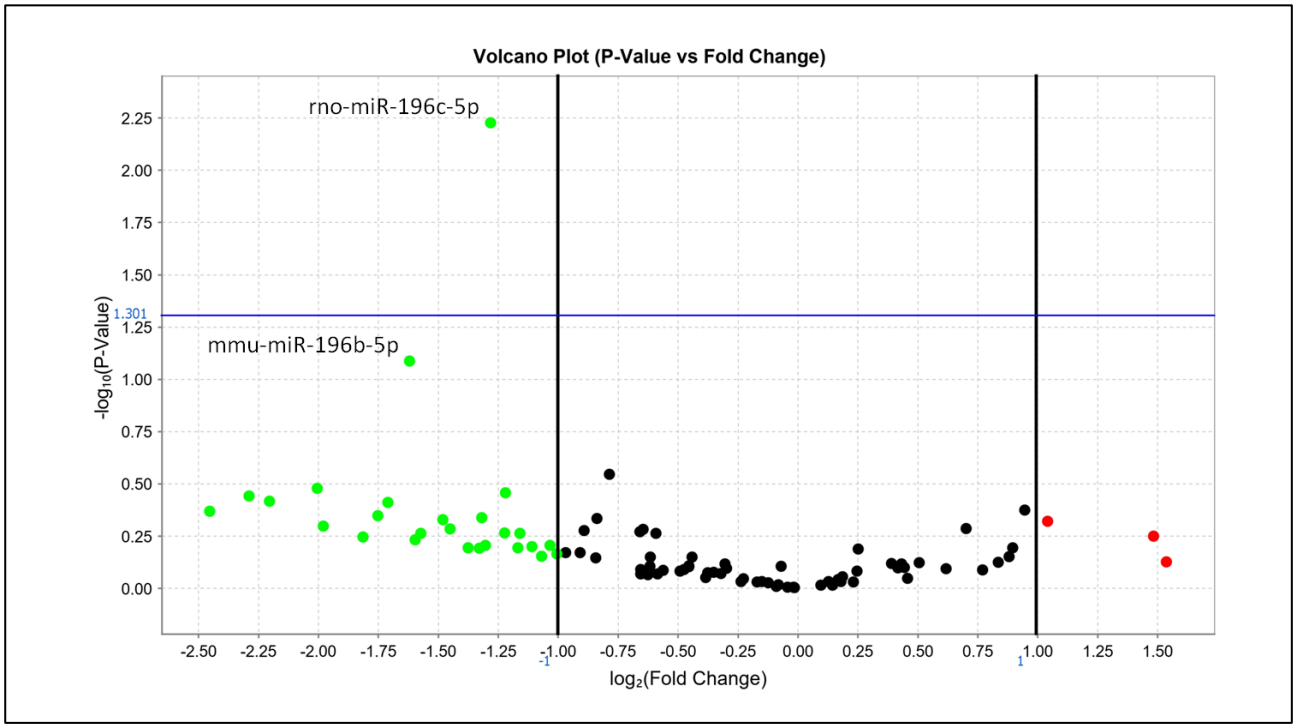

Volcano Plot – cochlea_BDNF1h vs CTRL Set A. miRNA's nomenclature refers to miRBase

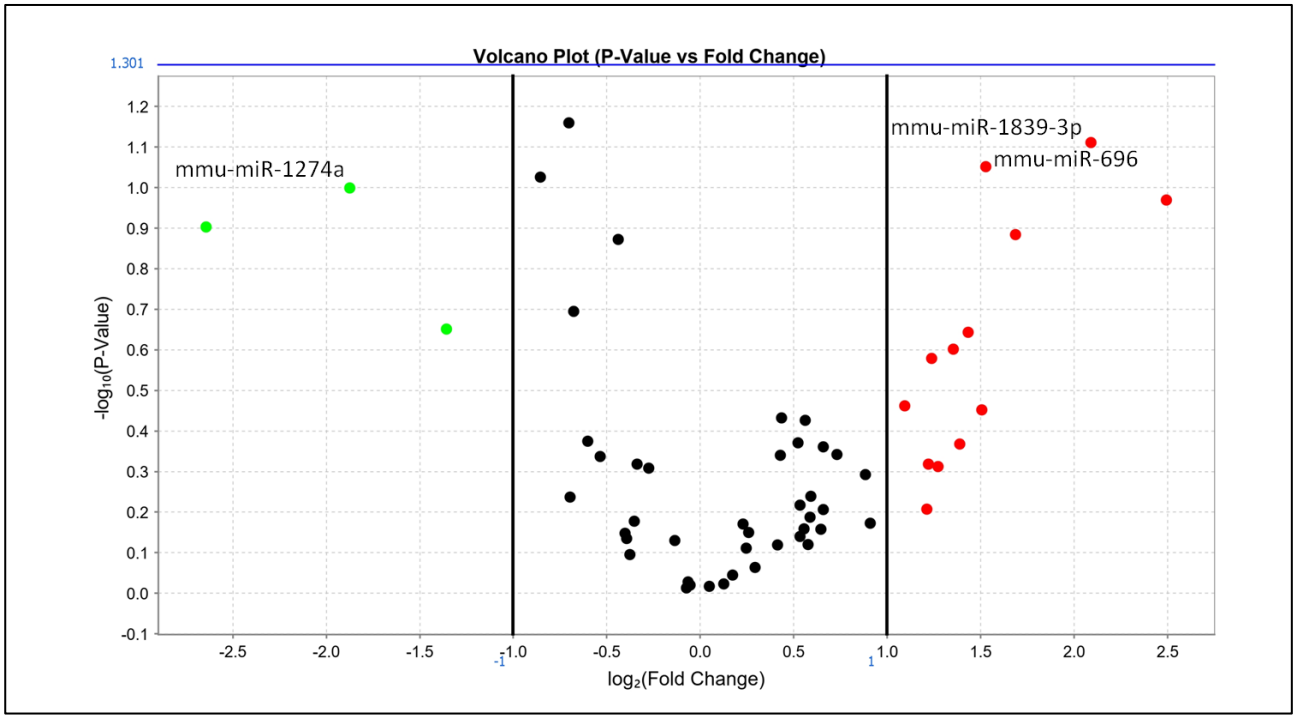

Volcano Plot – cochlea_BDNF1h vs CTRL Set B. miRNA's nomenclature refers to miRBase

Target Pathways

Target pathways of the miRNAs modulated by BDNF after 1h of treatment identified by Diana mirpath v3.0.

miRNAs	**Target genes**	**Target pathway**	**P value**
mmu-miR-196b-5p	*Igfbp1*	microRNA in cancer	0.0174918223646
mmu-miR-696	*Setd2, Whsc1l1, Ehmt1*	Lysine degradation	0.00605800896603
	Alg14,Man1a2, Mgat3	N-glycan biosynthesis	0.00605800896603
	Cds2, Plcg1, Pik3cb, Plcb1, Pik3c2a	Phosphatidylinositol signalling system	0.0100035403622
	Plcg1, Sos1, Camk2a, Pik3cb, Pdgfb	Glioma	0.00605800896603
	Tsc2, Pfkfb2, Dio2, Med13l, Plcg1, Pik3cb, Plcb1, Bmp4	Thyroid hormone signalling pathway	0.0100035403622
	Ptpn11, Sos1, Tgfb3, Pik3cb, Pdgfb	Renal cell carcinoma	0.0229833695166

4.2.2. 6h stimulation by BDNF

Volcano plots

Volcano Plots deriving from the analysis of the microfluidic card arrays by Expression Suite software showing the miRNAs modulated by BDNF after 6h of treatment.

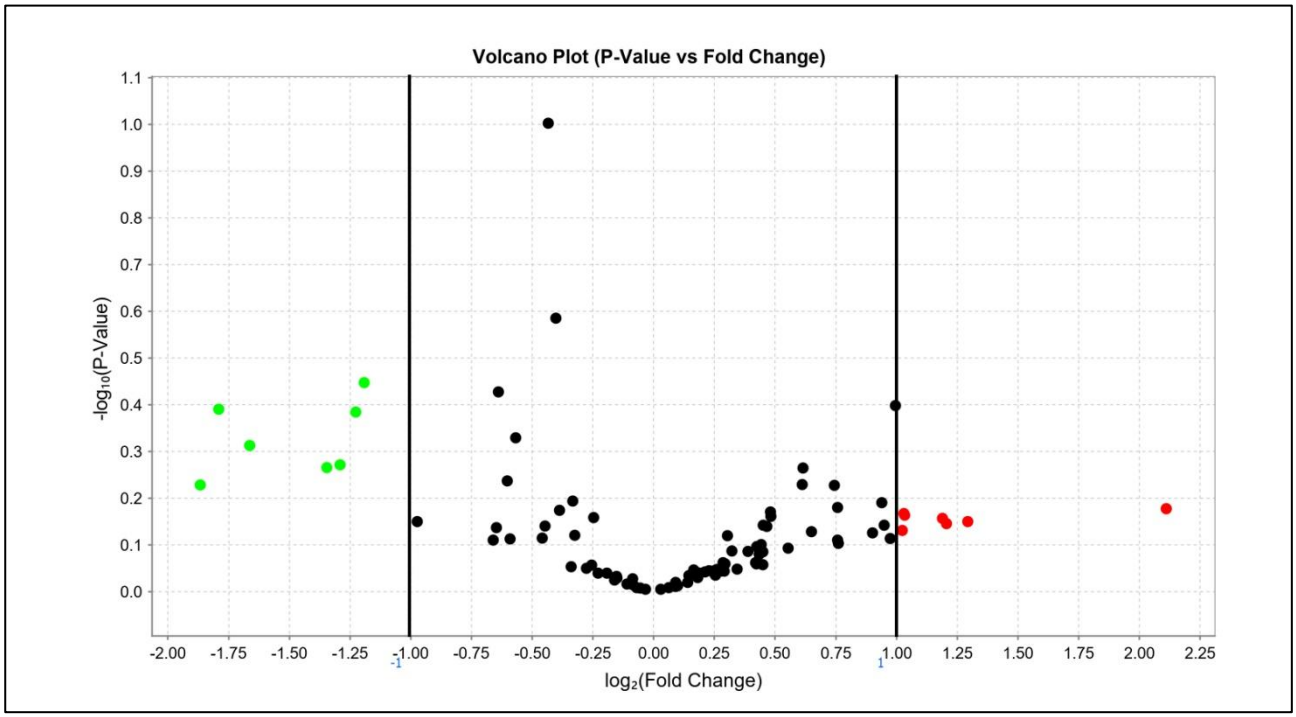

Volcano Plot – cochlea_BDNF6h vs CTRL Set A. miRNA's nomenclature refers to miRBase

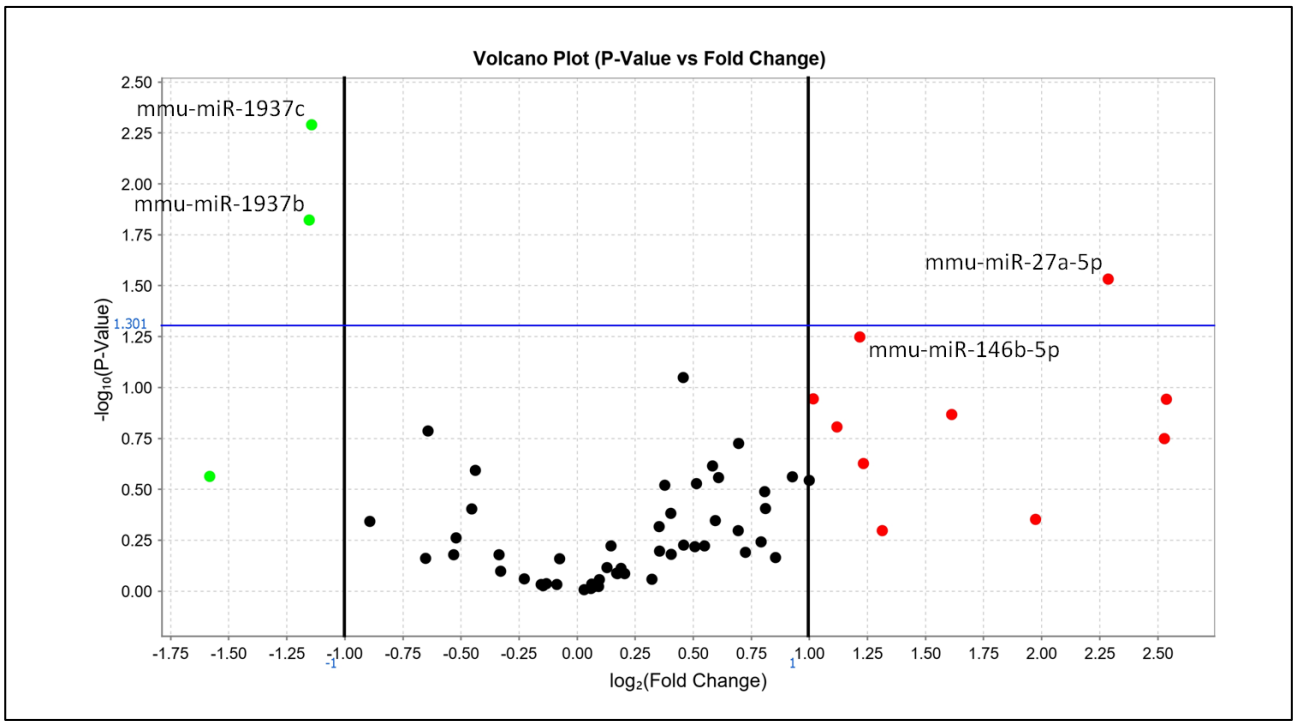

Volcano Plot – cochlea_BDNF6h vs CTRL Set B. miRNA's nomenclature refers to miRBase

Target Pathways

Target pathways of the miRNAs modulated by BDNF after 6h of treatment identified by Diana mirpath v3.0.

miRNAs	**Target genes**	**Target pathway**	**P value**
mmu-miR-146b-5p	*Pank1, Pank3*	Pantothenate and CoA biosynthesis	0.000245175351205
	Suv39h1, Setd1b, Suv420h1	Lysine degradation	0.00142669971241
	Id1, Smurf2, Smad4, Sp1, Rbl1	TGF-beta signaling pathway	0.00562877215941
	Pikfyve, Itpk1, Inpp4b	Inositol phosphate metabolism	0.0275663704754
mmu-miR-27a-5p	*Tars*	Aminoacyl-tRNA biosynthesis	0.00797573251436
	Epn2	Endocytosis	0.0147483273009

4.2.3. 24h stimulation by BDNF

Volcano plots

Volcano Plots deriving from the analysis of the microfluidic card arrays by Expression Suite software showing the miRNAs modulated by BDNF after 24h of treatment.

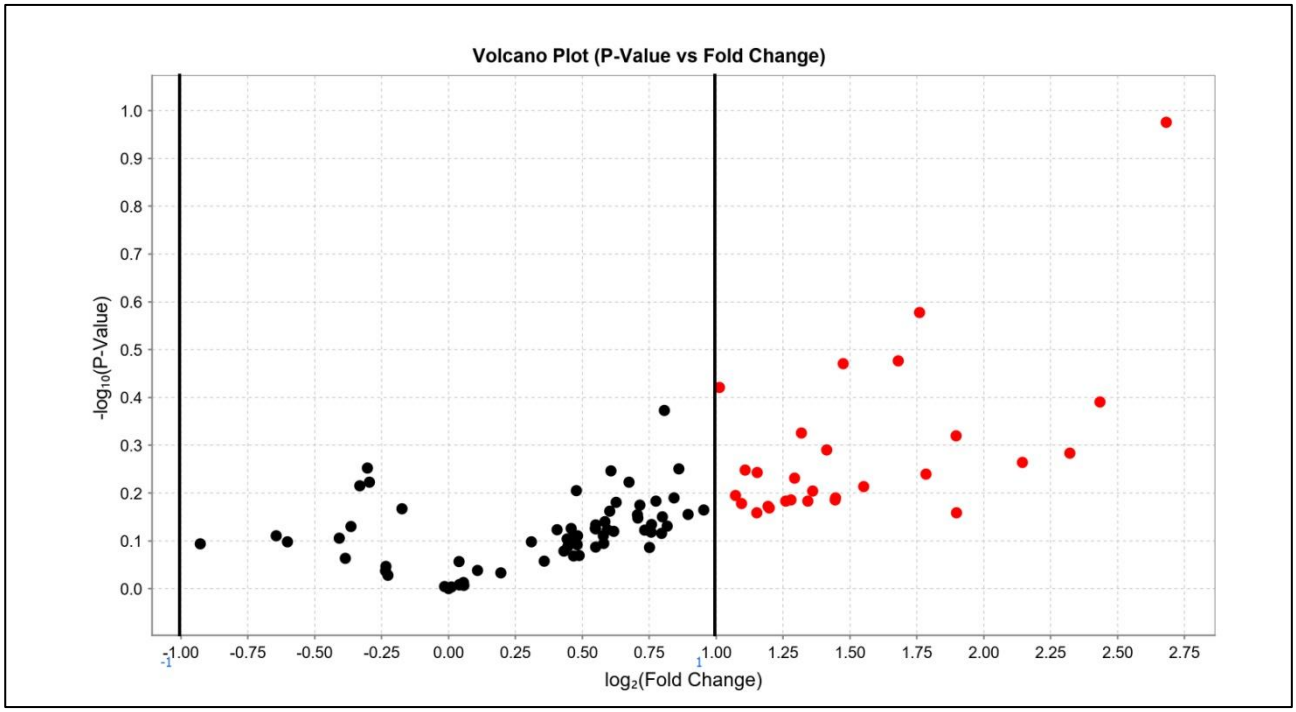

Volcano Plot – cochlea_BDNF24h vs CTRL Set A. miRNA's nomenclature refers to miRBase

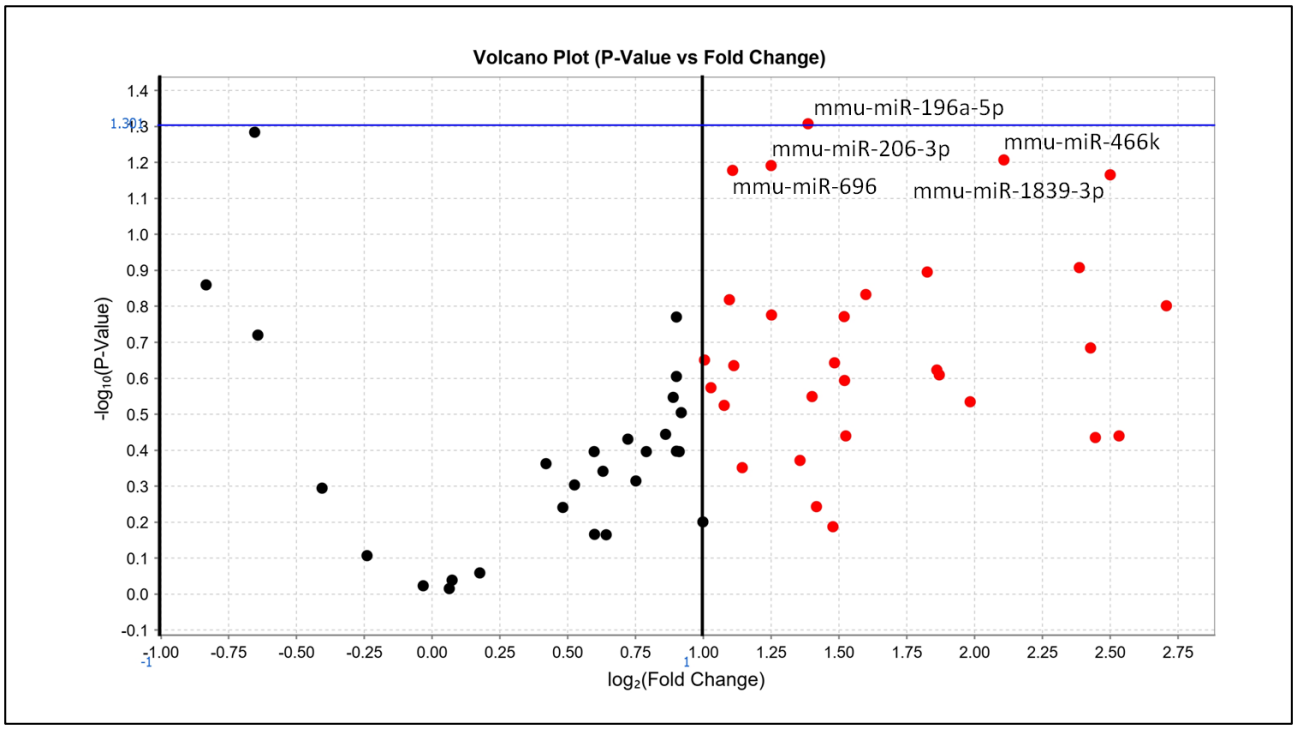

Volcano Plot – cochlea_BDNF24h vs CTRL Set B. miRNA's nomenclature refers to miRBase

Target Pathways

Target pathways of the miRNAs modulated by BDNF after 24h of treatment identified by Diana mirpath v3.0.

miRNAs	**Target genes**	**Target pathway**	**P value**
mmu-miR-466k, mmu-miR-696, mmu-miR-206-3p	*Fasn, Acadsb, Ptplb, Mcat, Acsl1, Cpt2, Acox3*	Fatty acid metabolism	1.38733364574e-08
	Vav2, Cbl, Pik3r3, Tlr4, Cblb, Tlr2, Flnb, Igf1, Itgb3, Timp3, Itga5, Actb, Arhgef12, Egfr, Ptpn11, Mapk3, Fzd7, Rdx, Ccnd1, Plcg1, Ank3, Nras, Erbb3, Sos1, Esr1, Camk2a, Pik3cb, Elk1, Frs2, Fzd5, Cd44, Sdc2, Prkacb, Met, Cdc42, Sdc4, Cav2	Proteoglycans in cancer	8.51509396763e-07
	Prkag3, Prkaa2, G6pc, Pik3r3, Plk2, Foxo1, Igf1, Skp2,Irs1,Nlk,Homer3, Cat, Egfr, Mapk3, Gabarapl1, Ccnd1, Nras, Sos1, Tgfb3, Pik3cb, Ccnd2, Stk4, Bcl2l11, Homer1, Mapk8, Crebbp	FoxO signalling pathway	0.00625564777652
	Tram1, Ern1, Os9, Sec63, Eif2ak1, Stt3a, Ssr3, Xbp1, Edem3, Hspa4l, Pdia3, Atf6, Dnajc3, Man1a2, Man1a, Ube2g2, Sec61a1, Atxn3, Ube2g1, Uggt1, Sec24c, March6, Mapk8, Ubqln1, Dnajb12, Dnajb2	Protein processing in endoplasmic reticulum	0.00973643196725
	Aldh2, Kmt2c, Nsd1, Setd2, Colgalt1, Whsc1, Hykk, Whsc1l1, Ehmt1, Dot1l	Lysine degradation	0.00158048327665
	Rasa2, Map4k3, Max, Flnb, Ppm1a, Map3k1, Gna12, Il1r1, Fgf11, Rps6ka3, Fgfr4, Nfatc3, Rapgef2, Nlk, Nf1, Ppp3cb, Egfr, Mapk3, Mecom, Nras, Sos1, Map4k2, Dusp3, Tgfb3, Pdgfb, Dusp10, Elk1, Stk4, Prkacb, Pla2g4a, Atf2, Map3k7, Cdc42, Map3k2, Mapk8, Zak	MAPK signalling pathway	0.0432711534982
	Prkaa2, Pik3r3, Ulk2, Igf1, Rps6ka3, Irs1, Tsc2, Rictor, Mapk3, Rragd, Rragc, Pik3cb, Cab39l	mTOR signalling pathway	0.0471528167276
	Cbl, Arf6, Pld1, Pld2, Cblb, Arap2, Stambp, Fgfr4, Chmp3, Vps37a, Arf3, Agap1, Ehd3, Cxcr4, Egfr, Pard6g, Acap2, Zfyve9, Iqsec1, Prkci, Erbb3, Tgfb3, Git1, Vps4b, Pdcd6ip, Ap2a2, Met, Cdc42, Tfrc, Cav2, Rab5c, Dab2	Endocytosis	0.00158048327665
	Ptpn1, Wasf2, Lef1, Ptprb, Nlk, Actb, Egfr, Mapk3, Mllt4, Pvrl3, Baiap2, Fer, Map3k7,	Adherens junctions	0.017801962

	Met, Cdc42, Snai2, Crebbp		2572
	Sptlc1, Pik3r3, Sgms2, Pld1, Pld2, Cers2, Ppp2r3a, Ppp2r2a, Gna12, Ctsd, Ppp2r5e, Smpd1, Gnaq, Mapk3, Nras, Pik3cb, Ppp2r5a, Plcb1, Mapk8, Adora1, Bid	Sphingolipid signalling pathway	0.024129743699
	Cbl, Pik3r3, Cblb, Nck2, Egfr, Mapk3, Plcg1, Nras, Erbb3, Sos1, Camk2a, Pik3cb, Elk1, Mapk8	ErbB signalling pathway	0.026811969 2163
	Lpar1, Egfr, Gnaq, Mapk3, Nras, Sos1, Adcy3, Pdgfb, Plcb1, Prkacb, Map3k2, Gja1	Gap junction	0.026811969 2163
	Vav2, Apc, Pik3r3, Mylk2, Wasf2, Gna12, Arhgap35, Itgb3, Fgf11, Fgfr4, Itga5, Actb, Arhgef12, Egfr, Mapk3, Rdx, Nras, Sos1, Pik3cb, Pdgfb, Mylk, Pikfyve, Git1, Tmsb4x, Diap2, Abi2, Arhgef7, Ssh2, Itga3, Baiap2, Enah, Mylk4, Cdc42	Regulation of actin cytoskeleton	0.026811969 2163
	Pik3r3, Igf1, Egfr, Mapk3, Ccnd1, Plcg1, Nras, Sos1, Camk2a, Pik3cb, Pdgfb, Rb1, Calm2, E2f3	Glioma	0.000920358 458548
	Med13, Pik3r3, Ncoa3, Foxo1, Itgb3, Tsc2, Actb, Pfkfb2, Mapk3, Dio2, Med13l, Ccnd1, Plcg1, Nras, Esr1, Pik3cb, Slc16a2, Notch3, Plcb1, Prkacb, Ncoa1, Bmp4, Med1, Ncoa2, Crebbp	Thyroid hormone signalling pathway	0.002834717 1187
	Pld1, Pld2, Map3k1, Egfr, Gnaq, Mapk3, Nras, Mmp14, Sos1, Adcy3, Camk2a, Calm2, Elk1, Plcb1, Prkacb, Pla2g4a, Cdc42, Map3k2, Mapk8	GnRH signalling pathway	0.005170258 42918
	Ppap2b, Pik3r3, Slc44a1, Pld1, Pld2, Wasf2, Tsc2, Egfr, Mapk3, Plcg1, Nras, Sos1, Pik3cb, Pdgfb, Sp1, Dgkg, Pla2g4a, Dgke, Mapk8	Choline metabolism in cancer	0.007130440 74477
	Pik3r3, Eml4, Egfr, Mapk3, Ccnd1, Plcg1, Nras, Sos1, Pik3cb, Rb1, Stk4, E2f3	Non-small cell lung cancer	0.024771114 4295
	Prkag3, Prkaa2, Pik3r3, Mylk2, Ryr3, Nfatc3, Actb, Ppp3cb, Egfr, Gnaq, Gnaq, Mapk3, Ccnd1, Nras, Adcy3, Camk2a, Pik3cb, Mylk, Kcnj2, Calm2, Elk1, Plcb1, Prkacb, Pla2g4a, Mylk4	Oxytocin signalling pathway	0.043271153 4982
	Pik3r3, Ptpn11, Mapk3, Nras, Sos1, Tgfb3, Pik3cb, Pdgfb, Epas1, Ets1, Met, Cdc42, Crebbp	Renal cell carcinoma	0.043271153 4982
mmu-miR-206-3p	*Fasn, Mcat, Acsl1*	Fatty acid	8.614589082

mmu-miR-466k		biosynthesis	$34e^{-20}$
	Pank1, *Bcat1*, *Pank2*, *Pank3*	Pantothenate and CoA biosynthesis	0.002834717 1187
mmu-miR-206-3p mmu-miR-696	*Alg14*, *Mgat5*, *Stt3a*, *Man1a2*, *Man2a1*, *Man1a*, *Mgat3*, *Glt28d2*, *Dpm1*	N-glycan biosynthesis	0.005604351 47903
	Pik3r3, *Synj2*, *Cds2*, *Plcg1*, *Impad1*, *Pik3cb*, *Pikfyve*, *Calm2*, *Dgkg*, *Plcb1*, *Pik3c2a*, *Pi4k2b*, *Dgke*, *Inpp4b*	Phosphatidylinositol signalling system	0.012110228 9793
	Chsy1, *Ust*, *Chst3*, *Chst11*, *Chst14*	Glycosaminoglycan biosynthesis – chondroitin sulfate/dermatan sulfate	0.026811969 2163

4.2.4. Summary of the most relevant target pathways of BDNF within 24h of treatment

The following table shows a summary of the pathways, that are relevant to the present study, identified within 24h of BDNF treatment.

Time of treatment by BDNF	Modulated miRNAs	Target genes	Predicted Pathways	p value
1h	mmu-miR-696	*Setd2, Whsc1l1, Ehmt1*	Lysine degradation	0.00605800896603
1h	mmu-miR-696	*Alg14, Man1a2, Mgat3*	N-glycan biosynthesis	0.00605800896603
1h	mmu-miR-696	*Cds2, Plcg1, Pik3cb, Plcb1, Pik3c2a*	Phosphatidylinositol signalling system	0.0100035403622
6h	mmu-miR-146b-5p	*Pank1, Pank3*	Pantothenate and CoA biosynthesis	0.000245175351205
6h	mmu-miR-146b-5p	*Id1, Smurf2, Smad4, Sp1, Rbl1*	TGF-beta signaling pathway	0.00562877215941
6h	mmu-miR-146b-5p	*Suv39h1,Setd1b, Suv420h1*	Lysine degradation	0.00142669971241
6h	mmu-miR-146b-5p	*Pikfyve, Itpk1, Inpp4b*	Inositol phosphate metabolism	0.0275663704754
6h	mmu-miR-27a-5p	*Epn2*	Endocytosis	0.0147483273009
6h	mmu-miR-27a-5p	*Tars*	Aminoacyl-tRNA biosynthesis	0.00797573251436
24h	mmu-miR-466k, mmu-miR-696, mmu-miR-206-3p	*Fasn, Acadsb, Ptplb, Mcat, Acsl1, Cpt2, Acox3*	Fatty acid metabolism	$1.38733364574e^{-08}$
24h	mmu-miR-466k, mmu-miR-696, mmu-miR-206-3p	*Vav2, Cbl, Pik3r3, Tlr4, Cblb, Tlr2, Flnb, Igf1, Itgb3, Timp3, Itga5, Actb, Arhgef12, Egfr, Ptpn11, Mapk3, Fzd7, Rdx, Ccnd1, Plcg1, Ank3, Nras, Erbb3, Sos1, Esr1, Camk2a, Pik3cb,*	Proteoglycans in cancer	$8.51509396763e^{-07}$

		Elk1, Frs2, Fzd5, Cd44, Sdc2, Prkacb, Met, Cdc42, Sdc4, Cav2		
24h	mmu-miR-466k, mmu-miR-206-3p	*Fasn, Mcat, Acsl1*	Fatty acid biosynthesis	$8.61458908234e^{-20}$
24h	mmu-miR-466k, mmu-miR-696 mmu-miR-206-3p	*Prkag3, Prkaa2, G6pc, Pik3r3, Plk2, Foxo1, Igf1, Skp2, Irs1,Nlk,Homer3, Cat, Egfr, Mapk3, Gabarapl1, Ccnd1, Nras, Sos1, Tgfb3, Pik3cb, Ccnd2, Stk4, Bcl2l11, Homer1, Mapk8, Crebbp*	FoxO signalling pathway	0.00625564777652
24h	mmu-miR-466k mmu-miR-696 mmu-miR-206-3p	*Tram1, Ern1, Os9, Sec63, Eif2ak1, Stt3a, Ssr3, Xbp1, Edem3, Hspa4l, Pdia3, Atf6, Dnajc3, Man1a2, Man1a, Ube2g2, Sec61a1, Atxn3, Ube2g1, Uggt1, Sec24c, March6, Mapk8, Ubqln1, Dnajb12, Dnajb2*	Protein processing in endoplasmic reticulum	0.00973643196725
24h	mmu-miR-466k mmu-miR-696 mmu-miR-206-3p	*Rasa2, Map4k3, Max, Flnb, Ppm1a, Map3k1, Gna12, Il1r1, Fgf11, Rps6ka3, Fgfr4, Nfatc3, Rapgef2, Nlk, Nf1, Ppp3cb, Egfr, Mapk3, Mecom, Nras, Sos1, Map4k2, Dusp3, Tgfb3, Pdgfb, Dusp10, Elk1, Stk4, Prkacb, Pla2g4a, Atf2, Map3k7, Cdc42, Map3k2, Mapk8, Zak*	MAPK signalling pathway	0.0432711534982
24h	mmu-miR-466k mmu-miR-696 mmu-miR-	*Prkaa2, Pik3r3, Ulk2, Igf1, Rps6ka3, Irs1, Tsc2, Rictor, Mapk3, Rragd, Rragc, Pik3cb, Cab39l*	mTOR signalling pathway	0.0471528167276

	206-3p			
24h	mmu-miR-466k mmu-miR-696 mmu-miR-206-3p	*Aldh2, Kmt2c, Nsd1, Setd2, Colgalt1, Whsc1, Hykk, Whsc1l1, Ehmt1, Dot1l*	Lysine degradation	0.00158048327665
24h	mmu-miR-466k mmu-miR-696 mmu-miR-206-3p	*Vav2, Apc, Pik3r3, Mylk2, Wasf2, Gna12, Arhgap35, Itgb3, Fgf11, Fgfr4, Itga5, Actb, Arhgef12, Egfr, Mapk3, Rdx, Nras, Sos1, Pik3cb, Pdgfb, Mylk, Pikfyve, Git1, Tmsb4x, Diap2, Abi2, Arhgef7, Ssh2, Itga3, Baiap2, Enah, Mylk4, Cdc42*	Regulation of actin cytoskeleton	0.0268119692163
24h	mmu-miR-466k mmu-miR-696 mmu-miR-206-3p	*Lpar1, Egfr, Gnaq, Mapk3, Nras, Sos1, Adcy3, Pdgfb, Plcb1, Prkacb, Map3k2, Gja1*	Gap junction	0.0268119692163
24h	mmu-miR-466k mmu-miR-696 mmu-miR-206-3p	*Cbl, Pik3r3, Cblb, Nck2, Egfr, Mapk3, Plcg1, Nras, Erbb3,Sos1, Camk2a, Pik3cb, Elk1, Mapk8*	ErbB signalling pathway	0.0268119692163
24h	mmu-miR-466k mmu-miR-696 mmu-miR-206-3p	*Sptlc1, Pik3r3, Sgms2, Pld1, Pld2, Cers2, Ppp2r3a, Ppp2r2a, Gna12, Ctsd, Ppp2r5e, Smpd1, Gnaq, Mapk3, Nras, Pik3cb, Ppp2r5a, Plcb1, Mapk8, Adora1, Bid*	Sphingolipid signalling pathway	0.024129743699
24h	mmu-miR-466k mmu-miR-696 mmu-miR-206-3p	*Ptpn1, Wasf2, Lef1, Ptprb, Nlk, Actb, Egfr, Mapk3, Mllt4, Pvrl3, Baiap2, Fer, Map3k7, Met, Cdc42, Snai2, Crebbp*	Adherens junctions	0.0178019622572

24h	mmu-miR-466k mmu-miR-696 mmu-miR-206-3p	*Cbl, Arf6, Pld1, Pld2, Cblb, Arap2, Stambp, Fgfr4, Chmp3, Vps37a, Arf3, Agap1, Ehd3, Cxcr4, Egfr, Pard6g, Acap2, Zfyve9, Iqsec1, Prkci, Erbb3, Tgfb3, Git1, Vps4b, Pdcd6ip, Ap2a2, Met, Cdc42, Tfrc, Cav2, Rab5c, Dab2*	Endocytosis	0.00158048327665
24h	mmu-miR-206-3p mmu-miR-466k	*Pank1, Bcat1, Pank2, Pank3*	Pantothenate and CoA biosynthesis	0.0028347171187
24h	mmu-miR-206-3p mmu-miR-696	*Alg14, Mgat5, Stt3a, Man1a2, Man2a1, Man1a, Mgat3, Glt28d2, Dpm1*	N-glycan biosynthesis	0.00560435147903
24h	mmu-miR-206-3p mmu-miR-696	*Pik3r3, Synj2, Cds2, Plcg1, Impad1, Pik3cb, Pikfyve, Calm2, Dgkg, Plcb1, Pik3c2a, Pi4k2b, Dgke, Inpp4b*	Phosphatidylinositol signalling system	0.0121102289793

4.2.5. Target pathways of the overall miRNA profile induced by BDNF

The following table shows the target pathways identified by Diana mirpath v3.0. for all the miRNAs modulated by BDNF within 24h of treatment. The most relevant pathways for this study are highlighted in the red frames.

Pathway	P value	Target genes	microRNA
Fatty acid biosynthesis	<0,001	3	206-3p, 466k
Fatty acid metabolism	<0,001	8	206-3p, 466k, 696, 146b-5p
Lysine degradation	<0,001	13	206-3p, 466k, 696, 146b-5p
Proteoglycans in cancer	<0,001	42	206-3p, 466k, 696, 146b-5p
Glioma	<0,001	16	206-3p, 466k, 696, 146b-5p
Endocytosis	<0,001	38	206-3p, 466k, 696, 146b-5p, 27a-5p
Thyroide hormone signalling pathway	<0,001	29	206-3p, 696, 146b-5p, 466k
FoxO signalling pathway	<0,001	30	466k, 206-3p, 696, 146b-5p
Choline metabolism in cancer	0.0032	22	466k, 206-3p, 696, 146b-5p
Renal cell carcinoma	0.0037	17	466k, 206-3p, 696, 146b-5p
Adherens junction	0.0039	20	466k, 206-3p, 696, 146b-5p
Chronic myeloid leukemia	0.0045	18	206-3p, 696, 146b-5p
Pantothenate and CoA biosynthesis	0.0049	4	206-3p, 146b-5p, 466k
Protein processing in endoplasmic reticulum	0.0058	30	466k, 206-3p, 696, 146b-5p
GnRH signalling pathway	0.0058	20	466k, 206-3p, 696, 146b-5p
Regulation of actin cytoskeleton	0.0080	39	466k, 206-3p, 696, 146b-5p
Hippo signalling pathway	0.0092	29	466k, 206-3p, 696, 146b-5p
ErbB signalling pathway	0.0093	17	466k, 206-3p, 696, 146b-5p
Dorso-ventral axis formation	0.0093	9	466k, 206-3p, 696, 146b-5p
Non-small cell lung cancer	0.0096	14	466k, 206-3p, 696, 146b-5p
N-Glycan biosynthesis	0.0152	9	206-3p, 696
Endometrial cancer	0.0184	14	466k, 206-3p, 696, 146b-5p
Phosphatydilinositol signalling system	0.0184	15	206-3p, 696, 146b-5p
Thyroid cancer	0.0185	7	206-3p, 146b-5p
mTOR signalling pathway	0.0190	15	466k, 206-3p, 696, 146b
Bacterial invasion of epithelial cells	0.0234	15	206-3p, 696, 146b
Estrogen signalling pathway	0.0246	16	466k, 206-3p, 696, 146b
Prostate cancer	0.0271	19	466k, 206-3p, 696, 146b
Focal adhesion	0.0297	35	466k, 206-3p, 696, 146b
Gap junction	0.0297	13	466k, 206-3p, 696, 146b
Huntington's disease	0.0324	22	466k, 206-3p, 696, 146b

Sphigolipid signalling pathway	0.0330	22	466k, 206-3p, 696, 146b
Colorectal cancer	0.0339	13	206-3p, 696, 146b
Melanoma	0.0431	13	466k, 206-3p, 696, 146b
Glycosaminoglycan biosynthesis - chondroitin sulfate / dermatan sulfate	0.0461	5	206-3p, 696
MAPK signalling pathway	0.0472	39	466k, 206-3p, 696, 146b
Viral carcinogenesis	0.0472	29	466k, 206-3p, 696, 146b

4.2.6. Network analysis of target genes involved in the mTOR signalling

We selected the mTOR signalling for network analysis through GeneMANIA server. The mTOR signalling is indeed of particular interest because of its role in cell survival, growth, proliferation and differentiation. A crass-talk between the MAPK, that is the primary signalling activated by neurotrophins, and mTOR pathways has already been highlighted [9]. Moreover, an important role of this signalling has been highligheted in differentiation processes of sensory cells from non-sensory cells in the organ of Corti [10].

The following figure shows two interaction network diagrams of genes after inputting in GeneMANIA the 15 screened target genes involved in the mTOR signalling, as reported in the table of paragraph 4.2.5. Genes interactions are marked with different colours, reported in the figure legend. The middle circles of the second diagram represent the target genes. As expected, function analysis correlated the target genes to the mTOR signalling, comprising 11/111 genes with an FDR of $3.26e^{-11}$.

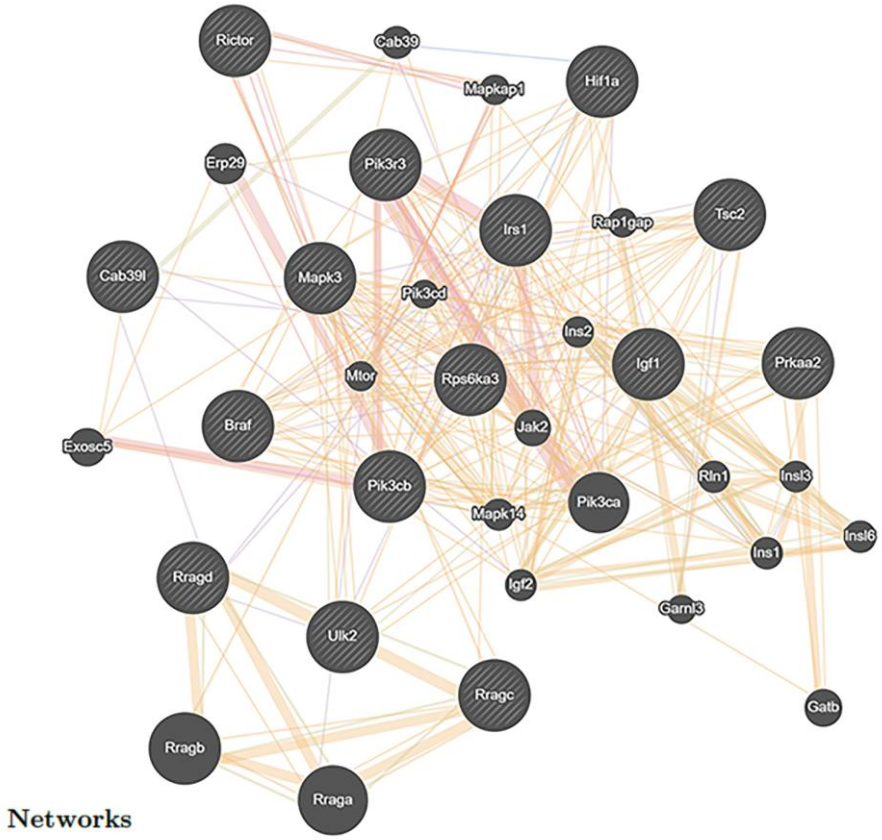

Networks

- Predicted
- Physical Interactions
- Co-expression
- Shared protein domains
- Co-localization
- Other

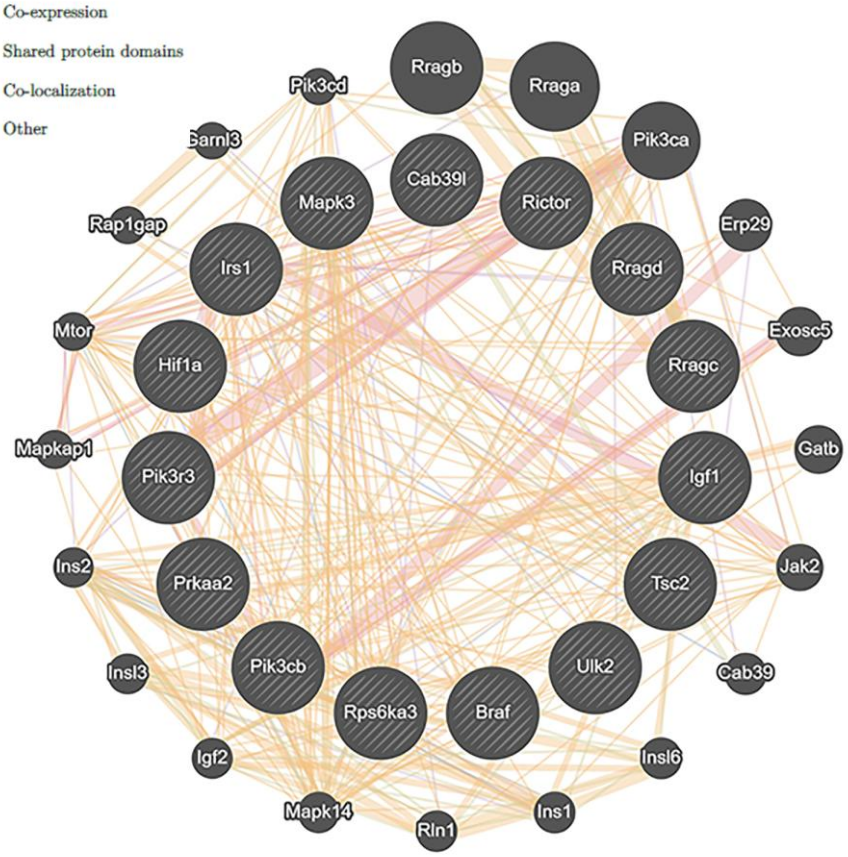

4.2.7. Analysis of selected miRNAs for each time point

For each time point the following table shows the relative quantification (RQ) (with respect to the CTRL) of the miRNAs found to be significantly modulated - or close to the statistical significance - by BDNF, together with the p values. The data showing a statistical significance (or close to 0,05) are reported in bold. Non significant data are reported as "n.s."

	1h		6h		24h	
miRNA	**RQ**	**pvalue vs CTRL**	**RQ**	**pvalue vs CTRL**	**RQ**	**pvalue vs CTRL**
rno-miR-196c-5p	**0.411**	**0.006**	0.74	n.s.	0.886	n.s.
mmu-miR-196b-5p	**0.325**	**0.082**	0.642	n.s.	1.597	n.s.
mmu-miR-1839-3p	**4.257**	**0.077**	0.792	n.s.	**5.660**	**0,068**
mmu-miR-696	**2.882**	**0,089**	1.277	n.s.	**2.156**	**0,066**
mmu-miR-27a-5p	1.353	n.s.	**4.879**	**0,029**	0.743	n.s.
mmu-miR-146b-5p	0.826	n.s.	**2.326**	**0,056**	0.778	n.s.
mmu-miR-196a-5p	0.791	n.s.	1.526	n.s.	**2.615**	**0,049**
mmu-miR-206-3p	0.626	n.s.	1.498	n.s.	**2.380**	**0,064**
mmu-miR-466k	2.843	n.s.	2.485	n.s.	**4.312**	**0,062**

Comparison between groups

The following tables show the **p values** deriving from the comparison of the expression levels of the miRNAs resulted to be significantly modulated - or close to the statistical significance - by BDNF between the different time points. The data with p<0,05 are highlighted in green; the data close to 0,05 are highlighted in yellow. Non significant data are reported as "n.s."

rno-miR-196c-5p

	1h	**6h**	**24h**
1h		0.006	0.077
6h	0.006		n.s.
24h	0.077	n.s.	

mmu-miR-196b-5p

	1h	**6h**	**24h**
1h		n.s.	0.013
6h	n.s.		n.s.
24h	0.013	n.s.	

mmu-miR-1839-3p

	1h	6h	24h
1h		0.073	n.s.
6h	0.073		n.s.
24h	n.s.	n.s.	

mmu-miR-696

	1h	6h	24h
1h		n.s.	n.s.
6h	n.s.		n.s.
24h	n.s.	n.s.	

mmu-miR-27a-5p

	1h	6h	24h
1h		0.028	n.s.
6h	0.028		n.s.
24h	n.s.	n.s.	

mmu-miR-146b-5p

	1h	6h	24h
1h		0.044	n.s.
6h	0.044		n.s.
24h	n.s.	n.s.	

mmu-miR-196a-5p

	1h	6h	24h
1h		n.s.	0.034
6h	n.s.		n.s.
24h	0.034	n.s.	

mmu-miR-206-3p

	1h	6h	24h
1h		0.002	0.013
6h	0.002		n.s.
24h	0.013	n.s.	

mmu-miR-466k

	1h	6h	24h
1h		n.s.	n.s.
6h	n.s.		n.s.
24h	n.s.	n.s.	

4.3. Comparison of the miRNA profiles between rhNGF and BDNF

miRNAs analysis between BDNF and NGF performed by Expression Suite software. The following table shows the miRNAs modulated by BDNF up to 24h of treatment in murine cochlear cells resulted to be significantly – or close to the statistical significance - compared to the miRNA profile induced by rhNGF.

Time of treatment	Set	miRNA Thermo	code	miRBase	p value
1h	A	-	-	-	-
1h	B	mmu-miR-183#	002270	mmu-miR-183-3p	0,066
6h	A	-	-	-	-
6h	B	-	-	-	-
24h	A	-	-	-	-
24h	B	hsa-miR-206	000510	mmu-miR-206-3p	0,032
		Mmu-miR-1839-3p	121203_mat	mmu-miR-1839-3p	0,053
	LEGEND	up-regulated	down-regulated		

4.3.1. Comparison after 1h of treatment

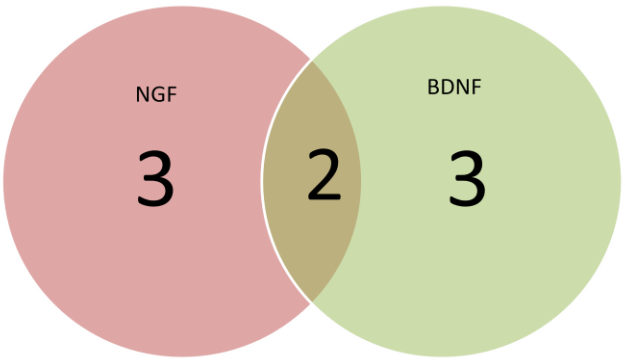

Venn diagram showing the number of miRNAs expressed by cochlear cells after 1h of NGF and BDNF treatment.

NGF	BDNF	SHARED
mmu-miR-183-3p	mmu-miR-1274-121150_mat	mmu-miR-196b-5p
mmu-miR-421-3p	mmu-miR-1839-3p	rno-miR-196c-5p
mmu-miR-206-3p	mmu-miR-696	

4.3.2. Comparison after 6h of treatment

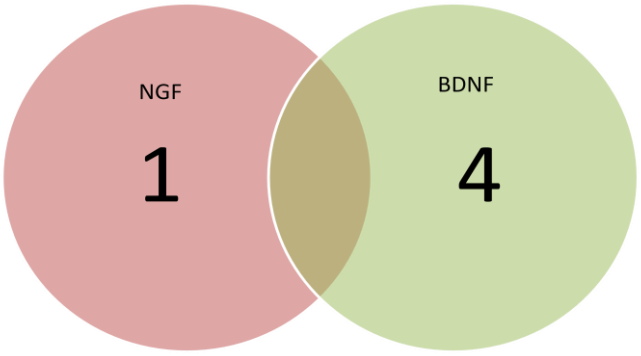

Venn diagram showing the number of miRNAs expressed by cochlear cells after 6h of NGF and BDNF treatment.

NGF	BDNF	SHARED
mmu-miR-99b-3p	mmu-miR-1937c-241011_mat	-
	mmu-miR-1937b-241023_mat	
	mmu-miR-27a-5p	
	mmu-miR-146b-5p	

4.3.3. Comparison after 24h of treatment

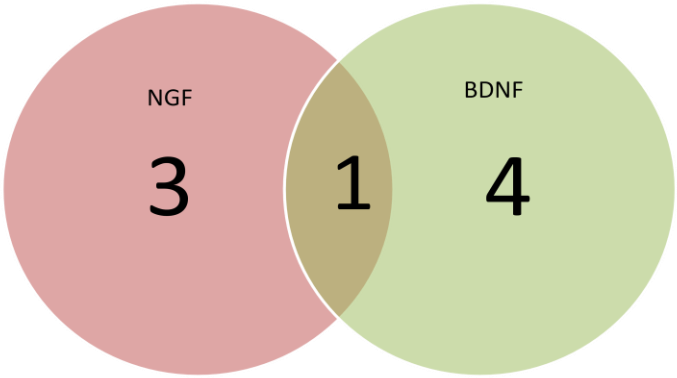

Venn diagram showing the numbers of miRNA expressed by cochlear cells after 24h of NGF and BDNF treatment

NGF	BDNF	SHARED
mmu-miR-34c-3p	mmu-miR-196a-5p	mmu-miR-466k
mmu-miR-146b-5p	mmu-miR-1839-3p	
mmu-miR-27a-5p	mmu-miR-696	
	mmu-miR-206-3p	

4.3.4. Overall miRNA profile

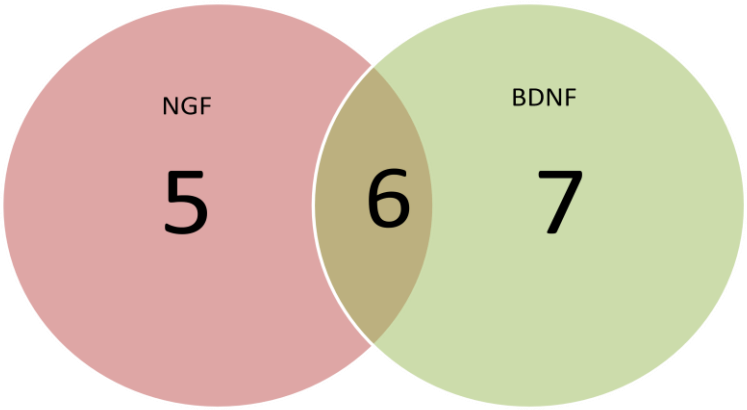

Venn diagram showing the overall number of miRNAs expressed by cochlear cells after NGF and BDNF treatment within 24h of treatment.

NGF	BDNF	SHARED
mmu-miR-183-3p	mmu-miR-1274a	mmu-miR-196b-5p
mmu-miR-421-3p	mmu-miR-1839-3p	rno-miR-196c-5p
mmu-miR-99b-3p	mmu-miR-696	mmu-miR-206-3p
rno-miR-196c-5p	mmu-miR-1937c	mmu-miR-466k
mmu-miR-34c-3p	mmu-miR-1937b	mmu-miR-146b-5p
	mmu-miR-196a-5p	mmu-miR-27a-5p
	mmu-miR-1839-3p	

4.3.5. Target pathways of the miRNAs exclusively modulated by rhNGF

The following table shows the target pathways identified by Diana mirpath v3.0. for the miRNAs modulated exclusively by rhNGF within 24h of treatment (Paragraph 4.4.).

KEGG pathway	p-value	genes	miRNAs
Glycosaminoglycan biosynthesis - heparan sulfate / heparin	0.013141064	1	34c-3p
Fat digestion and absorption	0.013141064	2	421-3p
Glycosaminoglycan biosynthesis - keratan sulfate	0.015357693	1	421-3p
Estrogen signaling pathway	0.015357693	4	99b-3p, 421-3p
Retinol metabolism	0.017533978	4	421-3p

4.3.6. Target pathways of the miRNAs exclusively modulated by BDNF

The following table shows the target pathways identified by Diana mirpath v3.0. for the miRNAs modulated exclusively by BDNF within 24h of treatment (Paragraph 4.4.).

KEGG pathway	p-value	#genes	#miRNAs
Lysine degradation	0.006058009	3	696
N-Glycan biosynthesis	0.006058009	3	696
Glioma	0.006058009	5	696
Phosphatidylinositol signaling system	0.01000354	5	696
Thyroid hormone signaling pathway	0.01000354	8	696
Renal cell carcinoma	0.02298337	5	696

4.3.7. Target pathways of the shared miRNAs

The following table shows the target pathways identified by Diana mirpath v3.0. for the miRNAs modulated by both rhNGF and BDNF within 24h of treatment (Paragraph 4.4.). The most relevant pathways for this study are highlighted in the red frames.

KEGG Pathway	p-value	genes	miRNAs
Fatty acid biosynthesis	<0,001	3	206-3p, 466k
Proteoglycans in cancer	<0,001	39	206-3p, 466k,146b-5p
Lysine degradation	<0,001	12	206-3p, 466k,146b-5p
Fatty acid metabolism	<0,001	7	206-3p, 466k,146b-5p
Endocytosis	<0,001	35	206-3p, 466k,146b-5p,27a-5p
Adherens junction	0.0022	19	206-3p, 466k,146b-5p
Pantothenate and CoA biosynthesis	0.0025	4	206-3p, 466k,146b-5p
FoxO signalling pathway	0.0025	26	206-3p, 466k,146b-5p
Thyroide hormone signalling pathway	0.0025	24	206-3p, 466k,146b-5p
Glioma	0.0025	13	206-3p, 466k,146b-5p
Dorso-ventral axis formation	0.0056	9	206-3p, 466k,146b-5p
Choline metabolism in cancer	0.0063	19	206-3p, 466k,146b-5p
Chronic myeloid leukemia	0.0066	16	206-3p, 146b-5p
GnRH signalling pathway	0.0086	18	206-3p, 466k,146b-5p
Thyroid cancer	0.0098	7	206-3p, 146b-5p
ErbB signalling pathway	0.0121	15	206-3p, 466k,146b-5p
Huntington's disease	0.0121	21	206-3p, 466k,146b-5p
Regulation of actin cytoskeleton	0.0136	34	206-3p, 466k,146b-5p
Bacterial invasion of epithelial cells	0.0165	14	206-3p, 146b-5p
Endometrial cancer	0.0182	13	206-3p, 466k,146b-5p
Non-small cell lung cancer	0.0185	13	206-3p, 466k,146b-5p
Protein processing in endoplasmic reticulum	0.0194	26	206-3p, 466k,146b-5p

Estrogen signalling pathway	0.0310	14	206-3p, 466k,146b-5p
Hippo signalling pathway	0.0344	24	206-3p, 466k,146b-5p
Renal cell carcinoma	0.0371	14	206-3p, 466k,146b-5p
Prostate cancer	0.0401	17	206-3p, 466k,146b-5p
Gap junction	0.0403	11	206-3p, 466k,146b-5p

5. Discussion

Pathways related to neuronal differentiation

- *Synaptic vesicles cycle*

The synaptic vescicles cycle signaling was associated with mmu-miR-183-3p. mmu-miR-183-3p resulted to be specifically modulated by rhNGF. Particularly, it was down regulated soon after stimulation (1h) compared to the control (p=0.025) and compared to BDNF (p=0.66), and it was progressively up-regulated up to 24h of treatment. One of the target gene of mmu-miR-183-3p is Cltc (Clathrin heavy chain 1).

	miRNAs significantly different from CTRL	
	NGF	BDNF
1h	✔	
6h		
24h		
all		

Clathrin is known to be a key component involved in the endocytosis pathway. Since its discovery, several studies have unveiled the multiple roles of chlatrin-mediated traffiking such as signaling, development, neuronal transmission, infection, immunity and genetic disorders [11]. Clathrin is also important for the synaptic vesicles cycle. Indeed, neurotransmitter release is mediated by exocytosis of synaptic vesicles at the presynaptic active zone. To support rapid and repeated rounds of release, synaptic vesicles undergo a trafficking cycle involving clathrin. It is known that NGF binding to TrkA enhances neurotransmitter release by increasing the number of Ca(2+)-responsive secretory vesicles [12]. The endocytic retrieval from the plasma membrane occurs by clathrin-dependent mechanisms and results in the formation of clathrin-coated vesicles [13]. Therefore, the down-regulation of mmu-miR-183-3p suggests that there is an increase in the expression of Cltc due to NGF stimulation.

Lysosome

The “lysosome” pathway was identified for mmu-miR-183-3p due to its target gene Cltc as fully described in the “synaptic vescicles cycle” section.

	miRNAs significantly different from CTRL	
	NGF	BDNF
1h	✔	
6h		
24h		
all		

In addition to the synaptic vescicle cycle and endocytosis, clathrin-based endocytosis is involved in lysosomal degradation and/or recycling to the plasma membrane [14]. A previous study on PC12 cells demonstrated that lysosome-mediated degradation of caspase 3 is a protective effect carried out by NGF to inhibit apoptosis and promote cell survival [15].

Pathways stimulating cell proliferation

- *Cell cycle*

The "cell cycle" pathway was associated with mmu-miR-183-3p, whose modulation is described in the "synaptic vesicles cycle" section. In fact, another target gene of mmu-miR-183-3p is Bdf4, which encodes for the Dbf4 zinc finger protein.

	miRNAs significantly different from CTRL	
	NGF	BDNF
1h	✔	
6h		
24h		
all		

Dbf4 zinc finger protein is a fundamental regulator of the cell cycle. Specifically, it is an activator of Cell division cycle 7-related protein kinase (CDC7). The Cdc7/Dbf4 complex allows the initiation of DNA replication in mitosis (phase S) [16]. Cell cycle and its control is essential for the proper development of organs, including the nervous system [17] and the cochlea [18]. It is known that NGF promotes cell proliferation [19][20] and its arrest [21][22], and is necessary in a variety of cell types. Hence, NGF plays a key role in the control of the cell cycle. On this basis, the down-regulation of mmu-miR-183-3p by NGF treatment could lead to

an increase in Dbf4 protein and, consequently, to an increase in cell proliferation. This is in accordance with the well known effects of NGF in promoting cell survival [23].

- *ErbB signaling pathway*

The "ErbB signaling pathway" was identified for rhNGF and BDNF after 24h of stimulation.

	miRNAs significantly different from CTRL	
	NGF	BDNF
1h		
6h		
24h	✔	✔
all	✔	✔

The ErbB family contains four receptor tyrosine kinases (RTKs) related to the epidermal growth factor receptor (EGFR). As the other RTKs, ErbB receptors play an important role in the control of most fundamental cellular processes including the cell cycle, cell migration, cell metabolism and survival, as well as cell proliferation and differentiation [24]. Moreover, it was suggested that EGF receptors can be activated by a "lateral propagation" initiated by local receptor activation or by cell adhesion [25]. An *in vivo* study demonstrated that the supporting cells of the vestibular sensory epithelium contribute to vestibular synapse formation and that this is mediated by reciprocal signals between sensory neurons and supporting cells involving ErbB and BDNF [26]. Even more interesting, NGF induced the down-regulation of EGFR in PC12 cells and this event could be a way to desensitize the cells from proliferative stimuli, while promoting NGF-induced neuronal differentiation [27],[28].

- *Hippo signaling pathway*

The "hippo signalling" was identified for the overall miRNA profile of both rhNGF and BDNF.

	miRNAs significantly different from CTRL	
	NGF	BDNF
1h		
6h		
24h		
all	✔	✔

The Hippo pathway drives gene expression programs that control cell proliferation, cell migration and invasion. The Hippo signaling also controls cell growth, organ size, proliferation and death. Moreover, several data indicate that the actin cytoskeleton [29] and cell junctions [30] are key mediators of the regulation of the Hippo signaling, in accordance with the other KEGG pathways resulted to be modulated by NGF and BDNF in this study. Recently, Xinyuan Yang and co-workers have identified a crosstalk between the NGF-TrkA and the Hippo signalling pathway. Although this study was focused on cancer, it showed that the suppression of TrkA inhibited the Hippo-mediated proliferation and migration of distinct cancer cell lines, indicating that the activation of NGF-TrkA signalling is involved in hippo-induced cell proliferation and migration [31]. A crosstalk between BDNF-TrkB and the Hippo signaling was also shown. In particular, aged cardiac microvascular endothelial cells were prompted to migrate through the activation of Hippo signaling due to TrkB stimulation by BDNF [32].

- *Multiple cancer pathways*
  e.g. miRNAs in cancer

Several cancer pathways were associated with the miRNA profiles deriving from NGF and BDNF treatment in cochlear cells. The shared feature of those pathways was the induction of cell proliferation mainly through the MAPK signaling. An example of these pathways is the "miRNAs in cancer" pathway, that is related to a single miRNA that was found down-regulated by both treatments: mmu-miR-196b-5p. Mmu-miR-196b-5p resulted to be down-regulated after 1h by both rhNGF and BDNF. Thereafter mmu-miR-196b-5p was progressively up-regulated by both treatments up to 24h. mmu-miR-196b-5p was related to "microRNAs in cancer" pathway by Diana mirpath v.3. due to its target gene "Igf2bp1". Igf2bp1 encodes for the β-actin mRNA zipcode binding protein 1 (ZBP1).

Igf2bp1 is associated with epithelial ovarian cancer and it is generally considered an oncogene, due to its role in promoting cell proliferation [33]. Although Igfbp1 was associated with the epithelial ovarian cancer by Diana mirpath, the down-regulation of mmu-miR-196b-5p suggests an up-regulation of Igfbp1 soon after BDNF or NGF treatment in cochlear cells, possibly promoting cell growth and differentiation. In fact, in neuronal development, Igfbp1 regulates the neurite outgrowth, neuronal cell migration, and axonal guidance, by controlling the spatiotemporal activation of protein synthesis [34]. It is also involved in controlling neuronal differentiation and matured neuronal system during regeneration [35][36]. There

are no published studies which elucidate the role of Igf2bp1 specifically in the cochlea. Sasaki and co-workers demonstrated that brain-derived neurotrophic factor (BDNF) signals the Src-dependent phosphorylation of Igf2bp1, which is necessary for β-actin synthesis and growth cone turning in developing neurons [37]. There are no published studies which correlate NGF with Igf2bp1.

Mineral absorption

The "mineral absorption" pathway was associated with mmu-miR-183-3p, whose modulation is described in the "synaptic vesicles cycle" section. In fact, another target gene of mmu-miR-183-3p is Mt2, which encodes for the Metallothionein-2.

	miRNAs significantly different from CTRL	
	NGF	BDNF
1h	✔	
6h		
24h		
all		

A previous role of metallothioneins was associated with the zinc metabolism. Today, it is known that metallothioneins cover a wide range of functions, including biological processes such as apoptosis and the regulation of neuronal outgrowth [38]. Even if there are no specific studies about the role of Mt2 in the cochlea, it was demonstrated that metallothionein-1a is overexpressed in cochlear cells of newborn rats following oxidative stress [39], suggesting that metallothioneins could have a role in the response to ototoxicity.

Fatty acids signalings

- *Fatty acid metabolism*
- *Fatty acids biosynthesis*

The "fatty acid metabolism" resulted to be a recurrent pathway associated with the miRNAs modulated both by rhNGF and BDNF, always with a p-value<0.001. The fatty acid biosynthesis was also identified for the miRNAs modulated by rhNGF and BDNF after 1h and 24h respectively. Moreover, fatty acids metabolism and synthesis are the most probable KEGG pathways identified by Diana mirpath for the overall microRNA profile induced by BDNF.

	miRNAs significantly different from CTRL	
	NGF	BDNF
1h	✔	
6h		
24h		✔
all	✔	✔

Fatty acids have been shown to be fundamental for growth of neurite processes from the cell body in nervous cells [40]. Moreover, it was shown that brain's energy is provided by mitochondrial oxidation of fatty acids and it was suggested that under conditions of neuronal excitation, both fatty acid and glucose (considered the first source of energy in the nervous system) metabolic pathways may exist simultaneously [41]. NGF was shown to be an effective regulator of fatty acid metabolism in PC12 cells [42]. In schizophrenic patients fatty acids levels have significant associations with BDNF levels [43]. It has also been suggested that decreased BDNF and altered metabolism of polyunsatured fatty acids could be associated with autism [44]. Based on the importance that fatty acids have in the nervous system in promoting neurite outgrowth [40,41,43], it is possible that the modulation of the miRNAs, involved in those pathways, could be related to cellular differentiation induced by rhNGF and BDNF.

Amino-acids signalings

- *Lysine degradation pathway*
- *Valine, leucine and isoleucine degradation*

The "lysine degradation" pathway resulted to be a recurrent pathway for the miRNAs modulated both by rhNGF and BDNF, always with a p-value<0.001. The "valine, leucine and isoleucine degradation" pathway was identified for the miRNAs modulated by BDNF after 1h and 24h of stimulation.

	miRNAs significantly different from CTRL	
	NGF	BDNF
1h	✔	✔
6h	✔	✔
24h	✔	✔
all	✔	✔

Lysine is an essential amino acid in humans. It is catabolized through the saccharopine pathway in liver mitochondria, leading to the production of acetyl-CoA. Defects involved in the lysine degradation pathway are associated with a neuro-metabolic pathology known as hyperlysinemia [45]. Leucine plays multiple functions in the nervous system. It is a metabolic precursor of fuel molecules, alpha-ketoisocaproate and ketone bodies. Leucine also participates in the maintenance of the nitrogen balance in the glutamate/glutamine cycle pertinent to the neurotransmitter glutamate and it is a major regulator of the activity of some enzymes important for brain energy metabolism [46]. Valine, leucine and isoleucine, constitute the group of branched-chain amino acids and are rapidly taken up into the brain parenchyma, where they serve several distinct functions including brain energy metabolism. In general, the amino acids play a critical role in neural function, including neurotransmission, neuromodulation, cellular metabolism, and protein construction.

FoxO signaling pathway

The "FoxO signaling pathway" was identified as target of both rhNGF and BDNF at multiple time points.

	miRNAs significantly different from CTRL	
	NGF	BDNF
1h	✔	
6h		
24h	✔	✔
all	✔	✔

Foxo signaling exerts a wide number of effects in cellular processes. In recent years mammalian FoxO transcription factors have arisen as crucial regulators of cell fate and function in the nervous system. FoxOs can trigger either neuronal apoptosis or survival in response to several type of stress. For example, Foxo proteins are effectors in mediating TGF-β signaling, leading to cell cycle arrest [47]. On the other side, it was demonstrated that FoxO signaling mediates neuronal plasticity [48]. The relevance of this signaling pathway was first shown in PC12-derived cells and in primary cultured sympathetic spinal cord neurons, in which the overexpression of FoxO signaling was associated with cell death [49]. It is well known that, in response to neurotrophic factors, AKT is activated and it phosphorylates FoxOs [50]. Recently, it has been demonstrated that NGF deprivation induces the up-regulation of the FoxO–related proteins, which in turn induce cell death in sympathetic neurons [51]. On this basis, we can conclude that the modulation of the FoxO signaling occurs also through several miRNAs as shown in this study.

Pathways invoving the cytoskeleton and cell junctions

- *Adherens junctions*

The "Adherens junctions" signaling was identified for both rhNGF and BDNF after 1h and 24h of treatment respectively.

	miRNAs significantly different from CTRL	
	NGF	BDNF
1h	✔	
6h		
24h		✔
all	✔	✔

Adherens junctions are protein complexes that constitute cell–cell junctions in epithelial and endothelial tissues linked to the actin cytoskeleton. They are fundamental regulators of cortical development [52]. Moreover, together with the tight junctions, they are essential in maintaining the correct structure of the blood brain barrier (BBB) [53], as well as of the blood-labyrinth barrier (BLB) [54]. Adherens junctions also contribute to the control of cell polarity, neuronal morphogenesis, growth cone guidance and migration during development [55]. It was previously demonstrated that in PC12 cells cultured on 3-dimensional substrata,

NGF supplementation induced the formation of networks of small aggregates interconnected by process-bearing cells [56].

- *Regulation of actin cytoskeleton*

The "regulation of actin cytoskeleton" pathway was associated with the overall miRNA profile induced by rhNGF and BDNF (5 miRNAs) and after 24h of stimulation by BDNF.

	miRNAs significantly different from CTRL	
	NGF	BDNF
1h		
6h		
24h		✔
all	✔	✔

Actin is a cytoskeletal protein that plays a key role in both the guidance and the maintenance of neuronal polarity. Actin structures spread along neuronal axons, dendrites and dendritic spines [57]. Reorganization of actin cytoskeleton is also a fundamental event occurring during cell proliferation as well as during differentiation, synaptogenesis and neuronal plasticity [58]. Moreover, cochlear hair cells present actin-based microvilli on the apical membrane, referred to as stereocilia, which allow to convert the sound-induced vibrations to electrical signals through mechanic-transduction. In fact, the deflection of the stereocilia leads to the mechanical opening of ion channels and cell depolarization. Actin stereocilia are structured as actin-bundling and can be classified in three major classes: villin, fimbrins/plastins and espins. Due to their fundamental role in cochlear hair cells, mutations in genes that encode for actin proteins lead to deafness [59]. The regulation of actin cytoskeleton is one of the pathways known to be regulated by Trk activation. Moreover, phosphorylation of synapsins by MAP kinase has been shown to regulate their interactions with the actin cytoskeleton, so that the MAP kinase cascade may potentiate synaptic transmission by releasing synaptic vesicles from the cytoskeleton [60]. Moreover, it has been demonstrated that NGF promotes collateral branching along sensory axons by increasing the emergence of axonal filopodia through the formation of filopodial precursors termed axonal actin patches. During branch formation, NGF regulates both the actin and microtubule cytoskeleton [61][62].

- *Gap junction*

The "gap junction" signaling is a target pathway of BDNF after 24h of stimulation.

	miRNAs significantly different from CTRL	
	NGF	BDNF
1h		
6h		
24h		✔
all		✔

The mammalian cochlea is a highly organized sensory organ for hearing composed of auditory hair cells and supporting cells. Cochlear supporting cells are electrically and metabolically coupled by gap junction channels. In contrast, gap junctions are not found between the sensory cells (inner and outer hair cells), or between sensory and non-sensory cells in mammals [63].

- *Focal adhesion*

The "focal adhesion" was predicted for the overall miRNA profile induced by BDNF.

	miRNAs significantly different from CTRL	
	NGF	BDNF
1h		
6h		
24h		
all		✔

Proper focal adhesion regulation is fundamental in order to allow a variety of cellular activities, including cell motility, proliferation, and differentiation. In fact, focal adhesion kinase, which is a key regulator of this process, has been found to be also involved in the effects due to BDNF stimulation [64],[65].

Endocytosis

The "endocytosis" pathway was identified for both rhNGF and BDNF treatments. Specifically, 7/9 of the microRNAs significantly modulated by rhNGF and 5/11 microRNAs significantly

modulated by rhBDNF were associated with endocytosis pathway, targeting 36 and 38 genes respectively. The pvalue for the endocytosis pathway was <0.001 for both neurotrophins.

	miRNAs significantly different from CTRL	
	NGF	BDNF
1h	✔	
6h		✔
24h		✔
all	✔	✔

Endocytosis is a cellular process which mediates material internalization by the formation of a vesicle containing the ingested material. It is essential in a variety of cellular processes [66]. A previous study demonstrated that in PC12 cells, NGF signaling through TrkA induced a general increase in clathrin-mediated membrane trafficking [67]. Moreover, after NGF treatment, NGF was bound to TrkA in endocytic organelles, and TrkA was tyrosine-phosphorylated and bound to PLC-gamma1, suggesting that these receptors were competent to initiate signal transduction [68]. Previous studies also demonstrated an increased endocytosis due to TrkA activation by NGF [68]. Moreover, a specialized NGF signaling system is initiated in distal axons and is axonally propagated back to the soma through a vesicular mechanism mediated by endosomal vesicle containing NGF, its receptor and associated signaling effectors [69]. Endocytosis is a also a process triggered by BDNF in order to induce TrkB internalization but also to regulate synaptic plasticity [70].

Neurotrophin signaling pathway and MAPK signalling

The correlation with the neurotrophin signaling pathway was identified for rhNGF after 6h of stimulation due to the down-regulation of mmu-miR-99b-3p, whose modulation was close to the statistical significance (p=0.062). The MAPK signaling, that is activated after Trk binding by NGF and BDNF, resulted to be modulated by BDNF after 24h of treatmentAlso the MAPK signaling alone was predicted for both treatments.

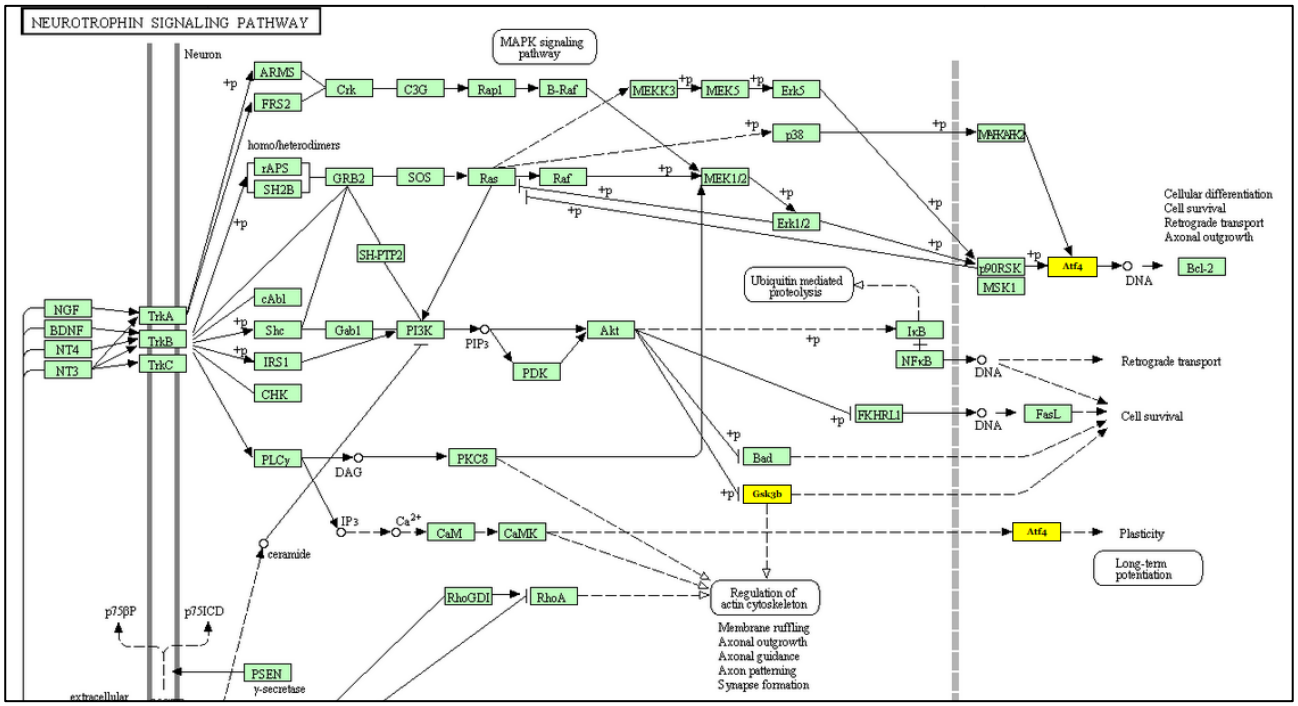

KEGG pathway related to mmu-miR-99b-3p

	miRNAs significantly different from CTRL	
	NGF	BDNF
1h		
6h	✔	
24h		✔
all		

The signaling mediated by rhNGF and BDNF plays a fundamental role in the nervous system as well as in the cochlea.

BDNF is an essential neurotrophic factor during development in the ear, as the knock down of its receptor resulted in alterations of ear maturation in mice. In the cochlea BDNF is physiologically expressed by the mechanosensory hair cells and by the surrounding supporting cells. The expression of BDNF by these cell types has been demonstrated to be fundamental both for the development and maintenance of the spiral ganglion neurons (SGNs). In fact, the degeneration of hair cells is inexorably associated with BDNF reduction, leading to subsequent SGNs degeneration. Therefore, the main studies involving the use of BDNF for the treatment of sensorineural hearing loss focus on the neuroprotection of SGNs as a strategy to improve the performance of cochlear implantations [71]. For these reasons BDNF is considered a major possible therapeutic approach to counteract sensorineural

hearing loss. Several experimental studies have been conducted to evaluate the neuroprotective effects of BDNF in cochlear neurodegenerative diseases.

Unlike BDNF, NGF is not required for the development of the inner ear. In fact, several studies have demonstrated that TrkA is not expressed in the ear during the development, suggesting that NGF is not necessary. This was confirmed by the development of transgenic animals, lacking the expression of NGF, which correctly developed the inner ear [72]. Conversely, NGF has been demonstrated to be a key player in the maintenance and survival of the post-natal ear. Accordingly, the immunolocalization of the TrkA receptor in the mouse inner ear revealed that there is not TrkA immunoreactivity during gestation, while TrkA immunolabeling progressively increases starting from post-natal day 12 up to adulthood in mice [73]. NGF could be involved in efferent cochlear innervations in post-natal ear [74]. All these findings suggest a major role of NGF in promoting cell survival and neuroprotection in the ear once it has matured, rather than promoting its development.

TGF- β signaling pathway

The TGF-beta signaling pathway was identified for rhNGF and BDNF after 24h and 6h of stimulation respectively.

	miRNAs significantly different from CTRL	
	NGF	BDNF
1h		
6h		✔
24h	✔	
all		

The "TGF-β signaling" is necessary for several important functions of the nervous system, such as differentiation and survival [75]. One of the well-studied functions of TGF-β is its cytostatic effect. The growth inhibitory effect of TGF-β is related to the cell-cycle arrest in a variety of cultured cell types. TGF-β suppresses the expression of several key transcription factors regulating growth control including the growth-promoting transcription factor c-Myc and cell differentiation inhibitor Id1 [47]. Among the target genes, RBI1 and Sp1 are key regulators of the cell cycle arrest also involved in TGF-β signalling. Another target gene, Smad4, encodes for a key protein of the TGF-β signalling. In particular it interacts with other SMAD proteins and forms a protein complex, which then moves to the cell nucleus, where

controls the activity of particular genes and regulates cell growth and division [76]. In the cochlea, TGF- β expression is finely regulated in order to allow proper development [77]. It was demonstrated that neurotrophic factors and TGF- β act in synergy to promote cell survival of spiral ganglion cells in the cochlea [78].

Metabolic pathways

- *Pantothenate and CoA biosynthesis*

The "Pantothenate and CoA biosynthesis" signaling was identified for rhNGF after 24h of treatment and for BDNF after 6h and 24h of stimulation.

	miRNAs significantly different from CTRL	
	NGF	BDNF
1h		
6h		✔
24h	✔	✔
all		✔

BDNF and NGF could mediate the modulation of metabolic signalings in order to regulate energy metabolism to promote cell growth and survival. Not surprisingly, several data indicate that NGF and BDNF can modulate energy metabolism [79]. Pantothenate is vitamin B_5 and is the key precursor for the biosynthesis of coenzyme A (CoA). CoA is an essential cofactor for cell growth and is involved in many metabolic reactions, including the synthesis of phospholipids, synthesis and degradation of fatty acids, and the operation of the tricarboxylic acid cycle [80]. Acetyl-CoA also allows to obtain ATP through the citrate cycle, being therefore fundamental for the energy metabolism [81]. Moreover, a previous study demonstrated that Panthothenate and CoA protect the cochlea from cysplantin-induced ototoxicity in guinea pigs [82]. A previous study showed that cytoplasmic acetyl-CoA levels were increased by NGF in cholinergic neuroblastoma cells [83].

Protein processing in endoplasmic reticulum (ER)

The "protein processing in endoplasmic reticulum" pathway was identified for the overall miRNA profile induced by rhNGF and BDNF and after 24h of stimulation by BDNF.

	miRNAs significantly different from CTRL	
	NGF	BDNF
1h		
6h		
24h		✔
all	✔	✔

ER stress-induced neuronal death plays a pivotal role in several neurodegenerative diseases. The final step of ER stress-induced neuronal death is the activation of C/EBP homologous protein (CHOP), which leads to apoptosis in several neurodegenerative disorders. For example, the CHOP gene is induced by parkinsonism-inducing neurotoxins [84]. Another study also showed that CHOP is a critical mediator of apoptotic death in the substantia nigra dopamine neurons in an animal model of parkinsonism [85]. The transcriptional up-regulation program in response to ER stress is conducted by three distinct types of ER stress transducers localized on the ER membrane, namely, PERK, ATF6 and IRE1. The role of NGF in inhibiting ER stress is widely documented in the literature. Remarkably, it has been demonstrated that NGF attenuates high glucose-induced ER Stress, preventing Schwann cell apoptosis through the activation of the PI3K/Akt/GSK3β and ERK1/2 Pathways [86]. Another study showed that NGF improved functional recovery by inhibiting endoplasmic reticulum stress-induced neuronal apoptosis in rats with spinal cord injury [87]. Several data indicate that also BDNF prevents ER stress [72],[73]. Remarkably, an *in vitro* study on cerebral cortical neurons showed that BDNF treatment was able to prevent ER stress-induced cell death through the PI3-K signaling and suppressing the activation of caspase-12 [89].

Huntington's disease

The Hungtington's disease pathway was predicted for the overall miRNA profile of both rhNGF and BDNF.

	miRNAs significantly different from CTRL	
	NGF	BDNF
1h		
6h		
24h		
all	✔	✔

Huntington's disease (HD) is a neurodegenerative disorder due to an abnormal expansion of polyglutamine repeats in the first exon of huntingtin gene, leading to deleterious effects in nervous cells [90]. Patients can also undergo hearing impairment mainly due to elevated levels of ROS [91]. A previous study showed that BDNF-TrkB interaction induces the regulation of Huntingtin-associated protein 1 (HAP1), which is a key protein involved in the Huntington's disease. In particular, HAP1 is involved in trafficking of vesicles intracellularly and also interacts with several membrane proteins including TrkB. This important evidence suggests that HAP1 may play a key role in BDNF signaling and its receptor endocytosis and may promote neuronal survival and proliferation [92]. Moreover, BDNF has been shown to be effective in ameliorating symptoms in several studies in preclinical models of Huntington's disease [93]. Some data indicate that also NGF could be effective in the management of HD patients. A previous study showed that NGF might protect against neuronal death by inhibiting the production of nitric oxide and decreasing the levels of superoxide radicals [94]. More recently, it was demonstrated that intracerebral injections of NGF rescued hippocampal cholinergic neuronal markers, restored neurogenesis, and improved spatial working memory in a mouse model of HD [95].

Glycans signalings

- *N-glycans biosynthesis*
- *Glycosaminoglycan biosynthesis – chondroitin sulfate/dermatan sulphate*
- *Proteoglycans in cancer*

The "N-glycan biosynthesis" signaling was identified for BDNF after 1h and 24h of stimulation. "Glycosaminoglycan biosynthesis – chondroitin sulfate/dermatan sulphate" signaling was predicted for BDNF after 24h of stimulation. The pathway "proteoglycans in cancer" was predicted for the miRNAs modulated by rhNGF after 1h of stimulation, and for the miRNAs modulated by BDNF after 24h of treatment. Among the shared miRNAs of the two treatments,

mmu-miR-206-3p,mmu-miR-466k,mmu-miR-146b-5p were associated with the pathway proteoglycans in cancer, involving 39 genes and with a pvalue<0,001.

	miRNAs significantly different from CTRL	
	NGF	BDNF
1h	✔	✔
6h		
24h		✔
all	✔	✔

N-glycans are critical for proper protein folding and quality control by chaperones in the endoplasmic reticulum (ER). More recently, N-glycans have been shown to modulate the function of many cell surface proteins involved in migration, adhesion and myelination [96]. N-glycans are also critical for the proportion of receptors expressed on the cell surface or for the retrograde transport of protein complexes between ligand and receptor. However, it has been demonstrated that N-glycans can also modulate the exocytotic transport and secretion of proteins with pathological effects such as amyloid or prion proteins [97]. On this basis, N-glycan-related pathways are studied as possible target for different pathological conditions of the nervous system [96]. Moreover, Glycosaminoglycans, have been shown to modulate axonal outgrowth in neural tissue [98]. Ihara and co-workers demonstrated that increased levels of N-glycans in PC12 cells correlate with inefficient neurite outgrowth following NGF treatment. In particular, the authors overexpressed N-acetylglucosaminyltransferase III, that is a fundamental enzyme involved in N-glycan biosynthesis. Its up-regulation increased N-glycans levels and impaired neurite outgrowth when PC12 cells were treated with NGF [99]. On the other hand, the immature BDNF form (proBDNF) carries an unusual type of N-glycans important for its processing and secretion [100]. Finally, proteoglycans control numerous normal and pathological processes, such as morphogenesis, tissue repair, inflammation, vascularization and cancer metastasis. Altered expression of proteoglycans on tumor and stromal cell membranes affects cancer cell signaling, growth and survival, cell adhesion, migration and angiogenesis [101]. Regardless of their role in cancer pathogenesis, proteoglycans cover important roles in the nervous system too. For example, proteoglycans have a pivoltal role in determining neuronal migration in the cerebral cortex during development [102]. They are also actively involved in axon guidance through the interaction

between signaling molecules and glycosaminoglycan chains [103]. Keratan sulfate (KS)-proteoglycans form perineuronal nets, that are dynamic neuroprotective structures with anti-oxidant properties, and are involved in neural differentiation, development and synaptic plasticity [104]. Proteoglycans are also important regulators of development and maturation of the cochlea [105]. Chondroitin sulfate proteoglycans (CSPGs) are required for proper maturation of axonal connections in the cochlea [106]. NGF induces hypersecretion and hypersulfation of neuroblastoma proteoglycans [107]. Another study highlighted structural changes in proteoglycans during the neuritogenesis of PC12 cells following NGF stimulation [108]. Interestingly, it was demonstrated that CSPGs dephosphorylate the BDNF high affinity receptor TrkB in embryonic cortical neurons *in vitro*. As a consequence, CSPGs inhibited the effects of BDNF, specifically by eliminating existing dendritic spines [109].

Inositol signalings

- *Phosphatidylinositol signaling system*
- *Inositol phosphate metabolism*

The inositol-related signalings resulted to be the target KEGG pathways of the miRNAs modulated by BDNF at each time point of stimulation.

	miRNAs significantly different from CTRL	
	NGF	BDNF
1h		✔
6h		✔
24h		✔
all		✔

After TrkB and TrkA binding by BDNF and rhNGF respectively, different signaling cascades can be activated. Among these, phosphatidylinositol trisphosphate (IP3) plays a crucial role in driving some cellular responses, such as activation of several enzymes. IP3 can be generated by Phosphoinositide phospholipase C (PLCγ), which hydrolyses PIP_2 to IP3 and diacylglycerol (DAG),or by PI3-kinases (PI3K) [70]. In particular, mmu-miR-696 is associated with the phosphatidylinositol signaling system and it resulted to be up-regulated after 1h of BDNF treatment. In particular, the target genes of mmu-miR-696 are specifically involved in the generation of IP3. For example Cds2 encodes for Phosphatidate cytidylyltransferase 2 enzyme, which regulates the amount of phosphatidylinositol available for signalling; Plcg1

and Plcb1 encode for Phospholipase C gamma 1 and 1-Phosphatidylinositol-4,5-bisphosphate phosphodiesterase beta-1 respectively; Pik3cb and Pik3c2a encode for hosphatidylinositol-4,5-bisphosphate 3-kinase and Phosphatidylinositol-4-phosphate 3-kinase C2 domain-containing alpha polypeptide respectively, belonging to the PI3K family .

Pathways involving RNAs

- *Aminoacyl-tRNA biosynthesis*

The "Aminoacyl-tRNA biosynthesis" pathway was identified for BDNF after 6h of treatment. Particularly, this is a target KEGG pathway of mmu-miR-27a-5p through the Tars gene.

	miRNAs significantly different from CTRL	
	NGF	BDNF
1h		
6h		✔
24h		
all		

Aminoacyl-tRNAs are essential substrates which determine the translation of the genetic code in amino acids. Indeed, they match amino acids with tRNAs containing the corresponding anticodon [110]. The Tars gene (involved in the aminoacyl-tRNA biosynthesis signaling) encodes for the Threonyl-tRNA synthetase, the enzyme that catalyzes aminoacylation of tRNA with the threonin amino acid. RNA transport from the nucleus to the cytoplasm is a fundamental process in order to allow proper gene expression and the different RNA species are exported from the nucleous to the cytoplasm through the nuclear pore complexes [111]. Due to the role of BDNF and NGF in triggering neuronal development, synaptic plasticity and neuronal survival, changes in protein synthesis are required to allow accomplishment of these functions. It was demonstrated that several proteins, identified to be modulated by BDNF, are actually involved in the translation activity [112]. Moreover, it has been demonstrated that BDNF mediates mRNA transport along dendrites to allow their translation at the synapses. As a consequence, this induces changes in the synaptic proteome [113]. On this basis, it is plausible that the modulation of tRNA biosynthesis and RNA transport pathways through selected miRNAs underlie an increased demand of protein synthesis due to neurotrophin-induced cellular differentiation and/or proliferation, also according to the literature [114][115]. On the other hand, sustained gene expression and protein synthesis

also need effective quality control of the abnormal mRNA. Not surprisingly, the RNA surveillance pathway was found to be modulated by neurotrophins as well.

mTOR signalling pathway

The mTOR signaling was associated with the miRNAs modulated by BDNF after 24h of stimulation.

	miRNAs significantly different from CTRL	
	NGF	BDNF
1h		
6h		
24h		✔
all		✔

The serine/threonine protein kinase mechanistic target of rapamycin (mTOR) is evolutionarily conserved and modulates protein synthesis, cell growth, and cellular autophagy in response to distinct intracellular and extracellular cues. A cross-talk between Ras-MAPK and mTOR has been established [9]. Moreover, mTOR-mediated autophagy was related to cell death during cisplatin-induced ototoxicity in cochlear hair cells. On this basis, the targeting of this pathway has been proposed as a neuroprotective strategy for cochlear hair cells [116]. Moreover, it was demonstrated that suppression of autophagy is required for BDNF-induced synaptic plasticity [117]. Moreover, several studies indicate that also NGF modulates the mTOR signaling in a variety of tissues [118],[119],[120].

Other pathways

In addition to the pathways described above, the Diana mirpath v.3.0 database also identified other signalings for the miRNA profilie deriving from NGF and BDNF treatments. Those signalings are not fully described here since they do not specifically match with the present study. However, they always involved downstream pathways, mainly MAPK and PIRK/AKT, that are described alongside this report. Examples of those pathways are: bacterial invasion of epithelial cells, oxytocin signaling pathway, GnRH signaling.

Conclusion

The present study investigated whether two major neurotrophic factors, NGF and BDNF, have the ability to modify the miRNA profiling in cochlear cells. The results of this study show that

both neurotrophic factors induce substantial changes of the miRNA profile, that also differs depending on the treatment duration. Through bioinformatics tools, it was possible to identify the target genes of those miRNAs and the relative target pathways. According to the well known effects that NGF and BDNF carry out in neuronal cells, pathways associated with cell cycle, differentiation, metabolism and others were predicted for the modulated miRNAs. Many of these have never been investigated in the cochlea in relationship with the neurotrophic factors. Moreover, the effects of NGF in the cochlea are poorly reported in the literature, since its role in promoting cochlear survival is only a recent outcome. On this basis, the present study demonstrates that NGF and BDNF target several signalings, that were already known to be modulated by NGF and BDNF, and that this is mediated by a wide range of miRNAs. Moreover, the results of this project also show new potential pathways that, through selective miRNAs, are likely to be modulated by NGF and BDNF in the cochlea.

Future studies will allow to deepen our understanding of the mechanisms underlying these processes and unveil the NGF- and BDNF-related signalings in cochlear cells.

6. References

1. Bartel, D.P. MicroRNAs: Genomics, Biogenesis, Mechanism, and Function. *Cell* 2004, *116*, 281–297.
2. Mittal, R.; Liu, G.; Polineni, S.P.; Bencie, N.; Yan, D.; Liu, X.Z. Role of microRNAs in inner ear development and hearing loss. *Gene* 2019, *686*, 49–55.
3. Vink, H.A.; Versnel, H.; Kroon, S.; Klis, S.F.L.; Ramekers, D. BDNF-mediated preservation of spiral ganglion cell peripheral processes and axons in comparison to that of their cell bodies. *Hear. Res.* **2021**, *400*, 108114, doi:10.1016/j.heares.2020.108114.
4. Vink, H.A.; van Dorp, W.C.; Thomeer, H.G.X.M.; Versnel, H.; Ramekers, D. Bdnf outperforms trkb agonist 7,8,3′-thf in preserving the auditory nerve in deafened guinea pigs. *Brain Sci.* **2020**, *10*, 1–20, doi:10.3390/brainsci10110787.
5. McGuinness, S.L.; Shepherd, R.K. Exogenous BDNF rescues rat spiral ganglion neurons in vivo. *Otol. Neurotol.* **2005**, *26*, 1064–1072, doi:10.1097/01.mao.0000185063.20081.50.
6. Chen, G.; Fan, Z.; Wang, X.; Ma, C.; Bower, K.A.; Shi, X.; Ke, Z.J.; Luo, J. Brain-derived neurotrophic factor suppresses tunicamycin-induced upregulation of CHOP in neurons. *J. Neurosci. Res.* **2007**, *85*, 1674–1684, doi:10.1002/jnr.21292.
7. Livak, K.J.; Schmittgen, T.D. Analysis of relative gene expression data using real-time quantitative PCR and the 2-ΔΔCT method. *Methods* **2001**, *25*, 402–408, doi:10.1006/meth.2001.1262.
8. Vlachos, I.S.; Zagganas, K.; Paraskevopoulou, M.D.; Georgakilas, G.; Karagkouni, D.; Vergoulis, T.; Dalamagas, T.; Hatzigeorgiou, A.G. DIANA-miRPath v3.0: Deciphering microRNA function with experimental support. *Nucleic Acids Res.* **2015**, *43*, W460–W466, doi:10.1093/nar/gkv403.
9. Mendoza, M.C.; Er, E.E.; Blenis, J. The Ras-ERK and PI3K-mTOR pathways: Cross-talk and compensation. *Trends Biochem. Sci.* 2011, *36*, 320–328.
10. Shu, Y.; Li, W.; Huang, M.; Quan, Y.Z.; Scheffer, D.; Tian, C.; Tao, Y.; Liu, X.; Hochedlinger, K.; Indzhykulian, A.A.; et al. Renewed proliferation in adult mouse cochlea and regeneration of hair cells. *Nat. Commun.* **2019**, *10*, doi:10.1038/s41467-019-13157-7.
11. Robinson, M.S. Forty Years of Clathrin-coated Vesicles. *Traffic* 2015, *16*, 1210–1238.
12. Amino, S.; Itakura, M.; Ohnishi, H.; Tsujimura, J.; Koizumi, S.; Takei, N.; Takahashi, M. Nerve growth factor enhances neurotransmitter release from PC12 cells by increasing Ca2+-responsible secretory vesicles through the activation of mitogen-activated protein kinase and phosphatidylinositol 3-kinase. *J. Biochem.* **2002**, *131*, 887–894, doi:10.1093/oxfordjournals.jbchem.a003179.
13. Gowrisankaran, S.; Milosevic, I. Regulation of synaptic vesicle acidification at the neuronal synapse. *IUBMB Life* 2020, iub.2235.
14. Luzio, J.P.; Pryor, P.R.; Bright, N.A. Lysosomes: Fusion and function. *Nat. Rev. Mol. Cell Biol.* 2007, *8*, 622–632.
15. Mnich, K.; Carleton, L.A.; Kavanagh, E.T.; Doyle, K.M.; Samali, A.; Gorman, A.M. Nerve growth factor-mediated inhibition of apoptosis post-caspase activation is due to removal of active caspase-3 in a lysosome-dependent manner. *Cell Death Dis.* **2014**, *5*,

doi:10.1038/cddis.2014.173.

16. Jackson, A.L.; Pahl, P.M.; Harrison, K.; Rosamond, J.; Sclafani, R.A. Cell cycle regulation of the yeast Cdc7 protein kinase by association with the Dbf4 protein. *Mol. Cell. Biol.* **1993**, *13*, 2899–2908, doi:10.1128/mcb.13.5.2899.

17. Götz, M.; Huttner, W.B. The cell biology of neurogenesis. *Nat. Rev. Mol. Cell Biol.* 2005, *6*, 777–788.

18. Schimmang, T.; Pirvola, U. Coupling the cell cycle to development and regeneration of the inner ear. *Semin. Cell Dev. Biol.* 2013, *24*, 507–513.

19. Hong, J.; Qian, T.; Le, Q.; Sun, X.; Wu, J.; Chen, J.; Yu, X.; Xu, J. NGF promotes cell cycle progression by regulating D-type cyclins via PI3K/Akt and MAPK/Erk activation in human corneal epithelial cells. *Mol. Vis.* **2012**, *18*, 758–764.

20. Zhang, L.; Li, X.; Lin, X.; Wu, M. Nerve growth factor promotes the proliferation of Müller cells co-cultured with internal limiting membrane by regulating cell cycle via Trk-A/PI3K/Akt pathway. *BMC Ophthalmol.* **2019**, *19*, doi:10.1186/s12886-019-1142-x.

21. Morillo, S.M.; Abanto, E.P.; Roman, M.J.; Frade, J.M. Nerve Growth Factor-Induced Cell Cycle Reentry in Newborn Neurons Is Triggered by p38MAPK-Dependent E2F4 Phosphorylation. *Mol. Cell. Biol.* **2012**, *32*, 2722–2737, doi:10.1128/mcb.00239-12.

22. Spittau, G.; Happel, N.; Behrendt, M.; Chao, T.I.; Krieglstein, K.; Spittau, B. Tieg1/Klf10 is upregulated by NGF and attenuates cell cycle progression in the pheochromocytoma cell line PC12. *J. Neurosci. Res.* **2010**, *88*, 2017–2025, doi:10.1002/jnr.22364.

23. Skaper, S.D. Neurotrophic Factors: An Overview. In; Humana Press, New York, NY, 2018; pp. 1–17.

24. Schlessinger, J. Cell signaling by receptor tyrosine kinases. *Cell* 2000, *103*, 211–225.

25. Sawano, A.; Takayama, S.; Matsuda, M.; Miyawaki, A. Lateral propagation of EGF signaling after local stimulation is dependent on receptor density. *Dev. Cell* **2002**, *3*, 245–257, doi:10.1016/S1534-5807(02)00224-1.

26. Gómez-Casati, M.E.; Murtie, J.C.; Rio, C.; Stankovic, K.; Liberman, M.C.; Corfas, G. Nonneuronal cells regulate synapse formation in the vestibular sensory epithelium via erbB-dependent BDNF expression. *Proc. Natl. Acad. Sci. U. S. A.* **2010**, *107*, 17005–17010, doi:10.1073/pnas.1008938107.

27. Cohen, G.; Ettinger, K.; Lecht, S.; Lelkes, P.I.; Lazarovici, P. Transcriptional Down-regulation of Epidermal Growth Factor (EGF) Receptors by Nerve Growth Factor (NGF) in PC12 Cells. *J. Mol. Neurosci.* **2014**, *54*, 574–585, doi:10.1007/s12031-014-0388-2.

28. Lazarovici, P.; Oshima, M.; Shavit, D.; Shibutani, M.; Jiang, H.; Monshipouri, M.; Fink, D.; Movsesyan, V.; Guroff, G. Down-regulation of epidermal growth factor receptors by nerve growth factor in PC12 cells is p140(trk)-, Ras-, and Src-dependent. *J. Biol. Chem.* **1997**, *272*, 11026–11034, doi:10.1074/jbc.272.17.11026.

29. Seo, J.; Kim, J. Regulation of Hippo signaling by actin remodeling. *BMB Rep.* 2018, *51*, 151–156.

30. Karaman, R.; Halder, G. Cell junctions in Hippo signaling. *Cold Spring Harb. Perspect. Biol.* **2018**, *10*, doi:10.1101/cshperspect.a028753.

31. Yang, X.; Shen, H.; Buckley, B.; Chen, Y.; Yang, N.; Mussell, A.L.; Chernov, M.; Kobzik, L.;

Frangou, C.; Han, S.X.; et al. NTRK1 is a positive regulator of YAP oncogenic function. *Oncogene* **2019**, *38*, 2778–2787, doi:10.1038/s41388-018-0609-1.

32. Wang, Z.; Chen, Y.; Chen, X.; Zheng, X.; Xu, G.; Yuan, Z.; Zhao, H.; Chen, W.; Li, L.; Zheng, N.; et al. The TrkB-T1 receptor mediates BDNF-induced migration of aged cardiac microvascular endothelial cells by recruiting Willin. *Aging Cell* **2019**, *18*, doi:10.1111/acel.12881.

33. Huang, X.; Zhang, H.; Guo, X.; Zhu, Z.; Cai, H.; Kong, X. Insulin-like growth factor 2 mRNA-binding protein 1 (IGF2BP1) in cancer. *J. Hematol. Oncol.* 2018, *11*.

34. Perycz, M.; Urbanska, A.S.; Krawczyk, P.S.; Parobczak, K.; Jaworski, J. Zipcode binding protein 1 regulates the development of dendritic arbors in hippocampal neurons. *J. Neurosci.* **2011**, *31*, 5271–5285, doi:10.1523/JNEUROSCI.2387-10.2011.

35. Boylan, K.L.M.; Mische, S.; Li, M.; Marqués, G.; Morin, X.; Chia, W.; Hays, T.S. Motility screen identifies Drosophila IGF-II mRNA-binding protein - Zipcode-binding protein acting in oogenesis and synaptogenesis. *PLoS Genet.* **2008**, *4*, doi:10.1371/journal.pgen.0040036.

36. Donnelly, C.J.; Willis, D.E.; Xu, M.; Tep, C.; Jiang, C.; Yoo, S.; Schanen, N.C.; Kirn-Safran, C.B.; Van Minnen, J.; English, A.; et al. Limited availability of ZBP1 restricts axonal mRNA localization and nerve regeneration capacity. *EMBO J.* **2011**, *30*, 4665–4677, doi:10.1038/emboj.2011.347.

37. Sasaki, Y.; Welshhans, K.; Wen, Z.; Yao, J.; Xu, M.; Goshima, Y.; Zheng, J.Q.; Bassell, G.J. Phosphorylation of zipcode binding protein 1 is required for brain-derived neurotrophic factor signaling of local β-actin synthesis and growth cone turning. *J. Neurosci.* **2010**, *30*, 9349–9358, doi:10.1523/JNEUROSCI.0499-10.2010.

38. Vašák, M.; Hasler, D.W. Metallothioneins: New functional and structural insights. *Curr. Opin. Chem. Biol.* 2000, *4*, 177–183.

39. Mazurek, B.; Amarjargal, N.; Haupt, H.; Fuchs, J.; Olze, H.; Machulik, A.; Gross, J. Expression of genes implicated in oxidative stress in the cochlea of newborn rats. *Hear. Res.* **2011**, *277*, 54–60, doi:10.1016/j.heares.2011.03.011.

40. Innis, S.M. Essential fatty acids in growth and development. *Prog. Lipid Res.* 1991, *30*, 39–103.

41. A, P.; Z, O.; V, V.; V, L. Fatty Acids in Energy Metabolism of the Central Nervous System. *Biomed Res. Int.* **2014**, *2014*, doi:10.1155/2014/472459.

42. Msika, O.; Brand, A.; Crawford, M.A.; Yavin, E. NGF blocks polyunsaturated fatty acids biosynthesis in n - 3 fatty acid-supplemented PC12 cells. *Biochim. Biophys. Acta - Mol. Cell Biol. Lipids* **2012**, *1821*, 1022–1030, doi:10.1016/j.bbalip.2012.04.007.

43. Chung, Y.C.; Cui, Y.; Sumiyoshi, T.; Kim, M.G.; Lee, K.H. Associations of fatty acids with cognition, psychopathology, and brain-derived neurotrophic factor levels in patients with first-episode schizophrenia and related disorders treated with paliperidone extended release. *J. Psychopharmacol.* **2017**, *31*, 1556–1563, doi:10.1177/0269881117731169.

44. Das, U.N. Autism as a disorder of deficiency of brain-derived neurotrophic factor and altered metabolism of polyunsaturated fatty acids. *Nutrition* 2013, *29*, 1175–1185.

45. Houten, S.M.; Te Brinke, H.; Denis, S.; Ruiter, J.P.N.; Knegt, A.C.; De Klerk, J.B.C.;

Augoustides-Savvopoulou, P.; Häberle, J.; Baumgartner, M.R.; Coşkun, T.; et al. Genetic basis of hyperlysinemia. *Orphanet J. Rare Dis.* **2013**, *8*, 57, doi:10.1186/1750-1172-8-57.

46. Murín, R.; Hamprecht, B. Metabolic and regulatory roles of leucine in neural cells. *Neurochem. Res.* **2008**, *33*, 279–284, doi:10.1007/s11064-007-9444-4.

47. Zhang, Y.; Alexander, P.B.; Wang, X.F. TGF-β family signaling in the control of cell proliferation and survival. *Cold Spring Harb. Perspect. Biol.* **2017**, *9*, doi:10.1101/cshperspect.a022145.

48. McLaughlin, C.N.; Broihier, H.T. Keeping Neurons Young and Foxy: FoxOs Promote Neuronal Plasticity. *Trends Genet.* 2018, *34*, 65–78.

49. Maxson & Mitchell FOXO in Neural Cells and Diseases of the Nervous System. *Physiol. Behav.* **2016**, *176*, 139–148, doi:10.1016/j.physbeh.2017.03.040.

50. Polter, A.; Yang, S.; Zmijewska, A.A.; van Groen, T.; Paik, J.H.; DePinho, R.A.; Peng, S.L.; Jope, R.S.; Li, X. Forkhead Box, Class O Transcription Factors in Brain: Regulation and Behavioral Manifestation. *Biol. Psychiatry* **2009**, *65*, 150–159, doi:10.1016/j.biopsych.2008.08.005.

51. Gilley, J.; Coffer, P.J.; Ham, J. FOXO transcription factors directly activate bim gene expression and promote apoptosis in sympathetic neurons. *J. Cell Biol.* **2003**, *162*, 613–622, doi:10.1083/jcb.200303026.

52. Veeraval, L.; O'Leary, C.J.; Cooper, H.M. Adherens Junctions: Guardians of Cortical Development. *Front. Cell Dev. Biol.* 2020, *8*.

53. Tietz, S.; Engelhardt, B. Brain barriers: Crosstalk between complex tight junctions and adherens junctions. *J. Cell Biol.* 2015, *209*, 493–506.

54. Shi, X. Pathophysiology of the cochlear intrastrial fluid-blood barrier (review). *Hear. Res.* 2016, *338*, 52–63.

55. Etienne-Manneville, S. Control of polarized cell morphology and motility by adherens junctions. *Semin. Cell Dev. Biol.* 2011, *22*, 850–857.

56. Keshmirian, J.; Bray, G.; Carbonetto, S. The extracellular matrix modulates the response of PC12 cells to nerve growth factor: cell aggregation versus neurite outgrowth on 3-dimensional laminin substrata. *J. Neurocytol.* **1989**, *18*, 491–504, doi:10.1007/bf01474545.

57. Konietzny, A.; Bär, J.; Mikhaylova, M. Dendritic actin cytoskeleton: Structure, functions, and regulations. *Front. Cell. Neurosci.* 2017, *11*.

58. Lei, W.; Omotade, O.F.; Myers, K.R.; Zheng, J.Q. Actin cytoskeleton in dendritic spine development and plasticity. *Curr. Opin. Neurobiol.* 2016, *39*, 86–92.

59. Sekerková, G.; Zheng, L.; Loomis, P.A.; Mugnaini, E.; Bartles, J.R. Espins and the actin cytoskeleton of hair cell stereocilia and sensory cell microvilli. *Cell. Mol. Life Sci.* 2006, *63*, 2329–2341.

60. Huang, E.J.; Reichardt, L.F. Neurotrophins: Roles in Neuronal Development and Function. *Annu. Rev. Neurosci.* **2001**, *24*, 677–736, doi:10.1146/annurev.neuro.24.1.677.

61. Ketschek, A.; Jones, S.; Spillane, M.; Korobova, F.; Svitkina, T.; Gallo, G. Nerve growth factor promotes reorganization of the axonal microtubule array at sites of axon

collateral branching. *Dev. Neurobiol.* **2015**, *75*, 1441–1461, doi:10.1002/dneu.22294.

62. Spillane, M.; Ketschek, A.; Jones, S.L.; Korobova, F.; Marsick, B.; Lanier, L.; Svitkina, T.; Gallo, G. The actin nucleating Arp2/3 complex contributes to the formation of axonal filopodia and branches through the regulation of actin patch precursors to filopodia. *Dev. Neurobiol.* **2011**, *71*, 747–758, doi:10.1002/dneu.20907.

63. Zhao, H.B.; Kikuchi, T.; Ngezahayo, A.; White, T.W. Gap junctions and cochlear homeostasis. *J. Membr. Biol.* **2006**, *209*, 177–186, doi:10.1007/s00232-005-0832-x.

64. Myers, J.P.; Gomez, T.M. Focal adhesion kinase promotes integrin adhesion dynamics necessary for chemotropic turning of nerve growth cones. *J. Neurosci.* **2011**, *31*, 13585–13595, doi:10.1523/JNEUROSCI.2381-11.2011.

65. Myers, J.P.; Robles, E.; Ducharme-Smith, A.; Gomez, T.M. Focal adhesion kinase modulates Cdc42 activity downstream of positive and negative axon guidance cues. *J. Cell Sci.* **2012**, *125*, 2918–2929, doi:10.1242/jcs.100107.

66. Ziello, J.E.; Huang, Y.; Jovin, I.S. Cellular endocytosis and gene delivery. *Mol. Med.* **2010**, *16*, 222–229, doi:10.2119/molmed.2009.00101.

67. Beattie, E.C.; Howe, C.L.; Wilde, A.; Brodsky, F.M.; Mobley, W.C. NGF signals through TrkA to increase clathrin at the plasma membrane and enhance clathrin-mediated membrane trafficking. *J. Neurosci.* **2000**, *20*, 7325–7333, doi:10.1523/jneurosci.20-19-07325.2000.

68. Grimes, M.L.; Zhou, J.; Beattie, E.C.; Yuen, E.C.; Hall, D.E.; Valletta, J.S.; Topp, K.S.; LaVail, J.H.; Bunnett, N.W.; Mobley, W.C. Endocytosis of activated trkA: Evidence that nerve growth factor induces formation of signaling endosomes. *J. Neurosci.* **1996**, *16*, 7950–7964, doi:10.1523/jneurosci.16-24-07950.1996.

69. Hendry, I.A.; Stöckel, K.; Thoenen, H.; Iversen, L.L. The retrograde axonal transport of nerve growth factor. *Brain Res.* **1974**, *68*, 103–121, doi:10.1016/0006-8993(74)90536-8.

70. Huang, E.J.; Reichardt, L.F. Trk Receptors: Roles in Neuronal Signal Transduction. *Annu. Rev. Biochem.* **2003**, *72*, 609–642, doi:10.1146/annurev.biochem.72.121801.161629.

71. Johnson Chacko, L.; Blumer, M.J.F.; Pechriggl, E.; Rask-Andersen, H.; Dietl, W.; Haim, A.; Fritsch, H.; Glueckert, R.; Dudas, J.; Schrott-Fischer, A. Role of BDNF and neurotrophic receptors in human inner ear development. *Cell Tissue Res.* **2017**, *370*, 347–363, doi:10.1007/s00441-017-2686-9.

72. Schimmang, T.; Alvarez-Bolado, G.; Minichiello, L.; Vazquez, E.; Giraldez, F.; Klein, R.; Represa, J. Survival of inner ear sensory neurons in trk mutant mice. *Mech. Dev.* **1997**, *64*, 77–85, doi:10.1016/s0925-4773(97)00047-6.

73. Dai, C.F.; Steyger, P.S.; Wang, Z.M.; Vass, Z.; Nuttall, A.L. Expression of Trk A receptors in the mammalian inner ear. *Hear. Res.* **2004**, *187*, 1–11, doi:10.1016/s0378-5955(03)00277-6.

74. Després, G.; Hafidi, A.; Romand, R. Immunohistochemical localization of nerve growth factor receptor in the cochlea and in the brainstem of the perinatal rat. *Hear. Res.* **1991**, *52*, 157–65, doi:10.1016/0378-5955(91)90195-f.

75. Meyers, E.A.; Kessler, J.A. TGF-β family signaling in neural and neuronal differentiation, development, and function. *Cold Spring Harb. Perspect. Biol.* **2017**, *9*,

doi:10.1101/cshperspect.a022244.

76. SMAD4 gene - Genetics Home Reference - NIH.

77. Paradies, N.E.; Sanford, L.P.; Doetschman, T.; Friedman, R.A. Developmental expression of the TGFβs in the mouse cochlea. *Mech. Dev.* **1998**, *79*, 165–168, doi:10.1016/S0925-4773(98)00184-1.

78. Marzella, P.L.; Gillespie, L.N.; Clark, G.M.; Bartlett, P.F.; Kilpatrick, T.J. The neurotrophins act synergistically with LIF and members of the TGF-β superfamily to promote the survival of spiral ganglia neurons in vitro. *Hear. Res.* **1999**, *138*, 73–80, doi:10.1016/S0378-5955(99)00152-5.

79. Chaldakov, G.N. The metabotrophic NGF and BDNF: An emerging concept. *Arch. Ital. Biol.* **2011**, *149*, 257–263, doi:10.4449/aib.v149i2.1366.

80. Leonardi, R.; Jackowski, S. Biosynthesis of Pantothenic Acid and Coenzyme A. *EcoSal Plus* **2007**, *2*, doi:10.1128/ecosalplus.3.6.3.4.

81. Akram, M. Citric Acid Cycle and Role of its Intermediates in Metabolism. *Cell Biochem. Biophys.* 2014, *68*, 475–478.

82. Ciges, M.; Fernández-Cervilla, F.; Crespo, P. V.; Campos, A. Pantothenic acid and coenzyme A in experimental cisplatin-induced ototoxia. *Acta Otolaryngol.* **1996**, *116*, 263–268, doi:10.3109/00016489609137837.

83. Szutowicz, A.; Madziar, B.; Pawełczyk, T.; Tomaszewicz, M.; Bielarczyk, H. Effects of NGF on acetylcholine, acetyl-CoA metabolism, and viability of differentiated and non-differentiated cholinergic neuroblastoma cells. *J. Neurochem.* **2004**, *90*, 952–961, doi:10.1111/j.1471-4159.2004.02556.x.

84. CHEN, G.; BOWER, K.A.; MA, C.; FANG, S.; THIELE, C.J.; LUO, J. Glycogen synthase kinase 3β (GSK3β) mediates 6-hydroxydopamine-induced neuronal death. *FASEB J.* **2004**, *18*, 1162–1164, doi:10.1096/fj.04-1551fje.

85. Silva, R.M.; Ries, V.; Oo, T.F.; Yarygina, O.; Jackson-Lewis, V.; Ryu, E.J.; Lu, P.D.; Marciniak, S.J.; Ron, D.; Przedborski, S.; et al. CHOP/GADD153 is a mediator of apoptotic death in substantia nigra dopamine neurons in an in vivo neurotoxin model of parkinsonism. *J. Neurochem.* **2005**, *95*, 974–986, doi:10.1111/j.1471-4159.2005.03428.x.

86. Li, R.; Wu, Y.; Zou, S.; Wang, X.; Li, Y.; Xu, K.; Gong, F.; Liu, Y.; Wang, J.; Liao, Y.; et al. NGF Attenuates High Glucose-Induced ER Stress, Preventing Schwann Cell Apoptosis by Activating the PI3K/Akt/GSK3β and ERK1/2 Pathways. *Neurochem. Res.* **2017**, *42*, 3005–3018, doi:10.1007/s11064-017-2333-6.

87. Zhang, H.; Wu, F.; Kong, X.; Yang, J.; Chen, H.; Deng, L.; Cheng, Y.; Ye, L.; Zhu, S.; Zhang, X.; et al. Nerve growth factor improves functional recovery by inhibiting endoplasmic reticulum stress-induced neuronal apoptosis in rats with spinal cord injury. *J. Transl. Med.* **2014**, *12*, 130, doi:10.1186/1479-5876-12-130.

88. Wei, L.; Kan, L.Y.; Zeng, H.Y.; Tang, Y.Y.; Huang, H.L.; Xie, M.; Zou, W.; Wang, C.Y.; Zhang, P.; Tang, X.Q. BDNF/TrkB Pathway Mediates the Antidepressant-Like Role of H2S in CUMS-Exposed Rats by Inhibition of Hippocampal ER Stress. *NeuroMolecular Med.* **2018**, *20*, 252–261, doi:10.1007/s12017-018-8489-7.

89. Shimoke, K.; Utsumi, T.; Kishi, S.; Nishimura, M.; Sasaya, H.; Kudo, M.; Ikeuchi, T. Prevention of endoplasmic reticulum stress-induced cell death by brain-derived

neurotrophic factor in cultured cerebral cortical neurons. *Brain Res.* **2004**, *1028*, 105–111, doi:10.1016/j.brainres.2004.09.005.

90. Pandey, M.; Rajamma, U. Huntington's disease: the coming of age. *J. Genet.* 2018, *97*, 649–664.

91. Lin, Y.S.; Wang, C.H.; Chern, Y. Besides Huntington's disease, does brain-type creatine kinase play a role in other forms of hearing impairment resulting from a commonpathological cause? *Aging (Albany. NY).* **2011**, *3*, 657–662, doi:10.18632/aging.100338.

92. Lim, Y.; Wu, L.L.; Chen, S.; Sun, Y.; Vijayaraj, S.L.; Yang, M.; Bobrovskaya, L.; Keating, D.; Li, X.; Zhou, X.; et al. HHS Public Access. **2018**, *55*, 1815–1830, doi:10.1007/s12035-016-0379-0.HAP1.

93. Gharami, K.; Xie, Y.; An, J.J.; Tonegawa, S.; Xu, B. Brain-derived neurotrophic factor over-expression in the forebrain ameliorates Huntington's disease phenotypes in mice. *J. Neurochem.* **2008**, *105*, 369–379, doi:10.1111/j.1471-4159.2007.05137.x.

94. Galpern, W.R.; Matthews, R.T.; Beal, M.F.; Isacson, O. NGF attenuates 3-nitrotyrosine formation in a 3-NP model of Huntington's disease. *Neuroreport* **1996**, *7*, 2639–2642, doi:10.1097/00001756-199611040-00046.

95. Zhang, H.; Petit, G.H.; Gaughwin, P.M.; Hansen, C.; Ranganathan, S.; Zuo, X.; Smith, R.; Roybon, L.; Brundin, P.; Mobley, W.C.; et al. NGF rescues hippocampal cholinergic neuronal markers, restores neurogenesis, and improves the spatial working memory in a mouse model of huntington's disease. *J. Huntingtons. Dis.* **2013**, *2*, 69–82, doi:10.3233/JHD-120026.

96. Bieberich, E. Synthesis, Processing, and Function of N-glycans in N-glycoproteins. In *Advances in neurobiology*; NIH Public Access, 2014; Vol. 9, pp. 47–70.

97. McFarlane, I.; Georgopoulou, N.; Coughlan, C.M.; Gillian, A.M.; Breen, K.C. The role of the protein glycosylation state in the control of cellular transport of the amyloid β precursor protein. *Neuroscience* **1999**, *90*, 15–25, doi:10.1016/S0306-4522(98)00361-3.

98. Menezes, R.; Hashemi, S.; Vincent, R.; Collins, G.; Meyer, J.; Foston, M.; Arinzeh, T.L. Investigation of glycosaminoglycan mimetic scaffolds for neurite growth. *Acta Biomater.* **2019**, *90*, 169–178, doi:10.1016/j.actbio.2019.03.024.

99. Ihara, Y.; Sakamoto, Y.; Mihara, M.; Shimizu, K.; Taniguchi, N. Overexpression of N-acetylglucosaminyltransferase III disrupts the tyrosine phosphorylation of Trk with resultant signaling dysfunction in PC12 cells treated with nerve growth factor. *J. Biol. Chem.* **1997**, *272*, 9629–9634, doi:10.1074/jbc.272.15.9629.

100. Benicky, J.; Sanda, M.; Kennedy, Z.B.; Goldman, R. N-Glycosylation is required for secretion of the precursor to brain-derived neurotrophic factor (proBDNF) carrying sulfated LacdiNAc structures. *J. Biol. Chem.* **2019**, *294*, 16816–16830, doi:10.1074/jbc.RA119.009989.

101. Iozzo, R. V.; Sanderson, R.D. Proteoglycans in cancer biology, tumour microenvironment and angiogenesis. *J. Cell. Mol. Med.* 2011, *15*, 1013–1031.

102. Maeda, N. Proteoglycans and neuronal migration in the cerebral cortex during development and disease. *Front. Neurosci.* **2015**, *9*, doi:10.3389/fnins.2015.00098.

103. Masu, M. Proteoglycans and axon guidance: a new relationship between old partners. *J. Neurochem.* **2016**, *139*, 58–75, doi:10.1111/jnc.13508.

104. Melrose, J. Keratan sulfate (<scp>KS</scp>)-proteoglycans and neuronal regulation in health and disease: the importance of <scp>KS</scp> -glycodynamics and interactive capability with neuroregulatory ligands. *J. Neurochem.* **2019**, *149*, 170–194, doi:10.1111/jnc.14652.

105. Go, S.; Yoshikawa, M.; Inokuchi, J. Glycoconjugates in the mammalian auditory system. *J. Neurochem.* **2011**, *116*, 756–763, doi:10.1111/j.1471-4159.2010.07099.x.

106. Friauf, E. Development of chondroitin sulfate proteoglycans in the central auditory system of rats correlates with acquisition of mature properties. *Audiol. Neuro-Otology* **2000**, *5*, 251–262, doi:10.1159/000013889.

107. Leveugle, B.; Ding, W.; Buée, L.; Fillit, H.M. Interleukin-1 and nerve growth factor induce hypersecretion and hypersulfation of neuroblastoma proteoglycans which bind β-amyloid. *J. Neuroimmunol.* **1995**, *60*, 151–160, doi:10.1016/0165-5728(95)00065-A.

108. Katoh-Semba, R.; Oohira, A.; Kashiwamata, S. Nerve Growth Factor-Induced Changes in the Structure of Sulfated Proteoglycans in PC 12 Pheochromocytoma Cells. *J. Neurochem.* **1992**, *59*, 282–289, doi:10.1111/j.1471-4159.1992.tb08902.x.

109. Kurihara, D.; Yamashita, T. Chondroitin sulfate proteoglycans down-regulate spine formation in cortical neurons by targeting tropomyosin-related kinase B (TrkB) protein. *J. Biol. Chem.* **2012**, *287*, 13822–13828, doi:10.1074/jbc.M111.314070.

110. Ibba, M.; Söll, D. Aminoacyl-tRNA Synthesis. *Annu. Rev. Biochem.* **2000**, *69*, 617–650, doi:10.1146/annurev.biochem.69.1.617.

111. Rodriguez, M.S.; Dargemont, C.; Stutz, F. Nuclear export of RNA. *Biol. cell* **2004**, *96*, 639–55, doi:10.1016/j.biolcel.2004.04.014.

112. Manadas, B.; Santos, A.R.; Szabadfi, K.; Gomes, J.R.; Garbis, S.D.; Fountoulakis, M.; Duarte, C.B. BDNF-induced changes in the expression of the translation machinery in hippocampal neurons: Protein levels and dendritic mRNA. *J. Proteome Res.* **2009**, *8*, 4536–4552, doi:10.1021/pr900366x.

113. Leal, G.; Comprido, D.; Duarte, C.B. BDNF-induced local protein synthesis and synaptic plasticity. *Neuropharmacology* 2014, *76*, 639–656.

114. Ruiz, C.R.; Shi, J.; Meffert, M.K. Transcript specificity in BDNF-regulated protein synthesis. *Neuropharmacology* 2014, *76*, 657–663.

115. Fujii, D.K.; Massoglia, S.L.; Savion, N.; Gospodarowicz, D. Neurite outgrowth and protein synthesis by PC12 cells as a function of substratum and nerve growth factor. *J. Neurosci.* **1982**, *2*, 1157–1175, doi:10.1523/jneurosci.02-08-01157.1982.

116. Youn, C.K.; Kim, J.; Park, J.-H.; Do, N.Y.; Cho, S. Il Role of autophagy in cisplatin-induced ototoxicity. *Int. J. Pediatr. Otorhinolaryngol.* **2015**, *79*, 1814–9, doi:10.1016/j.ijporl.2015.08.012.

117. Nikoletopoulou, V.; Sidiropoulou, K.; Kallergi, E.; Dalezios, Y.; Tavernarakis, N. Modulation of Autophagy by BDNF Underlies Synaptic Plasticity. *Cell Metab.* **2017**, *26*, 230-242.e5, doi:10.1016/j.cmet.2017.06.005.

118. Cao, G.F.; Liu, Y.; Yang, W.; Wan, J.; Yao, J.; Wan, Y.; Jiang, Q. Rapamycin sensitive mTOR activation mediates nerve growth factor (NGF) induced cell migration and pro-survival

effects against hydrogen peroxide in retinal pigment epithelial cells. *Biochem. Biophys. Res. Commun.* **2011**, *414*, 499–505, doi:10.1016/j.bbrc.2011.09.094.

119. Zhang, J.; Ma, W.Y. Nerve growth factor regulates the expression of vascular endothelial growth factor in human HaCaT keratinocytes via PI3K/mTOR pathway. *Genet. Mol. Res.* **2014**, *13*, 9324–9335, doi:10.4238/2014.January.24.14.

120. Good, D.W.; George, T.; Watts, B.A. Nerve growth factor inhibits Na+/H+ exchange and HCO3- absorption through parallel phosphatidylinositol 3-kinase-mTOR and ERK pathways in thick ascending limb. *J. Biol. Chem.* **2008**, *283*, 26602–26611, doi:10.1074/jbc.M803019200.

CHAPTER 3

Limited effects of rhNGF and rhBDNF on Hair Cells and Supporting Cells of the Organ of Corti in an animal model of sensorineural hearing loss

1. Abstract

*T*he administration of neurotrophic factors (NFs) represents a new promising therapeutic approach for sensorineural hearing loss and several *in vivo* studies already showed that NFs are effective in the neuroprotection of spiral ganglion cells (SGCs) of the cochlea. However, little is known about the protection of the organ of Corti by NFs. Here, we investigated the effects of recombinant human nerve growth factor NGF (rhNGF) and recombinant human brain-derived neurotrophic factor BDNF (rhBDNF) on hair cells (HCs) and supporting cells (SCs) of the organ of Corti in a model of sensorineural hearing loss. Adult albino guinea pigs were ototoxically deafened by furosemide- kanamycin administration, and two weeks after deafening the right cochleas of the animals were treated with gelatin sponge (gelfoam) soaked in rhNGF or rhBDNF, while the left cochleas were used as internal negative control. Four weeks after treatment, animals were euthanized and the cochleas processed for histological analysis. The HCs and the SCs of the organ of Corti were counted on all cochlear locations, from base to apex, of midmodiolar sections. The number of HCs and SCs was similar between treated and untreated ears. However, the rhBDNF-treated cochleas showed a small decrease in the number of outer hair cells (OHCs). Moreover, the survival of SGCs was not correlated with SC counts. which was similar between rhNGF treated and contralateral ears, but significantly higher in the basal turns of rhBDNF-treated ears compared to the untreated contralateral ears. Taken together, the data of this study show that rhNGF and rhBDNF did not improve the survival of SCs after cochlear ototoxic damage. Moreover, the number of SCs did not represent a determinant factor for SGC survival, and therefore the positive effects on the SGC packing density by rhBDNF administration leads one to consider a direct targeting of SGCs by the neurotrophin. However, additional studies on the molecular and functional aspects of the remaining supporting cells, as well as a more detailed time course analysis, could allow to better understand the most specific mechanisms underlying the crosstalk between the sensory epithelium, the SGCs and neurotrophic factors.

2. Introduction

The organ of Corti is the organ responsible for the auditory function and it is a complex epithelium constituted by several cell types located in the *scala media* of the cochlea. The mechanosensory hair cells (HCs) of the Organ of Corti allow the conversion of sound-induced vibrations into electrochemical signals [1]. They are organized in three rows of outer HCs (OHCs) and one row of inner HCs (IHCs), surrounded by non-sensory supporting cells (SCs), that have a major role in the maintenance of structural and functional properties of the sensory epithelium [1–3]. Five different types of SCs, organized in rows along the Organ of Corti, have been identified based on morphological, functional and expression patterns differences: (1) Hensen's cells, (2) Deiters' cells, (3) pillar cells, (4) inner phalangeal cells, and (5) border cells [2]. The structure and function of HCs and SCs vary significantly from base to apex in the cochlea [4], in accordance with the tonotopic organization of the cochlea, with the base responsible for transduction of high frequencies and the apex for that of low frequencies [5].

Unfortunately, the exposure to several damaging stimuli, such as ototoxic drugs, noise, genetic predisposition and aging, can induce degeneration of the Organ of Corti, leading to irreversible deafness [6]. Hearing loss represents the fourth cause of disability in the world according to the Global Burden of Disease Study, and the number of affected patients is expected to increase in the next years [7,8]. In particular, in sensorineural hearing loss the mechanosensory HCs are often the primary cells to degenerate, and their death is followed by progressive degeneration of afferent spiral ganglion cells (SGCs), a potential problem for the beneficial outcome of cochlear implants [9–11]. For instance, a significant correlation between the SGCs survival and the performance of cochlear implants has been previously demonstrated [12]. Recently, more attention has also been placed on the role of SCs in the Organ of Corti in pathological conditions, since the death of HCs is also accompanied by prominent structural alterations of the Organ of Corti involving the SCs, and resulting in their degeneration as well [13–15]. In the most advanced stages of the degeneration process, the Organ of Corti is then replaced by squamous and cuboidal cells, which constitute a "flat epithelium" [14]. It has been suggested that the remaining non-sensory cells in the deaf cochleas could be used for enhancing nerve survival and function, improving the beneficial effects of cochlear implants. For instance, these cells may be engineered in order to express survival and growth factors to prevent SGCs death [16,17] or to induce the regeneration of hair cells, as occurs in some animal species [18]. On this basis, the protection of the SCs in addition to that of the sensory cells, represents a challenging objective to be achieved for

therapeutic purposes. Nevertheless, to date effective treatments to prevent Organ of Corti's cell death or to restore its cells after degeneration, are not available and there is an increasing interest in the development of new therapies. Among these, the administration of neurotrophic factors (NFs) represents a new promising therapeutic approach and several *in vivo* studies already showed that the nerve growth factor (NGF) and the brain-derived neurotrophic factor (BDNF) are effective in the neuroprotection of SGCs [19]. Conversely, little is known about the protection of the Organ of Corti by neurotrophins, and the identification of NF receptors in both HCs and SCs [20,21] supports the possibility to develop targeted NFs-based therapies for the Organ of Corti.

On this basis, here we investigated the effects of recombinant human NGF (rhNGF) and recombinant human BDNF (rhBDNF) on HCs and SCs of the Organ of Corti in a model of kanamycin- and furosemide-induced severe hearing loss. We also compared the number of SCs with the survival of SGCs, in order to understand whether SCs protect SGCs even in absence of HCs.

3. Methods

3.1. Animals and Experimental Design

The present study was conducted on cochleas derived from previous studies conducted in the UMC Utrecht, including one published [22]. Young adult albino guinea pigs (Dunkin Hartley; Envigo, Horst, the Netherlands) were kept under standard housing conditions throughout the experiment (food and water ad libitum; lights on between 7:00 a.m. and 7:00 p.m.; temperature 21°C; humidity 60%). Animals were ototoxically deafened and two weeks thereafter the right cochleas were treated with gelatin sponge (gelfoam) soaked in rhNGF or rhBDNF, while the left cochleas were used as internal negative control. Four weeks after treatment, animals were euthanized and the cochleas processed for histological analysis. Normal-hearing (NH) animals were used as reference of number of SCs. An overview of the timeline and experimental groups involved in the study is reported in Figure 1.

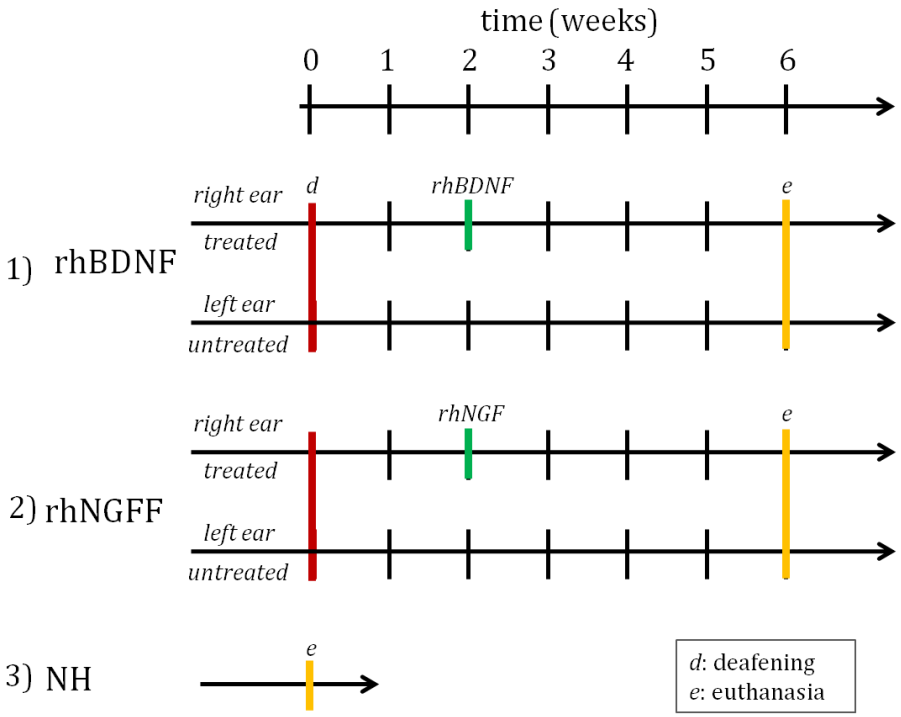

Figure 1. Schematic illustration of the experimental groups. The study was conducted on 3 groups of guinea pigs: (1) rhBDNF-treated and (2) rhNGF-treated animals, who received the treatment in the right ears, while the contralateral left ear was used as internal negative control; (3) normal hearing (NH) animals who did not receive any deafening or treatment procedure were used as baseline.

3.2. Deafening procedure and treatment administration

Surgical techniques and experimental procedures for both deafening and treatment administration were conducted according to previously published protocols [22]. In short, anesthesia for both procedures was induced with 40 mg/kg ketamine i.m. (Narketan;

Vetoquinol B.V., Breda, the Netherlands) and 0.25 mg/kg dexmedetomidine i.m. (Dexdomitor; Vetoquinol B.V.). Prior to the deafening procedure, normal hearing was verified with click-evoked auditory brainstem responses (ABRs). When normal hearing was confirmed, deafening was performed by systemic delivery of 400 mg/kg kanamycin subcutaneously (Sigma-Aldrich, St. Louis, MO, USA) and 100 mg/kg furosemide i.v. (Centrafarm, Etten-Leur, the Netherlands). Two weeks after deafening the animals were again anesthetized in order to confirm successful deafening through ABR recordings, and for the administration of the NFs to the right cochleas. The right bulla was exposed via retro-auricular approach. A small hole was drilled into the bulla to visualize the cochlear basal turn and round window niche. A ~1 mm^3 piece of gelatin sponge (Spongostan Dental; Ethicon, Somerville, NJ, USA) soaked in rhNGF (0.86 mg/ml; Dompé Pharmaceutici, Milan, Italy) or rhBDNF (6.67 mg/ml; PeproTech, Rocky Hill, NJ, USA) was placed into the round window niche, touching the perforated round-window membrane. The animals received non-ototoxic antibiotic enrofloxacin (Baytril; Bayer AG, Leverkusen, Germany; 5 mg/kg) and carprofen (Carporal; AST Farma, Oudewater, the Netherlands; 4 mg/kg) at the end of each surgery. Four weeks after treatment administration the animals were euthanized and the cochleas collected for subsequent analysis.

3.3. Tissue processing and histology

For histological analysis, the cochleas were fixed by an intra-labyrinthine infusion with a fixative solution containing 3% glutaraldehyde, 2% formaldehyde, 1% acrolein and 2.5% dimethyl sulfoxide (DMSO) in a 0.08 M sodium cacodylate buffer. The cochleas were then decalcified, post-fixated and embedded in Spurr's low-viscosity resin. Staining was performed using 1% methylene blue, 1% azur B and 1% borax in distilled water. The cochleas were subsequently divided into two halves along a standardized midmodiolar plane, then re-embedded in fresh resin, and cut to obtain semithin (1 μm) sections. More details about this procedure are reported in Kroon et al., 2017 [23]. The images were acquired by using a Leica DC300F digital camera mounted on a Leica DMRA light microscope with a 40x oil immersion objective (Leica Microsystems GmbH, Wetzlar, Germany).

3.4. Cell count analysis

Assessment of cell survival was conducted on the acquired images of the Organ of Corti from basal to apical turns and in the helicotrema (H): B1, B2, M1, M2, A1, A2, A3, H (Figure 2). B2 was excluded from statistical analysis because the organ of Corti was often missing due to technical processing of the cochlear sections. In addition to HCs, five types of supporting cells

were counted: Hensen's, Deiters', border, pillar, and inner phalangeal. In order to create a standardized method for cell counting, specific criteria, based on morphological aspects of the cells, were set up and used to include or exclude the cells from the analysis, as reported in Table 1. The average number of cells for each cytotype determined in NH guinea pigs was used to normalize the cell count, and data were therefore expressed as % of NH. Specific SC number of NH animals for each cochlear location is reported in paragraph 3.5.

Cell count results of SCs were correlated with SGC packing density of the same animal for each turn. SGC data were obtained from previous analysis [22].

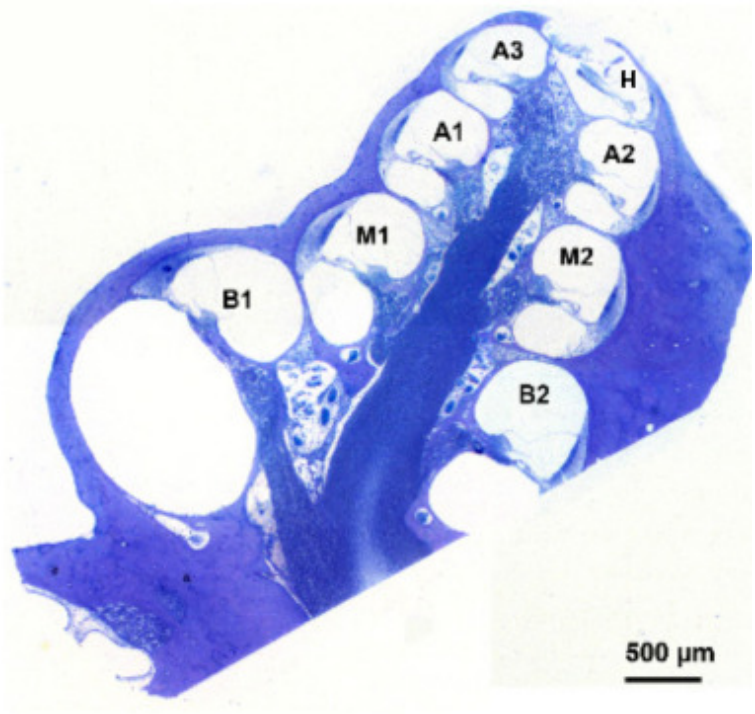

Figure 2. Representative cochlear cross-section. The image is representative of a cochlear midmodiolar section in which all the cochlear locations have been indicated by appropriate lettering: B1, B2, M1, M2, A1, A2, A3, H. The image has been modified from Vink et al., 2020 [22].

Cytotype	*Criteria for counting*	*Inclusion criteria*
IHC	1) Presence of the cuticular plate; 2) Nucleus at appropriate position; 3) Evident IHC cell edges at the expected position.	Cells included as IHC comply with point 1 and at least one of point 2 and 3.
OHC	1) Presence of the cuticular plate; 2) Nucleus at appropriate position; 3) Evident OHC cell edges at the expected OHC position.	Cells included as OHC comply with point 1 and at least one of point 2 and 3.
Deiters'	1) Evident cell edges; 2) Contact with the basilar membrane; 3) If visible, appropriate nucleus position	Cells included as Deiters' cells comply at least with points 1 and 2.
Pillar	1) Presence of a triangular cell shape in contact with the basilar membrane; 2) Presence of extensions that widen in the superior part of the Organ of Corti.	Cells included as Pillar comply with one of the counting criteria.
Phalangeal	1) Evident morphological cell edges; 2) Position immediately under the IHC or along the IHC side close to Pillar cells; 3) Presence of peculiar white spots; 4) If visible, appropriate nucleus position.	Cells included as Phalangeal comply with at least point 1 and 2.
Border	1) Evident morphological cell edges; 2) Cell counting starts from cells in contact with IHC to the inner sulcus cells (identified as bigger, cuboid and often white cells); 3) If visible, appropriate nucleus position.	Cells included as Border cells comply with at least point 1 and 2.
Hensen's	1) Evident morphological cell edges; 2) Presence of a nucleus; 3) If visible, presence of vacuoles.	Cells included as Hensen's comply with at least point 1 or 2.

Table 1. Criteria for the identification of specific sensory and non-sensory cells of the Organ of Corti. For each cell type, morphological aspects for their identification were determined and used to perform the cell count along the cochlear turns.

3.5. Determination of normalization factors

As a first step of the study, we focused on NH guinea pig cochleas and analyzed the number of SCs for each cochlear turn in order to set up the normalization numbers to be used for the other analysis. To better identify the cell types present in the Organ of Corti, a color coding cell signature was performed on the images to highlight the cell edges (Figure 3A,B,C). HCs were included in the analysis. SCs number did not differ between the cochlear turns for pillar, Deiters' and phalangeal cells. Small differences were found in the number of border cells that

did not vary between the cochlear locations (not shown). On this basis, the normalization values were the same for each cochlear turn: pillar (2 cells/turn=100%), Deiters' (3 cells/turn=100%), phalangeal (1 cell/turn=100%), border (3 cells/turn=100%). Conversely, Hensen's cell number increased from base to apex (Figure 3D). On this basis, different normalization factors were set up for Hensen's cells depending on the turn considered based on the average number obtained from NH cochleas: B1,B2:3cells/turn=100%; M1,M2:4 cells/turn=100%; A1:5 cells/turn=100%; A2,A3,H:6 cells/turn=100%. The increase of Hensen's cell number towards the apex was accompanied by a change in morphology, with the apical Hensen's cells rich in lipid droplets (Figure 3 C, black arrows), as also reported in the literature [24].

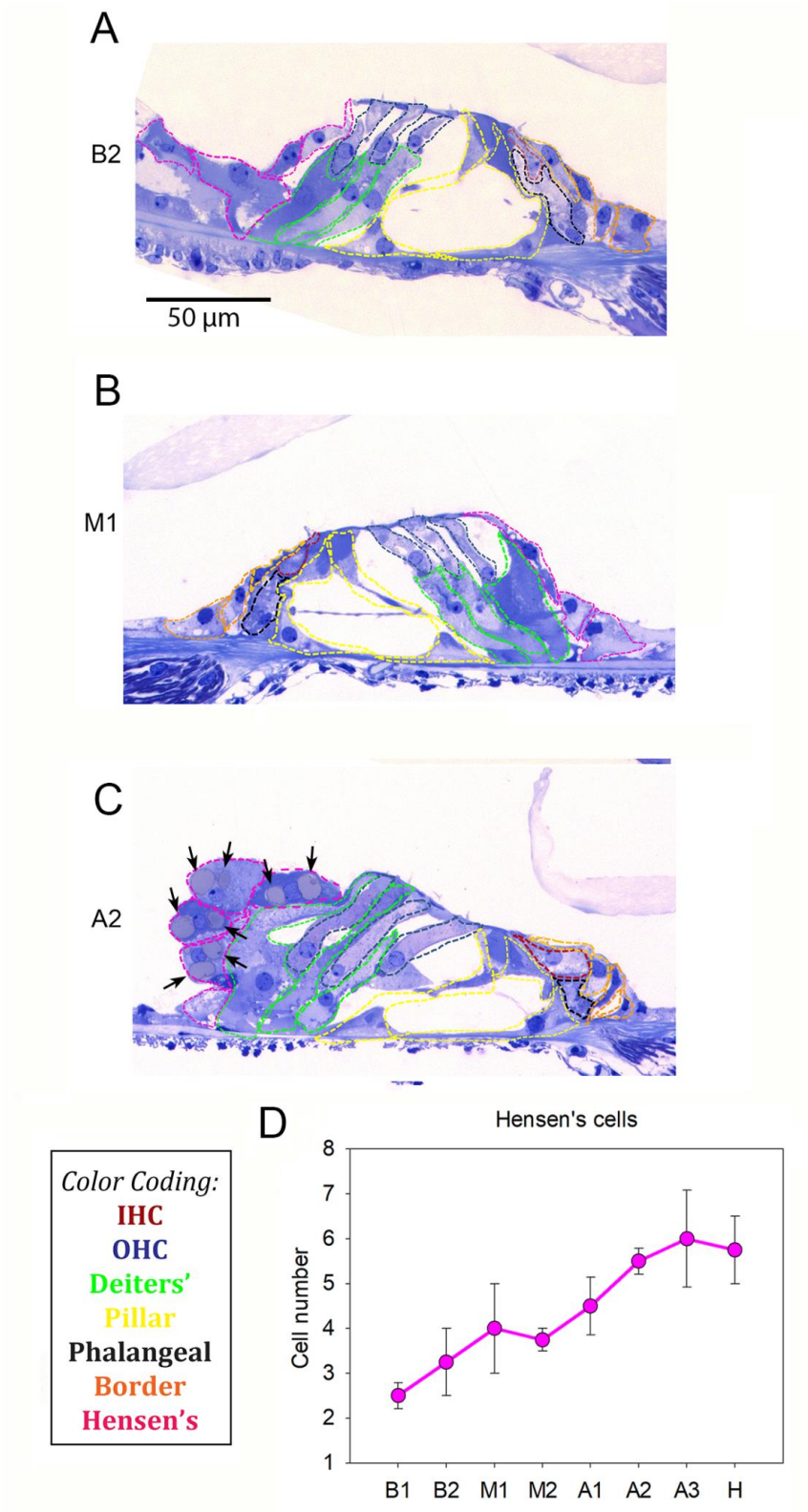

Figure 3. The Organ of Corti in Normal Hearing guinea pigs. Representative images of a (A) B2, (B) M1 and (C) A2 turn from a NH guinea pig cochlea. Hair cells and supporting cells were identified by using the color coding reported in the black frame: Inner Hair Cells (red), Outer Hair Cells (blue), Deiters' (green), pillar (yellow), phalangeal (black), border (orange) and Hensen's (pink). The black arrows indicate the vacuoles present in the hensen's cells of the apical turn. (D) Hensen's cell count along the cochlear turns of NH guinea pigs shows an increase from base to apex.

3.6. Statistical analysis

For statistical analysis of cell count in the Organ of Corti, non-parametric statistical tests were applied, that are the Mann Whitney and Wilcoxon tests. The Student's t-test was performed for the analysis of SGC packing density. The statistical analysis was conducted by using the SigmaPlot 12.0 software. Data are shown as mean ± SE.

4. Results

4.1. Analysis of rhNGF-treated animals

We proceeded by analyzing the rhNGF-treated animals. At 6 weeks after deafening, the organ of Corti appeared clearly damaged in both treated and untreated animals (Figure 4). A more severe degeneration was observed in the basal turns compared to the apical ones, which is in agreement with the literature [9].

A first analysis on the sensory hair cells (Figure 5) revealed that the number of cells was not different between treated and untreated ears in each turn for both OHC (Figure 5A) and IHC (Figure 5C). We also analyzed the total number of HCs over all cochlear locations for individual animals (Figure 5B,D). The data distribution observed in the scatter plot graphs shows that no differences in the number of OHC (Figure 5B) and IHC (Figure 5D) existed between treated right ear and untreated left ear within individual animals. Figure 4E shows representative images of the organ of Corti of treated and untreated ears, in which OHC and IHC were highlighted in blue and red respectively.

Also the number of SCs did not differ between treated and untreated ears in each cochlear turn for Deiters' (Figure 6A), phalangeal (Figure 6C), pillar (Figure 6E), border (Figure 6G) and Hensen's cells (Figure 6I). The same trend was confirmed when comparing the total number of each SC type for individual animals (Figure 6B, D, F, H, L).

As observed for the degree of damage observed in the Organ of Corti, the SGC packing density was similar between treated and untreated ears in basal, middle and apical turns. SGC packing density plotted against the total number of SCs (Figure 7), showed no correlation between the two parameters either considering the average number of the experimental groups (Figure 7A) and the cochleas of individual animals (Figure 7B, C, D, E).

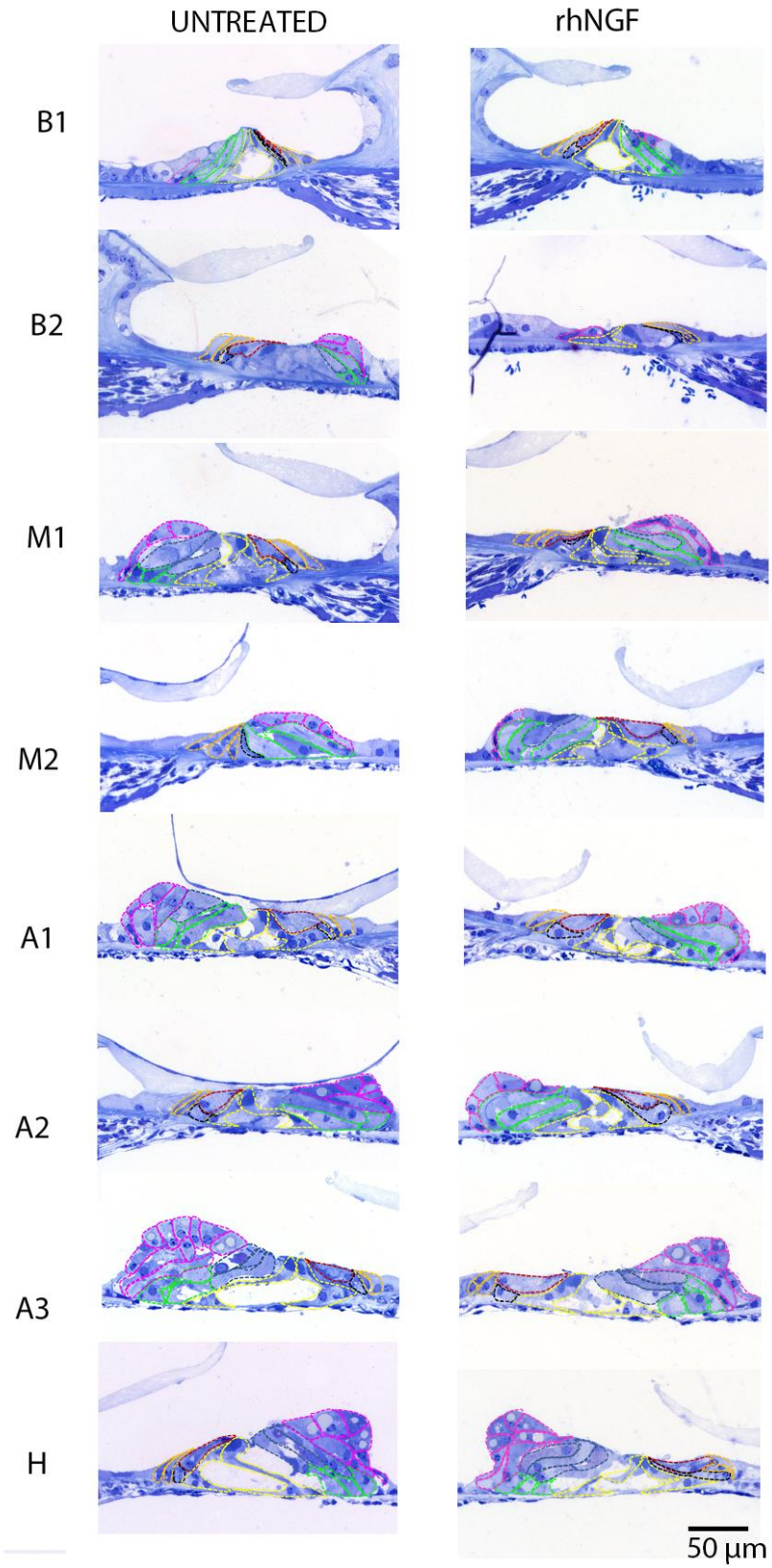

Figure 4. Representative images of the Organ of Corti from rhNGF-treated animals. Microscope picture are representative of the Organ of Corti of untreated (left) and rhNGF-treated cochleas (right) over all cochlear locations: B1, B2, M1, M2, A1, A2, A3, H. Hair cells and supporting cells were identified by using the color coding reported in the black frame: Inner Hair Cells (red), Outer Hair Cells (blue), Deiters' (green), pillar (yellow), phalangeal (black), border (orange) and Hensen's (pink).

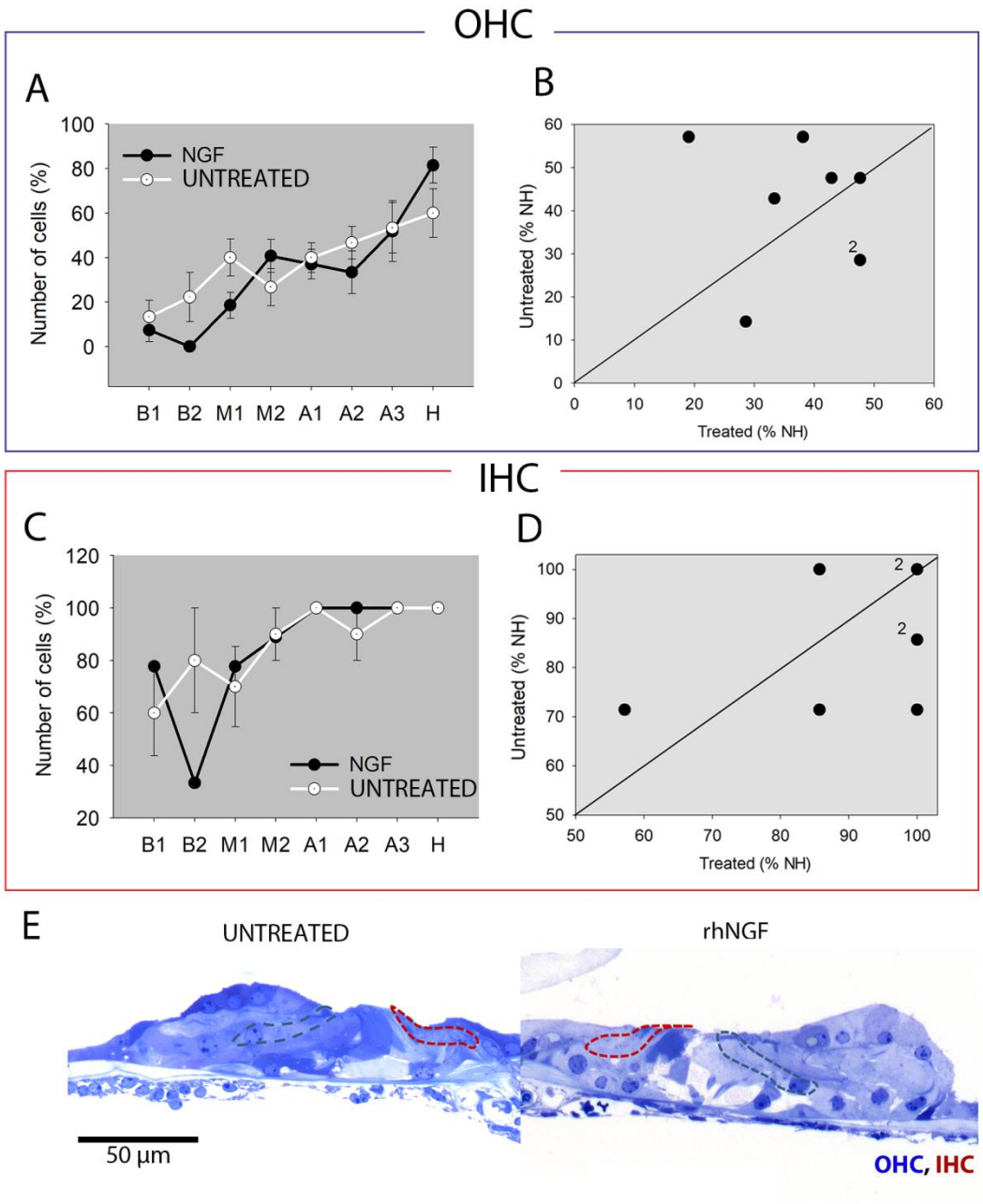

Figure 5. Cell count of sensory cells in the Organ of Corti of rhNGF-treated animals. (A,B) Cell count of Outer Hair cells (OHC) and (C,D) Inner Hair cells (IHC). (A, C) Cell count of OHC and IHC respectively for each cochlear turn of rhNGF-treated and untreated ears; graphs are shown as mean ± SE (rhNGF: B1:n=8, B2:n=2, M1-H:n=9; UNTREATED: B1, M1-H:n=10, B2:n=3). (B, D) Scatter plot showing the number of OHC and IHC respectively of untreated versus treated cochleas of individual animals (n=8). Data are expressed as % of NH (100%). (E) Representative images of the Organ of Corti of A1 location in treated and untreated cochleas; OHC and IHC are highlighted in blue and red respectively.

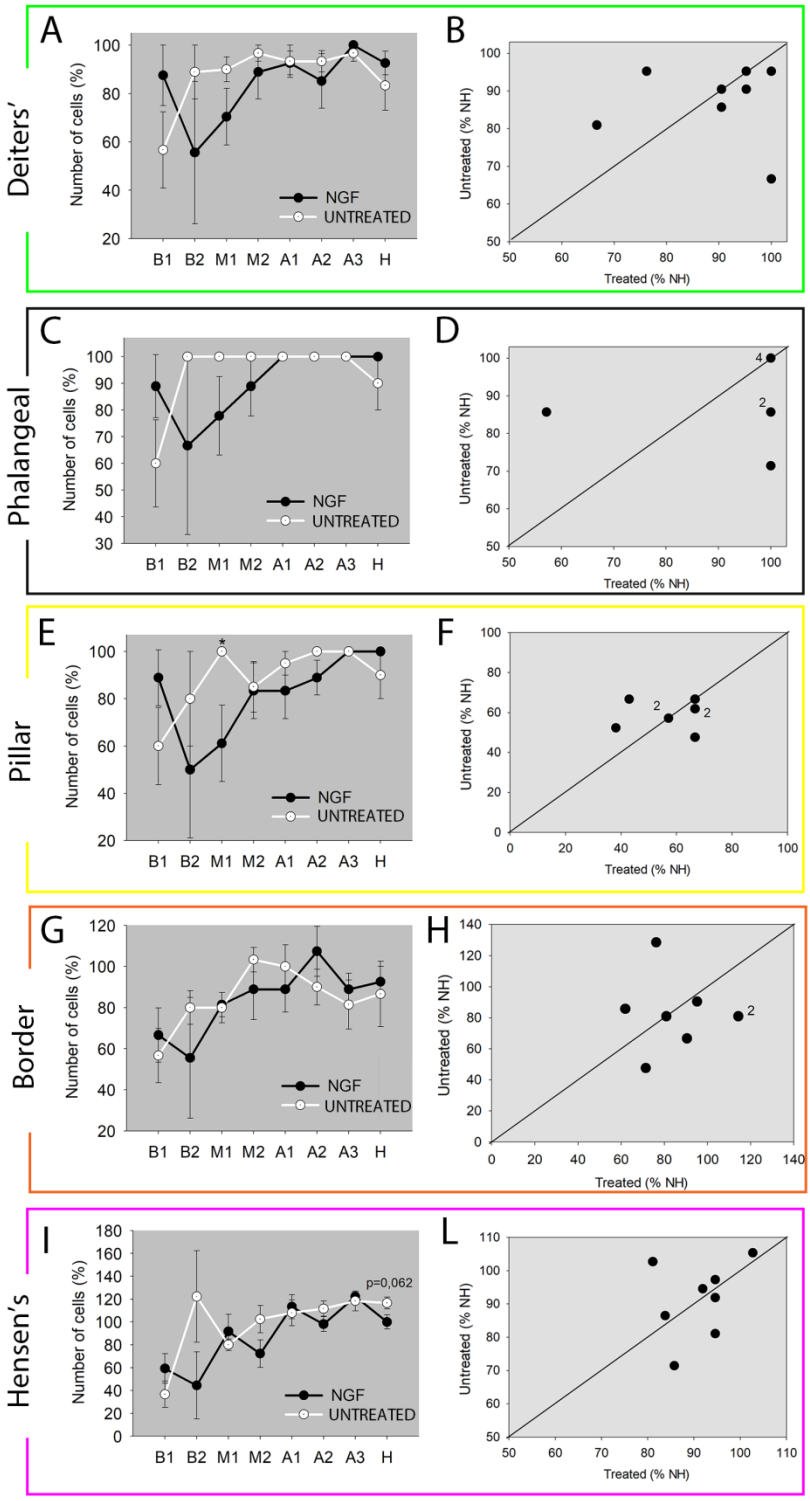

Figure 6. Cell count of non-sensory cells in the Organ of Corti of rhNGF-treated animals. Cell count of (A,B) deiters', (C,D) phalangeal, (E,F) pillar, (G,H) border, and (I,L) hensen's cells. (A, C, E, G, I) Cell count of each SC type for each cochlear turn of rhNGF-treated and untreated ears; graphs are shown as mean ± SE (rhNGF: B1:n=8, B2:n=3, M1-H:n=9; UNTREATED: B1, M1-H:n=10, B2:n=3-5). Statistical analysis: Mann-Whitney test. (B, D, F, H, I) Scatter plot showing the total number of SCs of untreated versus treated cochleas of individual animals (n=8). Data are expressed as % of NH (100%).

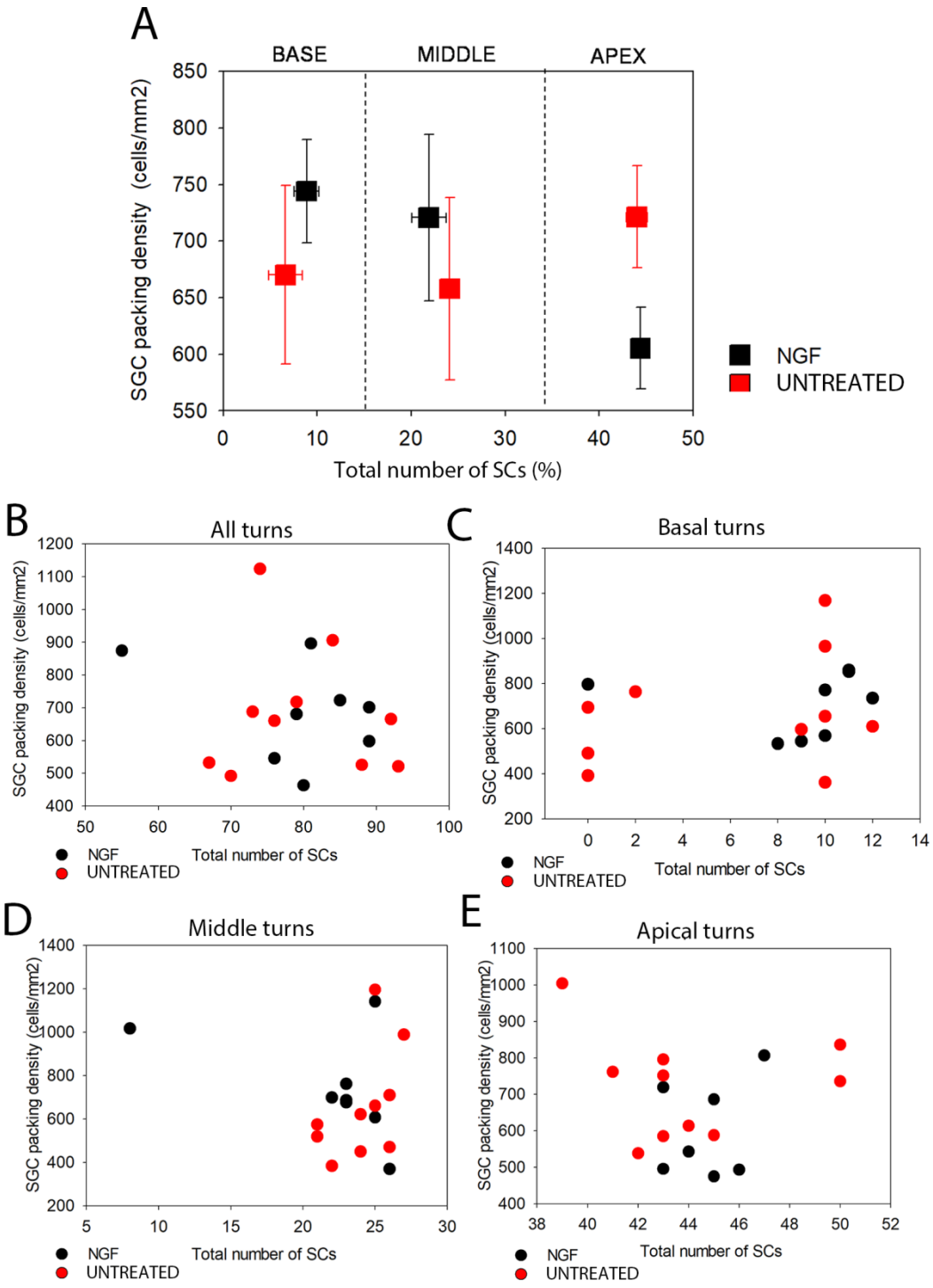

Figure 7. Correlation between SGC packing density and SCs number of rhNGF-treated animals. (A) Correlation between the Spiral Ganglion cells (SGC) packing density and the total number of Supporting Cells in basal, middle and apical turns of rhNGF-treated and untreated cochleas averaged by treatment group. The graph is expressed as mean ± SE. (B,C,D,E) Scatter plot correlating SGC packing density and SCs number for individual animals comparing the treated and untreated ears. (SGC packing density rhNGF and UNTREATED n=10; Supporting cells 6WD n=10 (B and M), n=9 (A and all turns); Supporting cells rhNGF n=8). Basal turn: B1 (B2 was excluded because the Organ of Corti of that location was often missing); Middle turns: M1, M2; Apical turns: A1, A2, A3; Total: B1, M1, M2, A1, A2, A3.

4.2. Analysis of rhBDNF-treated animals

As observed in rhNGF-treated animals, also the rhBDNF-treated ones displayed evident signs of degeneration in both treated and untreated cochleas. Figure 7 shows some representative images of the Organ of Corti from treated and untreated ears for each cochlear location.

Cell count of OHC revealed that the rhBDNF-treated group presented fewer cells at A3 location compared to the untreated one, with a statistically significant difference ($p=0.041$) (Figure 8A). The difference in OHC number was even more evident in the scatter plot obtained comparing the total number of OHC over all cochlear locations for individual animals (Figure 8B). Accordingly, the overall difference of OHC number between treated and untreated ears of individual animals was statistically significant ($p=0.019$). Conversely, the IHC number averaged by experimental group did not vary between treated and untreated ears for each cochlear turn (Figure 8C). Similarly, no differences were found between treated and untreated cochleas of individual animals considering the total number of IHC over all cochlear locations (Figure 8D).

The analysis of SCs (Figure 9) demonstrated very similar cell numbers for each supporting cell type for all the cochlear turns (Figure 9A, C, E, G, I). Similarly, the comparison of total cell number between treated and untreated cochleas of individual animals was not different for all the supporting cell types, except for the Hensen's cells, which resulted to be increased in the untreated ears compared to the contralateral treated ones (Figure 9B, D, F, H, L).

Finally, we correlated the SGC packing density with the total number of SCs, considering the total amount derived from the sum of all the SC types (Figure 10). The rhBDNF-treated group showed a significantly increased SGC packing density in the basal turns compared to the untreated group ($p<0.001$) (Figure 10 A) as previously reported [22]. Conversely, the SGC packing density was similar between treated and untreated ears in the middle and apical turns (Figure 10 A). Moreover, this data was not associated with any differences in the total SC number, that instead was similar between treated and untreated ears in the basal, middle and apical turns (Figure 10 A). Likewise, SGC packing density plotted against the total number of SCs of individual animals, showed no correlation between the two parameters (Figure 10 B, C, D, E).

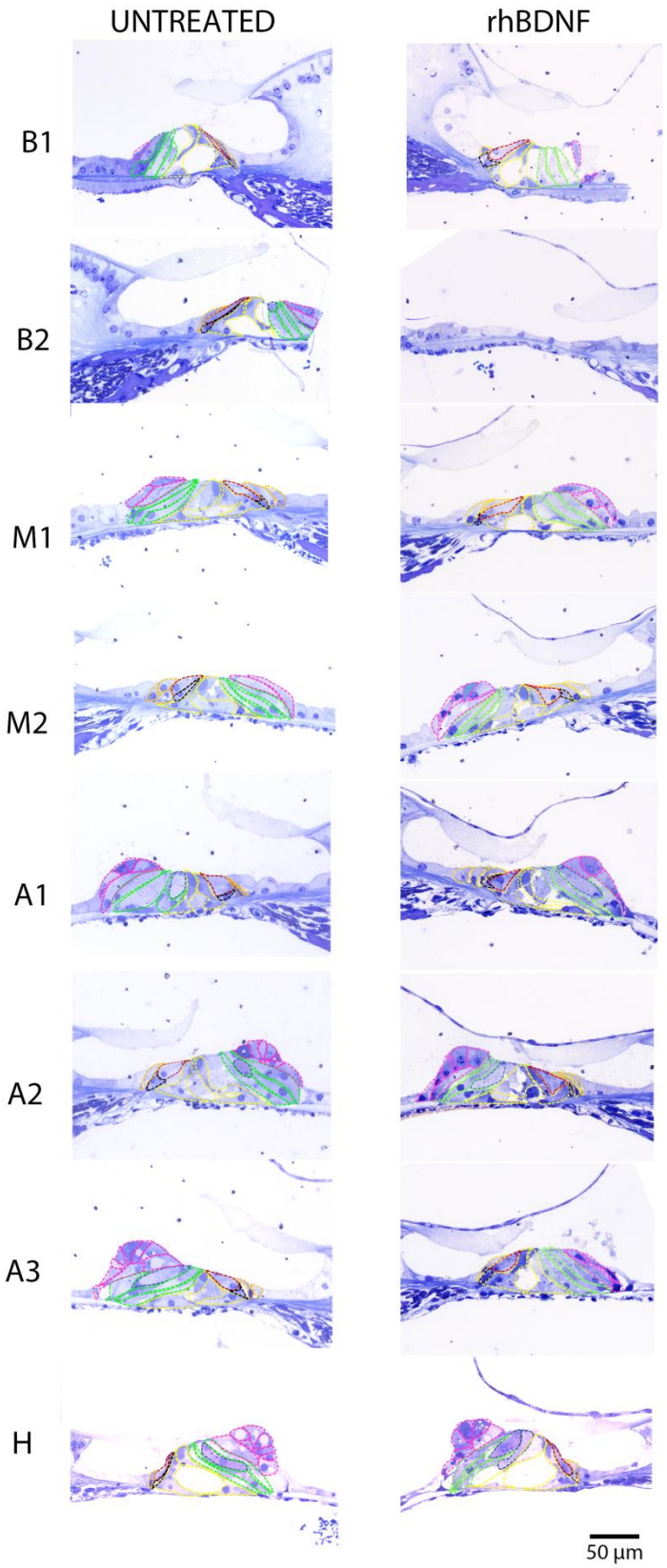

Figure 7. Representative images of the Organ of Corti from rhBDNF-treated animals. Microscope picture are representative of the Organ of Corti of untreated (left) and rhBDNF-treated cochleas (right) of all cochlear locations: B1, B2, M1, M2, A1, A2, A3, H. Hair cells and supporting cells were identified by using the color coding reported in the black frame: Inner Hair Cells (red), Outer Hair Cells (blue), Deiters' (green), pillar (yellow), phalangeal (black), border (orange) and Hensen's (pink).

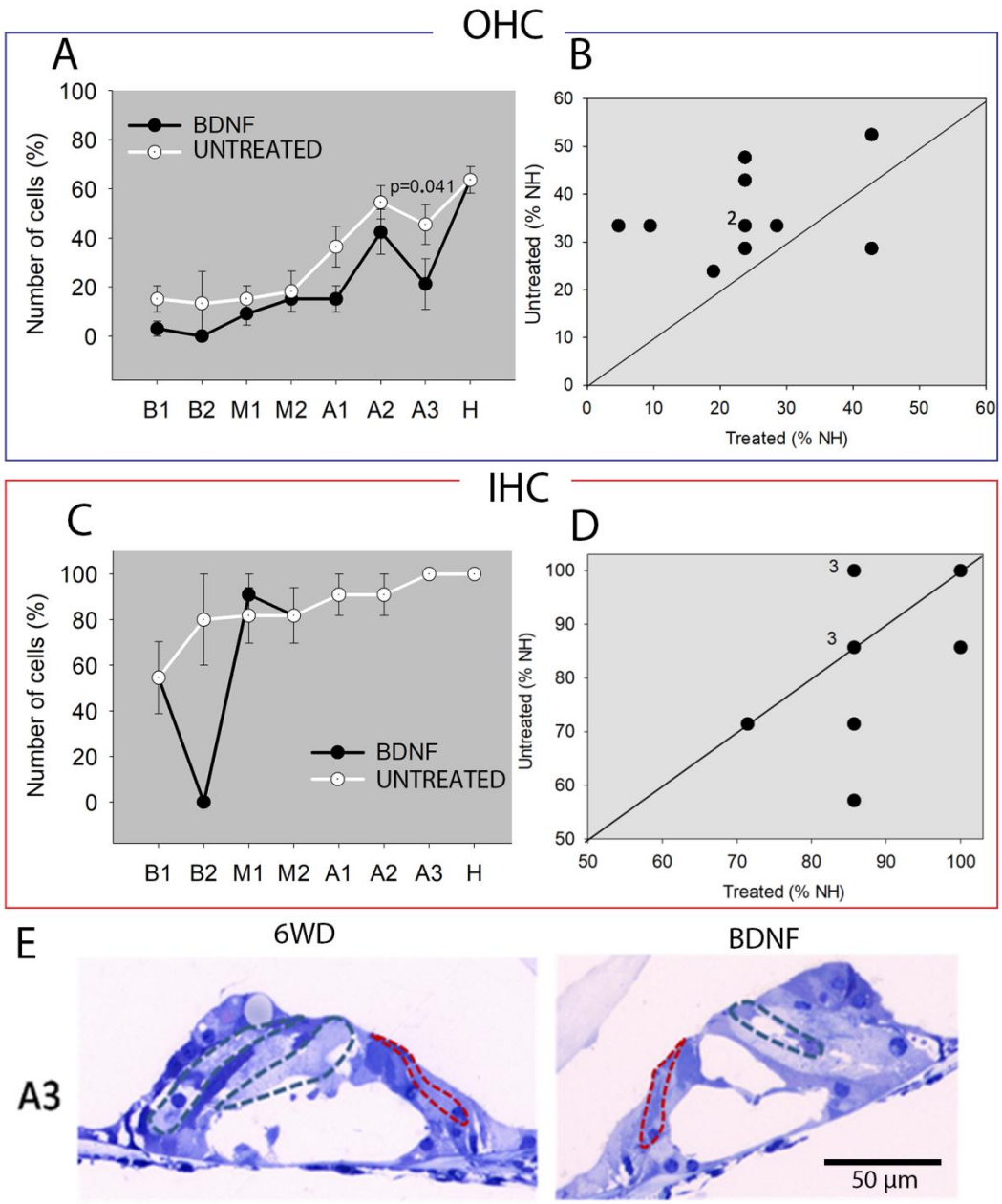

Figure 8. Cell count of sensory cells in the Organ of Corti of rhBDNF-treated animals. (A,B) Cell count of Outer Hair cells (OHC) and (C,D) Inner Hair cells (IHC). (A, C) Cell count of OHC and IHC respectively for each cochlear turn of rhBDNF-treated and untreated ears; graphs are shown as mean ± SE (n=11). (B, D) Scatter plot showing the number of OHC and IHC respectively of untreated versus treated cochleas of individual animals; statistical analysis: Wilcoxon test (n=11). Data are expressed as % of NH (100%). (E) Representative images of the Organ of Corti of A3 location in treated and untreated cochleas; OHC and IHC are highlighted in blue and red respectively.

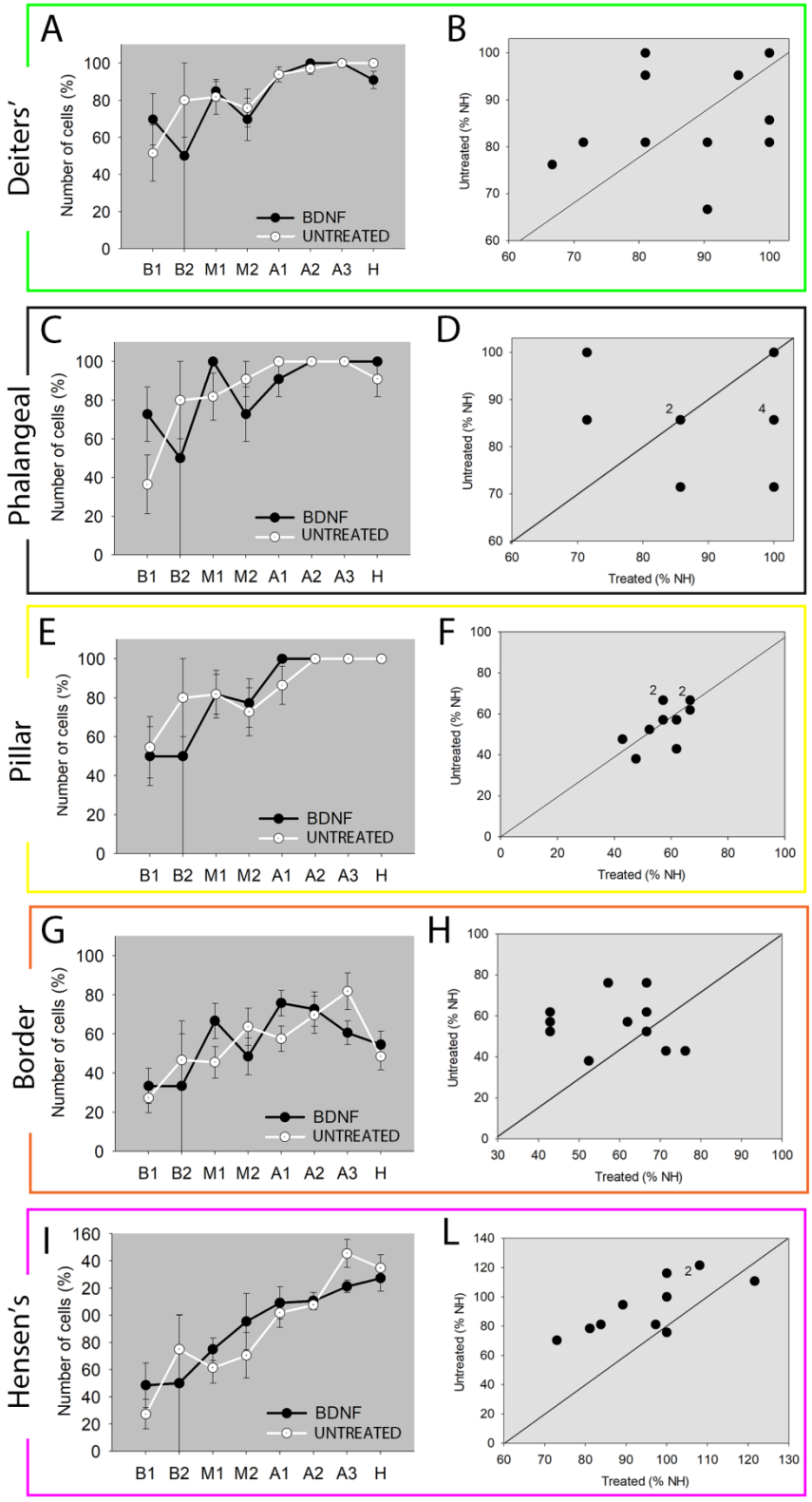

Figure 9. Cell count of non-sensory cells in the Organ of Corti of rhBDNF-treated animals. Cell count of (A,B) deiters', (C,D) phalangeal, (E,F) pillar, (G,H) border, and (I,L) hensen's cells. (A, C, E, G, I) Cell count of each SC type for each cochlear turn of rhBDNF-treated and untreated ears; graphs are shown as mean ± SE (n=11). (B, D, F, H, I) Scatter plot showing the total number of SCs of untreated versus treated cochleas of individual animals (n=11). Data are expressed as % of NH (100%).

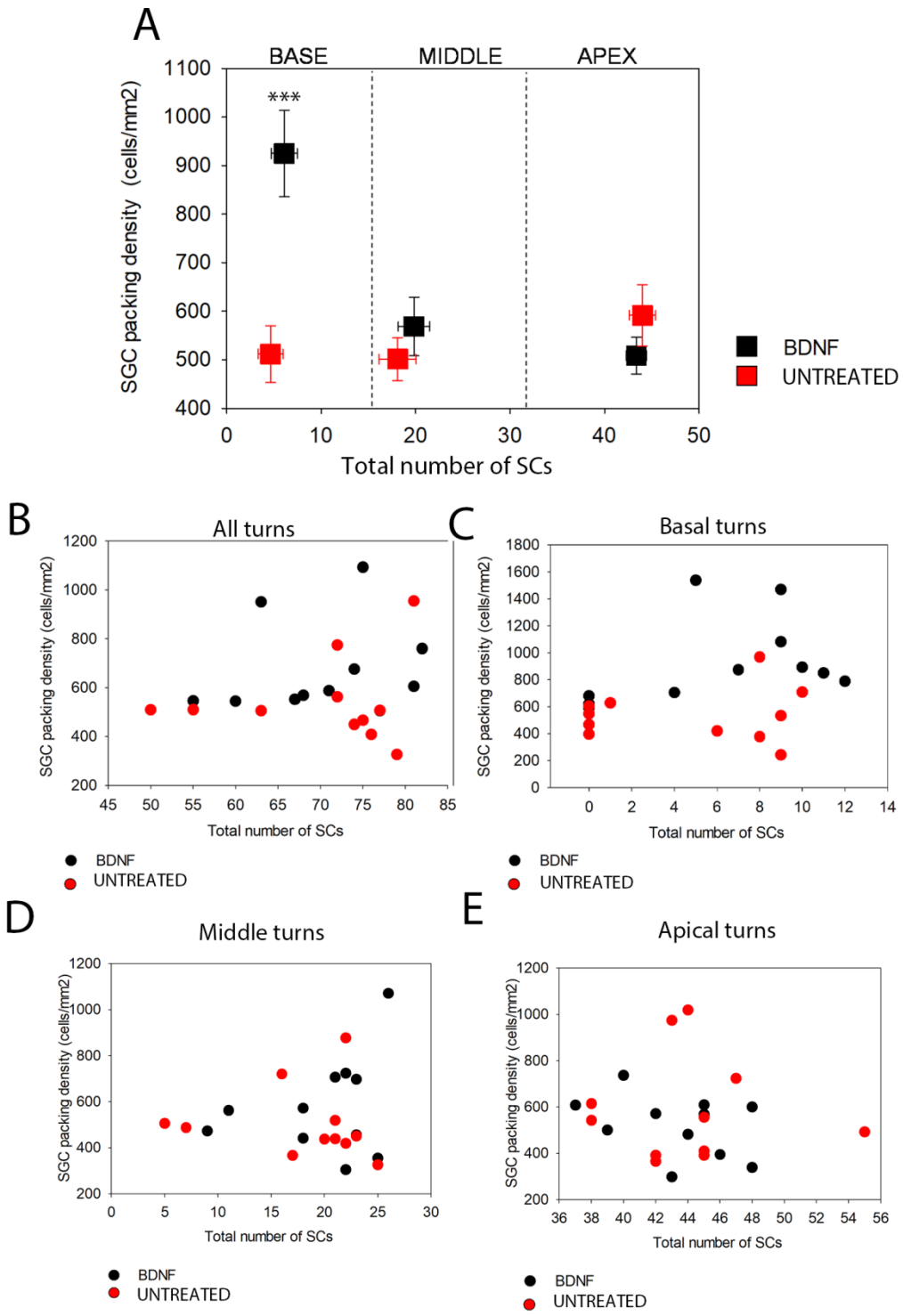

Figure 10. Correlation between SGC packing density and SCs number of rhBDNF-treated animals. (A) Correlation between the Spiral Ganglion cells (SGC) packing density and the total number of Supporting Cells in basal, middle and apical turns of rhBDNF-treated and untreated cochleas averaged by treatment group. The graph is expressed as mean ± SE (SGC packing density: n=12; Total number of supporting cells: n=11). Statistical analysis refers to SGC packing density; statistical test: Student's t-test, *** p<0.001. (B,C,D,E) Scatter plot correlating SGC packing density and SCs number for individual animals comparing the treated and untreated ears (*n=11*). *Basal turn: B1 (B2 was excluded because the Organ of Corti of that location was often missing); Middle turns: M1, M2; Apical turns: A1, A2, A3; Total: B1, M1, M2, A1, A2, A3.*

5. Discussion

Neurotrophic factors (NFs) are a family of proteins, which have been demonstrated to have an essential role in the development, survival, plasticity and protection of the peripheral and central nervous system [25]. Among these, the neurotrophins form a subclass of NFs and include: nerve growth factor (NGF), brain-derived neurotrophic factor (BDNF), neurotrophin-3 (NT-3) and neurotrophin-4/5 (NT-4/5; also called neurotrophin-4 or NT-4) [26]. BDNF is the most abundant neurotrophin of the brain and is essential for ear development and survival [27,28]. Conversely, NGF is not required for the development of the inner ear, but plays a major role in the mature cochlea [29–31]. BDNF administration resulted to be effective in preventing SGCs death following hair cells degeneration in vivo [32–36]. Conversely, the therapeutic efficacy of NGF in the treatment of hearing loss has been only sparsely investigated compared to BDNF [37,38].

In the present study, we investigated the effects of rhNGF and rhBDNF on the different cytotypes of the organ of Corti in ototoxically deafened guinea pigs. Our analysis was mainly focused on the cell number of both sensory and non-sensory cells and did not take into account any functional aspects of those cells. The findings of our study seem to indicate that rhNGF and rhBDNF do not protect the HCs and SCs from degeneration after ototoxic trauma. However, some considerations regarding this result are in order. First, the treatment was administered two weeks after damage induction. In principle, the experiment was designed with the aim of investigating the protective effects of the neurotrophic factors on SGCs [20], which degenerate as a consequence of HCs death. For this reason, the treatment was administered when a high degree of damage had already occurred in the organ of Corti. It is therefore possible that the effects of the treatments may not be appreciable in these experimental conditions, although the organ of Corti was not completely degenerated and a sufficient number of HCs and SCs was still detectable. Nonetheless, a previous study from Shoji and colleagues demonstrated that BDNF administered through osmotic pump was not able to prevent OHC degeneration in noise-induced deafened guinea pigs even when the treatment started 4 days before damage and continued until one week after [39]. Likewise, BDNF administered through osmotic pump was not effective in protecting HCs in guinea pigs deafened by kenamycin [40]. Our data, together with the literature, suggest that BDNF is likely not effective in protecting the organ of Corti. However, in our experimental design we did not consider any other intermediate time points that would allow to have a wider overview of degeneration processes and the possible protective effects by both NFs.

An interesting result is related to the small decrease of OHC number in the BDNF-treated ears. This data could be associated with surgical trauma due to BDNF administration and/or electrode array insertion [22], however there is apparently no clear explanation for this evidence since the same interventions were performed in the NGF experiments. Nevertheless, the SGC packing density was significantly increased in the basal turns of BDNF-treated ears. Note that OHCs are unlikely to protect SGCs which for about 95% innervate IHCs, and therefore SGC survival is not related to OHC survival [23,41]. Unlike BDNF, NGF did not enable a preservation of the SGC packing density. A direct comparison with the BDNF-treated animals cannot be made due to the different concentrations used for NGF (0.86 mg/ml) and BDNF (6.67 mg/ml), that could importantly affect the result of the study. Nevertheless, for both treatments the number of SCs did not represent a determinant factor for SGC survival. Therefore, the positive effects on the SGC packing density associated with rhBDNF administration leads one to consider a direct targeting of SGCs by the neurotrophin. Another hypothesis is that the treatment could allow a preservation of the function of surviving supporting cells, for instance promoting the secretion of additional growth and survival factors, that in turn could influence the health of SGCs. Additional studies on the molecular and functional aspects of the remaining supporting cells, as well as a more detailed time course analysis, could allow a deeper understanding of the most specific mechanisms underlying the crosstalk between the sensory epithelium, the SGCs and neurotrophic factors.

6. References

1. Lim, D.J. Functional structure of the organ of Corti: a review. *Hear. Res.* 1986, *22*, 117–146.
2. Wan, G.; Corfas, G.; Stone, J.S. Inner ear supporting cells: Rethinking the silent majority. *Semin. Cell Dev. Biol.* 2013, *24*, 448–459.
3. Monzack, E.L.; Cunningham, L.L.; Gov, E.M. Lead roles for supporting actors: critical functions of inner ear supporting cells. *Hear Res.* **2013**, *303*, 20–29, doi:10.1016/j.heares.2013.01.008.
4. Waldhaus, J.; Durruthy-Durruthy, R.; Heller, S. Quantitative High-Resolution Cellular Map of the Organ of Corti. *Cell Rep.* **2015**, *11*, 1385–1399, doi:10.1016/j.celrep.2015.04.062.
5. Pujol, R.; Lenoir, M.; Ladrech, S.; Tribillac, F.; Rebillard, G. Correlation Between the Length of Outer Hair Cells and the Frequency Coding of the Cochlea. In *Auditory Physiology and Perception*; Elsevier, 1992; pp. 45–52.
6. Cunningham, L.L.; Tucci, D.L. Hearing Loss in Adults. *N. Engl. J. Med.* **2017**, *377*, 2465–2473, doi:10.1056/NEJMra1616601.
7. GBD 2015 Disease and Injury Incidence and Prevalence Collaborators, G. 2015 D. and I.I. and P. Global, regional, and national incidence, prevalence, and years lived with disability for 310 diseases and injuries, 1990-2015: a systematic analysis for the Global Burden of Disease Study 2015. *Lancet (London, England)* **2016**, *388*, 1545–1602, doi:10.1016/S0140-6736(16)31678-6.
8. Haile, L.M.; Kamenov, K.; Briant, P.S.; Orji, A.U.; Steinmetz, J.D.; Abdoli, A.; Abdollahi, M.; Abu-Gharbieh, E.; Afshin, A.; Ahmed, H.; et al. Hearing loss prevalence and years lived with disability, 1990–2019: findings from the Global Burden of Disease Study 2019. *Lancet* **2021**, *397*, 996–1009, doi:10.1016/S0140-6736(21)00516-X.
9. Versnel, H.; Agterberg, M.J.H.; de Groot, J.C.M.J.; Smoorenburg, G.F.; Klis, S.F.L. Time course of cochlear electrophysiology and morphology after combined administration of kanamycin and furosemide. *Hear. Res.* **2007**, *231*, 1–12, doi:10.1016/j.heares.2007.03.003.
10. Shepherd, R.K.; Hardie, N.A. Deafness-Induced Changes in the Auditory Pathway: Implications for Cochlear Implants. *Audiol. Neuro-Otology* **2001**, *6*, 305–318, doi:10.1159/000046843.
11. Webster, M.; Webster, D.B. Spiral ganglion neuron loss following organ of corti loss: A quantitative study. *Brain Res.* **1981**, *212*, 17–30, doi:10.1016/0006-8993(81)90028-7.

12. Kamakura, T.; Nadol, J.B. Correlation between word recognition score and intracochlear new bone and fibrous tissue after cochlear implantation in the human. *Hear. Res.* **2016**, *339*, 132–141, doi:10.1016/j.heares.2016.06.015.
13. Sugawara, M.; Corfas, G.; Liberman, M.C. Influence of Supporting Cells on Neuronal Degeneration After Hair Cell Loss. *JARO - J. Assoc. Res. Otolaryngol.* **2005**, *6*, 136–147, doi:10.1007/s10162-004-5050-1.
14. Raphael, Y.; Kim, Y.-H.; Osumi, Y.; Izumikawa, M. Non-sensory cells in the deafened organ of Corti: approaches for repair. *Int. J. Dev. Biol.* **2007**, *51*, 649–654, doi:10.1387/ijdb.072370yr.
15. Taylor, R.R.; Jagger, D.J.; Forge, A. Defining the Cellular Environment in the Organ of Corti following Extensive Hair Cell Loss: A Basis for Future Sensory Cell Replacement in the Cochlea. *PLoS One* **2012**, *7*, e30577, doi:10.1371/journal.pone.0030577.
16. Takada, Y.; Beyer, L.A.; Swiderski, D.L.; O'Neal, A.L.; Prieskorn, D.M.; Shivatzki, S.; Avraham, K.B.; Raphael, Y. Connexin 26 null mice exhibit spiral ganglion degeneration that can be blocked by BDNF gene therapy. *Hear. Res.* **2014**, *309*, 124–135, doi:10.1016/j.heares.2013.11.009.
17. Budenz, C.L.; Wong, H.T.; Swiderski, D.L.; Shibata, S.B.; Pfingst, B.E.; Raphael, Y. Differential effects of AAV.BDNF and AAV.Ntf3 in the deafened adult guinea pig ear. *Sci. Rep.* **2015**, *5*, doi:10.1038/srep08619.
18. Shu, Y.; Li, W.; Huang, M.; Quan, Y.Z.; Scheffer, D.; Tian, C.; Tao, Y.; Liu, X.; Hochedlinger, K.; Indzhykulian, A.A.; et al. Renewed proliferation in adult mouse cochlea and regeneration of hair cells. *Nat. Commun.* **2019**, *10*, doi:10.1038/s41467-019-13157-7.
19. Bezdjian, A.; Kraaijenga, V.J.C.; Ramekers, D.; Versnel, H.; Thomeer, H.G.X.M.; Klis, S.F.L.; Grolman, W. Towards clinical application of neurotrophic factors to the auditory nerve; assessment of safety and efficacy by a systematic review of neurotrophic treatments in humans. *Int. J. Mol. Sci.* 2016, *17*.
20. Schulze, J.; Staecker, H.; Wedekind, D.; Lenarz, T.; Warnecke, A. Expression pattern of brain-derived neurotrophic factor and its associated receptors: Implications for exogenous neurotrophin application. *Hear. Res.* **2020**, doi:10.1016/j.heares.2020.108098.
21. Dai, C.F.; Steyger, P.S.; Wang, Z.M.; Vass, Z.; Nuttall, A.L. Expression of Trk A receptors in the mammalian inner ear. *Hear. Res.* **2004**, *187*, 1–11, doi:10.1016/S0378-5955(03)00277-6.
22. Vink, H.A.; van Dorp, W.C.; Thomeer, H.G.X.M.; Versnel, H.; Ramekers, D. Bdnf

outperforms trkb agonist 7,8,3′-thf in preserving the auditory nerve in deafened guinea pigs. *Brain Sci.* **2020**, *10*, 1–20, doi:10.3390/brainsci10110787.

23. Kroon, S.; Ramekers, D.; Smeets, E.M.; Hendriksen, F.G.J.; Klis, S.F.L.; Versnel, H. Degeneration of auditory nerve fibers in guinea pigs with severe sensorineural hearing loss. *Hear. Res.* **2017**, *345*, 79–87, doi:10.1016/j.heares.2017.01.005.
24. Merchan, M.A.; Merchan, J.A.; Ludena, M.D. Morphology of Hensen's cells. *J. Anat.* **1980**, *131*, 519–523.
25. Skaper, S.D. Neurotrophic Factors: An Overview. In; Humana Press, New York, NY, 2018; pp. 1–17.
26. Ramekers, D.; Versnel, H.; Grolman, W.; Klis, S.F.L. Neurotrophins and their role in the cochlea. *Hear. Res.* 2012, *288*, 19–33.
27. Schimmang, T.; Tan, J.; Müller, M.; Zimmermann, U.; Rohbock, K.; Köpschall, I.; Limberger, A.; Minichiello, L.; Knipper, M. Lack of Bdnf and TrkB signalling in the postnatal cochlea leads to a spatial reshaping of innervation along the tonotopic axis and hearing loss. *Development* **2003**, *130*, 4741–4750, doi:10.1242/dev.00676.
28. Ylikoski, J.; Pirvola, U.; Moshnyakov, M.; Palgi, J.; Arumäe, U.; Saarma, M. Expression patterns of neurotrophin and their receptor mRNAs in the rat inner ear. *Hear. Res.* **1993**, *65*, 69–78, doi:10.1016/0378-5955(93)90202-C.
29. Schimmang, T.; Alvarez-Bolado, G.; Minichiello, L.; Vazquez, E.; Giraldez, F.; Klein, R.; Represa, J. Survival of inner ear sensory neurons in trk mutant mice. *Mech. Dev.* **1997**, *64*, 77–85, doi:10.1016/s0925-4773(97)00047-6.
30. Després, G.; Hafidi, A.; Romand, R. Immunohistochemical localization of nerve growth factor receptor in the cochlea and in the brainstem of the perinatal rat. *Hear. Res.* **1991**, *52*, 157–65, doi:10.1016/0378-5955(91)90195-f.
31. Dai, C.F.; Steyger, P.S.; Wang, Z.M.; Vass, Z.; Nuttall, A.L. Expression of Trk A receptors in the mammalian inner ear. *Hear. Res.* **2004**, *187*, 1–11, doi:10.1016/s0378-5955(03)00277-6.
32. Gillespie, L.N.; Clark, G.M.; Marzella, P.L. Delayed neurotrophin treatment supports auditory neuron survival in deaf guinea pigs. *Neuroreport* **2004**, *15*, 1121–1125, doi:10.1097/00001756-200405190-00008.
33. Agterberg, M.J.H.; Versnel, H.; de Groot, J.C.M.J.; Smoorenburg, G.F.; Albers, F.W.J.; Klis, S.F.L. Morphological changes in spiral ganglion cells after intracochlear application of brain-derived neurotrophic factor in deafened guinea pigs. *Hear. Res.* **2008**, *244*, 25–34, doi:10.1016/j.heares.2008.07.004.

34. McGuinness, S.L.; Shepherd, R.K. Exogenous BDNF rescues rat spiral ganglion neurons in vivo. *Otol. Neurotol.* **2005**, *26*, 1064–1072, doi:10.1097/01.mao.0000185063.20081.50.
35. Ramekers, D.; Versnel, H.; Strahl, S.B.; Klis, S.F.L.; Grolman, W. Temporary neurotrophin treatment prevents deafness- induced auditory nerve degeneration and preserves function. *J. Neurosci.* **2015**, *35*, 12331–12345, doi:10.1523/JNEUROSCI.0096-15.2015.
36. Vink, H.A.; Versnel, H.; Kroon, S.; Klis, S.F.L.; Ramekers, D. BDNF-mediated preservation of spiral ganglion cell peripheral processes and axons in comparison to that of their cell bodies. *Hear. Res.* **2021**, *400*, 108114, doi:10.1016/j.heares.2020.108114.
37. Han, Z.; Wang, C.P.; Cong, N.; Gu, Y.Y.; Ma, R.; Chi, F.L. Therapeutic value of nerve growth factor in promoting neural stem cell survival and differentiation and protecting against neuronal hearing loss. *Mol. Cell. Biochem.* **2017**, *428*, 149–159, doi:10.1007/s11010-016-2925-5.
38. Shah, S.B.; Gladstone, H.B.; Williams, H.; Hradek, G.T.; Schindler, R.A. An extended study: Protective effects of nerve growth factor in neomycin-induced auditory neural degeneration. In Proceedings of the American Journal of Otology; Am J Otol, 1995; Vol. 16, pp. 310–314.
39. Shoji, F.; Miller, A.L.; Mitchell, A.; Yamasoba, T.; Altschuler, R.A.; Miller, J.M. Differential protective effects of neurotrophins in the attenuation of noise-induced hair cell loss. *Hear. Res.* **2000**, *146*, 134–142, doi:10.1016/S0378-5955(00)00106-4.
40. Ruan, R.S.; Leong, S.K.; Mark, I.; Yeoh, K.H. Effects of BDNF and NT-3 on hair cell survival in guinea pig cochlea damaged by kanamycin treatment. *Neuroreport* **1999**, *10*, 2067–2071, doi:10.1097/00001756-199907130-00014.
41. Raphael, Y.; Altschuler, R.A. Structure and innervation of the cochlea. *Brain Res. Bull.* **2003**, *60*, 397–422, doi:10.1016/s0361-9230(03)00047-9.

CHAPTER 4

BDNF-induced mTOR modifications in the organ of Corti of ototoxically deafened guinea pigs

1. Abstract

The mammalian target of rapamycin (mTOR) signaling plays a critical role in cell homeostasis, and is implicated in cell growth and survival. In the present study, we investigated whether a modulation of the mTOR signaling was induced by brain-derived neurotrophic factor (BDNF) in the organ of Corti of guinea pigs undergoing ototoxic deafening procedure. Animals were ototoxically deafened by systemic administration of furosemide-kanamycin, and one week after deafening the right cochleas of the animals were treated with gelatin sponge (gelfoam) soaked in rhBDNF, while the left cochleas were used as negative control. Twenty-four hours after treatment, animals were euthanized and the cochleas processed for subsequent analysis. Western blot technique was used to quantify the protein levels of AKT, pAKT (Thr308), mTOR, pmTOR and PTEN, and the same markers were localized through immunofluorescence on cochlear cryosections and acquired through confocal microscopy. We did not find a modulation of AKT, pAKT and PTEN protein levels, suggesting that the mTORC1 is not involved. Conversely, mTOR and pmTOR showed a general increase in the BDNF-treated Organs of Corti as shown by immunofluorescence and western blot techniques respectively. These findings suggest that a brief exposure to BDNF is able to modulate the mTOR signaling in the organ of Corti of deaf animals, and could potentially act to induce cell survival and synaptic plasticity.

2. Introduction

Brain-derived neurotrophic factor (BDNF) is a neurotrophin, which plays a pivotal role in the development of the cochlea [1] and its maintenance in the post-natal ear [2]. BDNF binds to the p75 neurotrophin receptor ($p75^{NTR}$), that is the receptor shared between all neurotrophins, but also has a second more specific receptor belonging to the tropomyosin-related kinase (Trk) family, that is the TrkB [3,4]. In the cochlea, the BDNF receptors are expressed on sensory and non-sensory cells of the organ of Corti, as well as on the spiral ganglion cells (SGCs)[4,5]. It has been demonstrated that BDNF is particularly important for the survival of SGCs, and accordingly several *in vivo* studies demonstrated that BDNF administration positively prevented SGCs from degeneration following that of the sensory hair cells (HCs) located in the organ of Corti [6–11]. Conversely, few studies focused on the effects of BDNF in the protection of the Organ of Corti [12,13].

In recent years, particular attention has also been placed on the molecular mechanisms underlying sound perception and degenerative diseases of the cochlea [14–16]. Important findings deriving from those studies highlight the possibility to develop targeted therapies, based on selective gene regulatory networks. Additionally, the investigation of the molecular basis underlying the diseases and treatments could allow to have a wider overview of the degenerative/protective mechanisms.

Likewise, more attention has also been placed on the downstream signalings occurring upon BDNF interaction with TrkB. The results derived from those studies identified interesting pathways that may serve as therapeutic targets in several diseases of the nervous system in the years to come. Among these, it has been demonstrated that BDNF may activate the mammalian target of rapamycin (mTOR), thereby preventing neuronal death [17].

mTOR is a protein kinase, which is involved in the activation or repression of multiple cell functions, including cell growth, survival, synaptic plasticity, autophagy. [18]. Specifically, mTOR is the central component of two major protein complexes, mTORC1 and mTORC2 [19,20]. The major function of mTORC1 is the regulation of translation, but it is also involved in the regulation of the activity of phosphatases, such as the protein phosphatase 2A (PP2A), [20] and of the autophagic flux [21]. mTORC2, instead, has different targets compared to mTORC1, and is involved in several functions including cytoskeleton remodeling, cell survival and migration [19]. Compared to mTORC2, the mTORC1 upstream pathway has been better characterized. Specifically, upon different kinds of stimuli, including the exposure to growth factors, the phosphatidylinositide 3 kinase (PI3K) is activated and initiates a phosphorylation cascade which involves the AKT protein, also known as Protein Kinase B. AKT

phosphorylation at Threonine 308 in turn induces the activation of the mTORC1 complex. The cascade may be inhibited by the Phosphatase And Tensin Homolog (PTEN), that acts as a phosphatase and blocks the PI3K/AKT activation axis [20].

Contradicting data indicate that either activation or inhibition of the mTOR signaling could be involved in the degeneration or protection of the Organ of Corti [22–24]. Intriguingly, a recent study also showed that the mTOR signaling could play a major role in the regeneration of the hair cells in the mammalian cochlea [25]. Therefore, the mTOR signaling represents an interesting target for therapeutic purposes, but its specific role in physiological and pathological conditions of the cochlea still needs to be elucidated. In this context, to date the mTOR signaling has never been investigated in the cochlea in relationship to stimulation with exogenous BDNF.

In order to increase the knowledge in the field, in the present study we investigated whether a modulation of the mTOR signaling occurred in ototoxically deafened and BDNF-treated cochleas *in vivo*.

3. Methods

3.1. Animals and experimental design

Eighteen young adult female albino guinea pigs (Dunkin Hartley; Envigo, Horst, the Netherlands) were kept under standard housing conditions throughout the experiment (food and water ad libitum; lights on between 7:00 a.m. and 7:00 p.m.; temperature 21°C; humidity 60%). All experimental procedures were approved by the Dutch Central Authority for Scientific Procedures on Animals (CCD: 1150020174315).

Six normal-hearing (NH) guinea pigs without any deafening or treatment procedure were used as healthy control group. Twelve guinea pigs underwent deafening procedure and in each of these animals the right ear was treated with rhBDNF 7 days after the damage induction, while the other ear was used as internal negative control without receiving any treatments. One day thereafter, i.e., eight days after deafening, the animals were euthanized and the cochleas collected for subsequent molecular (10 animals for the deafened group; 5 animals for the NH group) and morphological analysis (2 animals for the deafened group 1; 1 animal for the NH group).

A schematic illustration of the experimental conditions is shown in Figure 1.

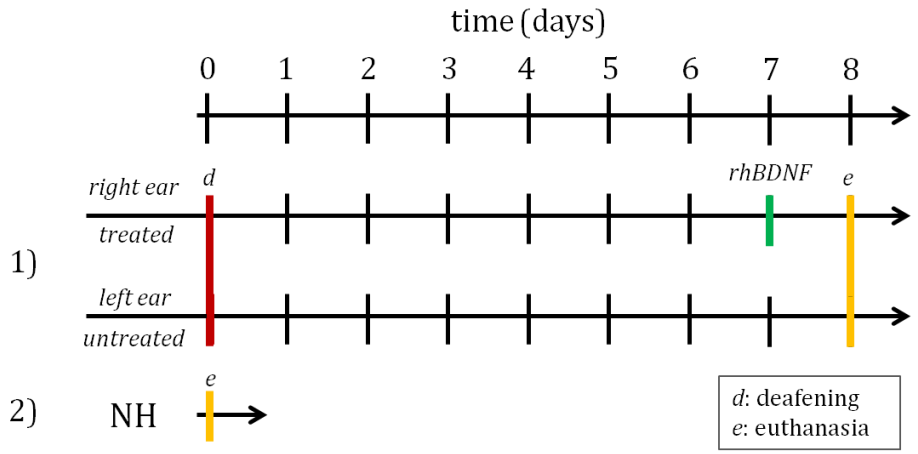

Figure 1. Schematic Illustration of the experimental design. Group 1 of young adult female albino guinea pigs underwent deafening procedure; the right ear was treated after 7 days from the injury, while the left ear was left untreated; the animals were euthanized 8 days from deafening induction. Group 2 is formed by Normal Hearing (NH) young adult female albino guinea pigs.

3.2. Deafening procedure, BDNF administration and extraction of the cochlea

Surgical techniques and experimental procedures for both deafening and BDNF administration were identical to previously reported procedures [26]. In short, anesthesia for both procedures was induced with 40 mg/kg ketamine i.m. (Narketan; Vetoquinol B.V., Breda, the Netherlands) and 0.25 mg/kg dexmedetomidine i.m. (Dexdomitor; Vetoquinol B.V.). Prior to the deafening surgery, normal hearing was verified with click-evoked auditory brainstem

responses (ABRs). When normal hearing was confirmed, deafening was performed by systemic delivery of 400 mg/kg kanamycin subcutaneously (Sigma-Aldrich, St. Louis, MO, USA) and 100 mg/kg furosemide i.v. (Centrafarm, Etten-Leur, the Netherlands). One week after deafening the animals were again anesthetized. Successful deafening was confirmed with ABR recordings (ABR threshold shifts for all animals was ≥57 dB), after which the right bulla was exposed via retro-auricular approach. A small hole was drilled into the bulla to visualize the cochlear basal turn and round window niche. A ~1 mm^3 piece of gelatin sponge (Spongostan Dental; Ethicon, Somerville, NJ, USA) soaked in 3 µL BDNF solution (PeproTech, London, UK; 3.33 µg/µL) was placed into the round window niche, touching the perforated round-window membrane. The animals received non-ototoxic antibiotic enrofloxacin (Baytril; Bayer AG, Leverkusen, Germany; 5 mg/kg) and carprofen (Carporal; AST Farma, Oudewater, the Netherlands; 4 mg/kg) at the end of each surgery.

Approximately 24 hours after the placement of the BDNF-soaked gelatin sponge, the animals were sacrificed by intraperitoneal injection of an overdose of pentobarbital (Euthanimal 20%; Alfasan B.V., Woerden, the Netherlands). Both cochleas were harvested and stored at -80 °C.

3.3. Protein extraction

After thawing, the bony wall of the cochlea was removed and the basilar membrane, containing the Organ of Corti, and the modiolus dissected out. The basilar membrane was cut into separate turns, the modiolus was removed and the remaining parts of the turns of the basilar membrane were collected and stored at -80ºC.

Each sample was obtained from a pool of two Organs of Corti in order to have enough protein quantity for subsequent analysis. Samples were homogenized on ice in a lysis buffer composed as follows: 50 mM Tris.Cl pH 7.8, 1% Triton X100, 0.1% SDS, 250 mM NaCl, 5 mM EDTA, Inhibitors of proteases and phosphatases inhibitor 100X (Thermo Fisher Scientific, Waltham, MA, USA, #1861281). After homogenization the samples were kept in ice for 20 minutes and then centrifuged at 14000 rpm in a refrigerated centrifuge (4°C). The soluble phase containing the proteins was recovered and stored at -80°C for the subsequent analysis. Protein concentration was quantified by using the Bradford assay (Bio-Rad Laboratories, Milan, Italy).

3.4. Western Blot

33 µg of total protein extracts were run on a Bolt 4–12% Bis-Tris Plus (Thermo Fisher Scientific, Waltham, MA, USA) at 200 V for 20 min. The proteins were transferred to a Polyvinylidene fluoride (PVDF) membrane (Millipore, Milan, Italy) through the iBlot 2 Dry Blotting System (Invitrogen IB21001). Membranes were blocked with 5% of blotting grade milk in Tris-Buffered Saline containing 0.1% Tween20 (TBST) for 1h at room temperature (R.T.). Specific proteins were detected with primary antibodies (Table 1) diluted in 5% non-fat dry milk in TBST or in 5% Bovine Serum Albumine (BSA) in TBST (for detection of phosphorylated proteins). Secondary antibodies were anti-rabbit or anti-mouse (depending on the primary antibody) Horseradish Peroxidase (HRP)-conjugated mixture (Bio-Rad Laboratories, Milan, Italy) diluted 1:2000 in TBST containing 5% non-fat milk or 5% BSA. The membranes were developed with SuperSignal West Pico chemiluminescent substrate (Thermo Fisher Scientific Inc., Rockford, IL, USA). The protein bands were detected using a BioRad ChemiDoc XRS-plus imaging system (Bio-Rad Laboratories, Milan, Italy). Densitometric analysis was conducted by using the ImageJ software (U.S. National Institutes of Health, Bethesda, MD, USA) and the amount of proteins was normalized versus the housekeeping protein (GAPDH). Data are reported as relative fold change with samples normalized to control (NH group), which was set to 1.

Antibody	Company	Catalogue number	MW(kDa)
anti-mTOR	Rockland	#600-401-897	250
anti-pmTOR	Rockland	#600-401-422	250
anti-AKT	Cell Signaling	#9272S	60
anti-pAKT (Thr 308)	Cell Signaling	#2965S	60
anti-PTEN	Cell Signaling	#9552S	54
anti-GAPDH	Thermo Fisher	#AM4300	37

Table 1. Primary antibodies used in the study.

3.5. Cryosections

After euthanizing by intraperitoneal injection of sodium pentobarbital, the cochleas were removed and the bulla opened. Intralabyrinthine fixation with 2% paraformaldehyde (Merck: 1.04005.1000) in 0.1M cacodylate (Sigma: C0250) buffer of the cochlea was performed through an opening in the apex and puncture of the round and oval window. Prolonged storage was in the same fixative at 4ºC. Next, the cochleas were decalcified with 10% EDTA

(Sigma: ED2SS) in aqua dest for at least 7 days at room temperature under constant agitation. After decalcification, cochleas were infiltrated with graded sucrose (Merck: 1.07653.1000) solutions in PBS till 30% sucrose, followed by embedding in OCT compound (Sakura Finetek Europe B.V. Alphen aan den Rijn, the Netherlands) and storage at -80ºC. O.C.T. embedded cochleas were cryosectioned using a Leica CM1850 cryostat. 14-µm thick midmodiolar cryosections were collected on Superfrost PLUS coated slides (Thermo Fisher Scientific, Waltham, MA, USA) for subsequent analysis. Sections containing all the cochlear turns (from base to helicotrema) were selected to perform immunofluorescence staining.

3.6. Immunofluorescence staining

Immunofluorescence staining was performed on cochlear cryosections in order to identify the localization of the factors investigated through western blot technique in the different cochlear regions and at the cellular level. Specifically, non-specific bindings were blocked with 5% BSA (bovine serum albumin) and 0.1% Triton-x-100 for 1h R.T. Primary antibodies (Table 1) were diluted 1:200 in 1% BSA and 0.1% Triton-X-100 and incubated overnight at 4 °C. Secondary antibody was anti-rabbit IgG conjugated to green fluorescent dye (Alexa Fluor 488, Molecular Probes, Invitrogen, Carlsbad, CA, USA) diluted 1:1000 in phosphate buffered saline (PBS 1X) and incubated at 37°C for 2 h.

All sections were counterstained with nuclear staining Bisbenzimide (Hoechst) and confocal images were acquired in all cochlear locations (B1, B2, M1, M2, A1, A2, A3, H:helicotrema) (Figure 2) by setting up the same parameters, using a Leica TCS SP5 confocal microscope. ~22 planes at a distance of 0.5 µm were acquired for the final images. The fluorescence intensity of all markers was quantified for each cochlear location through ImageJ software, by selecting the organ of Corti and normalizing the values to the field area.

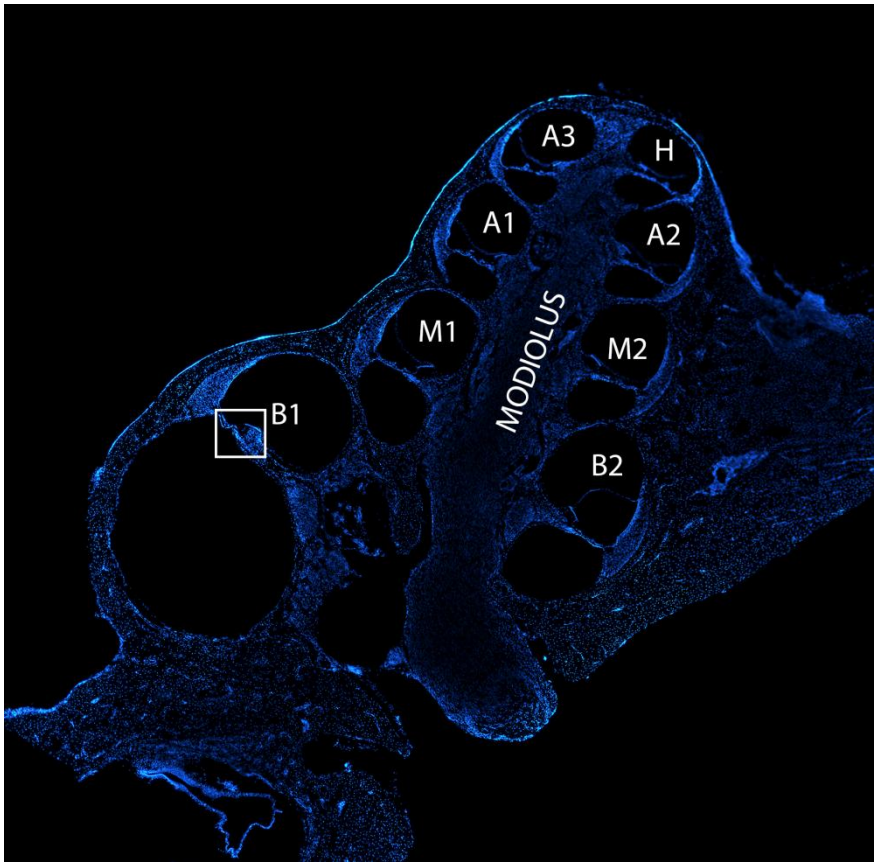

Figure 2. Cochlear cryosection and locations. The image is representetative of a midmodiolar cochlear cryosection stained with bisbenzimide nuclear dye. Each cochlear location is signed by a different lettering: basal turns (B1, B2), middle turns (M1, M2), apical turns (A1, A2, A3) and helicotrema (H). The white frame borders the area of the Organ of Corti for B1 turn and is an example showing the localization of the Organ of Corti in the cochlear turns.

3.7. Statistical analysis

For western blot, statistical analysis was performed by one-way ANOVA test followed by Tukey test. First type error was set at 5%. The statistical analysis was conducted using the SigmaPlot 12.0 software.

4. Results

4.1. AKT and pAKT analysis

As a first step of the study, we performed molecular investigations in order to evaluate a possible modulation of the mTOR signaling in the organ of Corti of the experimental groups through protein quantification. We focused on AKT, mTOR and PTEN proteins. Importantly, we also considered the phosphorylated forms of AKT (Thr 308) and mTOR (Ser2448), which provide more information about the activation state of the signaling.

The first marker that was analyzed was AKT and its phosphorylated form at Threonine 308 (pAKT). We did not find significant differences between the experimental groups considering the ratio between pAKT and its basal form (pAKT/AKT) (Figure 3A), pAKT and the housekeeping protein (pAKT/GAPDH) (Figure 3B) and the ratio between AKT and the housekeeping (AKT/GAPDH) (Figure 3C). The BDNF treated organs of Corti showed a more similar trend to the NH ones as for AKT/GAPDH expression than the untreated ones (Figure 3C), but the variability between samples did not lead to statistically significant differences. Figure 3D shows representative western blot bands of pAKT and AKT from the three experimental groups.

In addition, we analyzed the immunolocalization of AKT and pAKT on cochlear cryosections, focusing on the organ of Corti. AKT was homogeneously expressed in the organ of Corti of all cochlear locations in all the experimental groups (Figure 4A). No differences in the signal intensity were identified between samples, as clearly visible looking at the green signal of the confocal images (Figure 4A) and confirmed by fluorescence intensity analysis of each cochlear location for individual samples (Figure 4B).

Localization of pAKT varied in the organ of Corti (Figure 5). The signal was observed in all cell types of the organ of Corti, but was particularly highly expressed in the apex of pillar cells (Figure 5 A, B, C). In Figure 5C pillar cells have been highlighted by a yellow outline in order to show the localization and the expression of pAKT signal in those cells. Intriguingly, during the scanning of the cryosections, we noticed that the pAKT signal was localized distally to the apical part of the cell body rather than in the centre, a detail that was often not appreciable looking at the final confocal acquisition. Therefore, in Figure 5 D we reported the single acquisitions (every 0.5 μm) of an organ of Corti of a NH cochlea, showing the localization of the pAKT signal across the cryosection thickness. The same specific localization was observed in all cochlear locations of all the experimental groups (Figure 6 A). Additionally, we did not find any differences in the fluorescence intensity of pAKT for all cochlear locations between groups (Figure 6B).

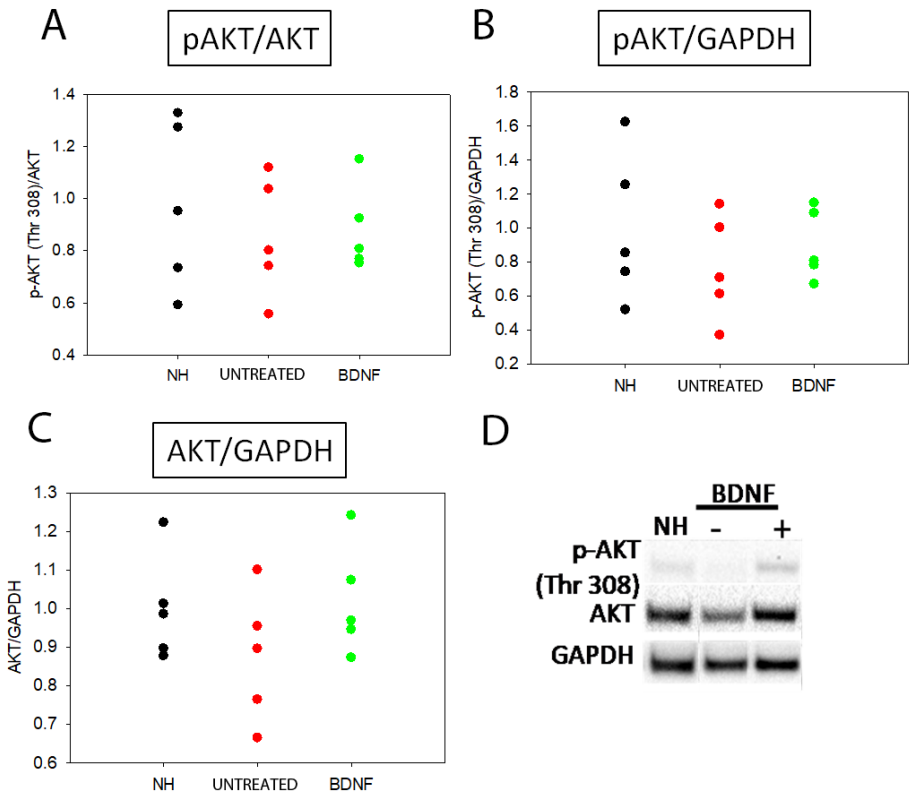

Figure 3. Protein quantification of AKT and pAKT (Thr 308). Western blot analysis of pAKT/AKT (A), pAKT/GAPDH (B) and AKT/GAPDH (C) on Organ of Corti samples of all the experimental groups**.** Graphs show the densitometric values for individual samples; each sample is a pool of two organs of Corti (n=5). (D) Representative western blot bands.

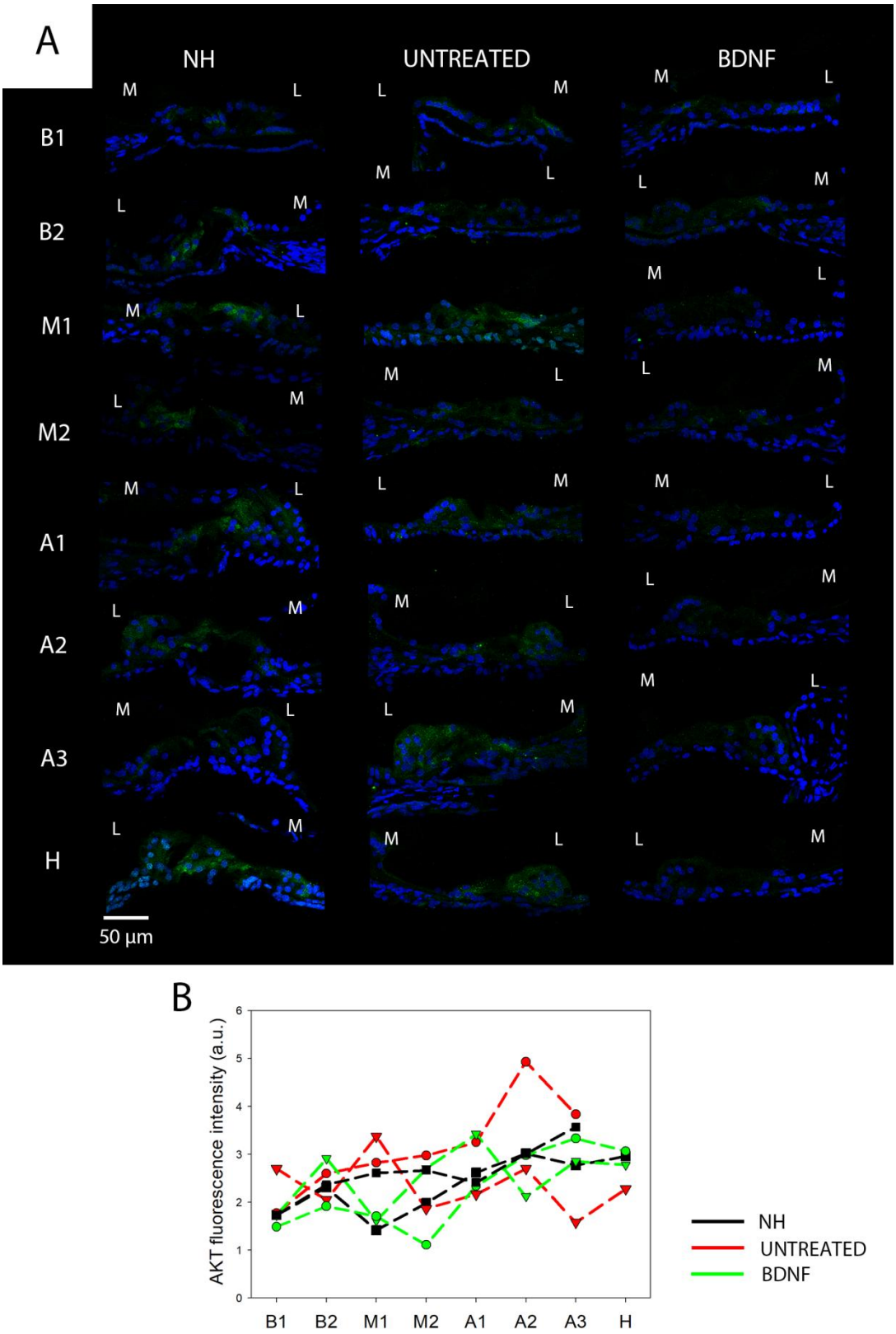

Figure 4. Immunolocalization and fluorescence intensity of AKT. (A) Representative confocal images showing the organ of Corti immunolabelled with anti-AKT (green) and counterstained with bisbenzimide nuclear dye (blue) of all experimental groups and for each cochlear location (from B1 to H). Scale bar: 50 µm. L: lateral, M: medial. (B) Fluorescence intensity analysis of AKT immunostaining for 6 cochleas (2 NH, 2 untreated, 2 BDNF treated). The graph shows the signal intensity of each sample for all cochlear locations (black: NH, red: untreated, green: BDNF-treated). The same symbol was used to identify the BDNF-treated and contralateral untreated ears within individual animals.

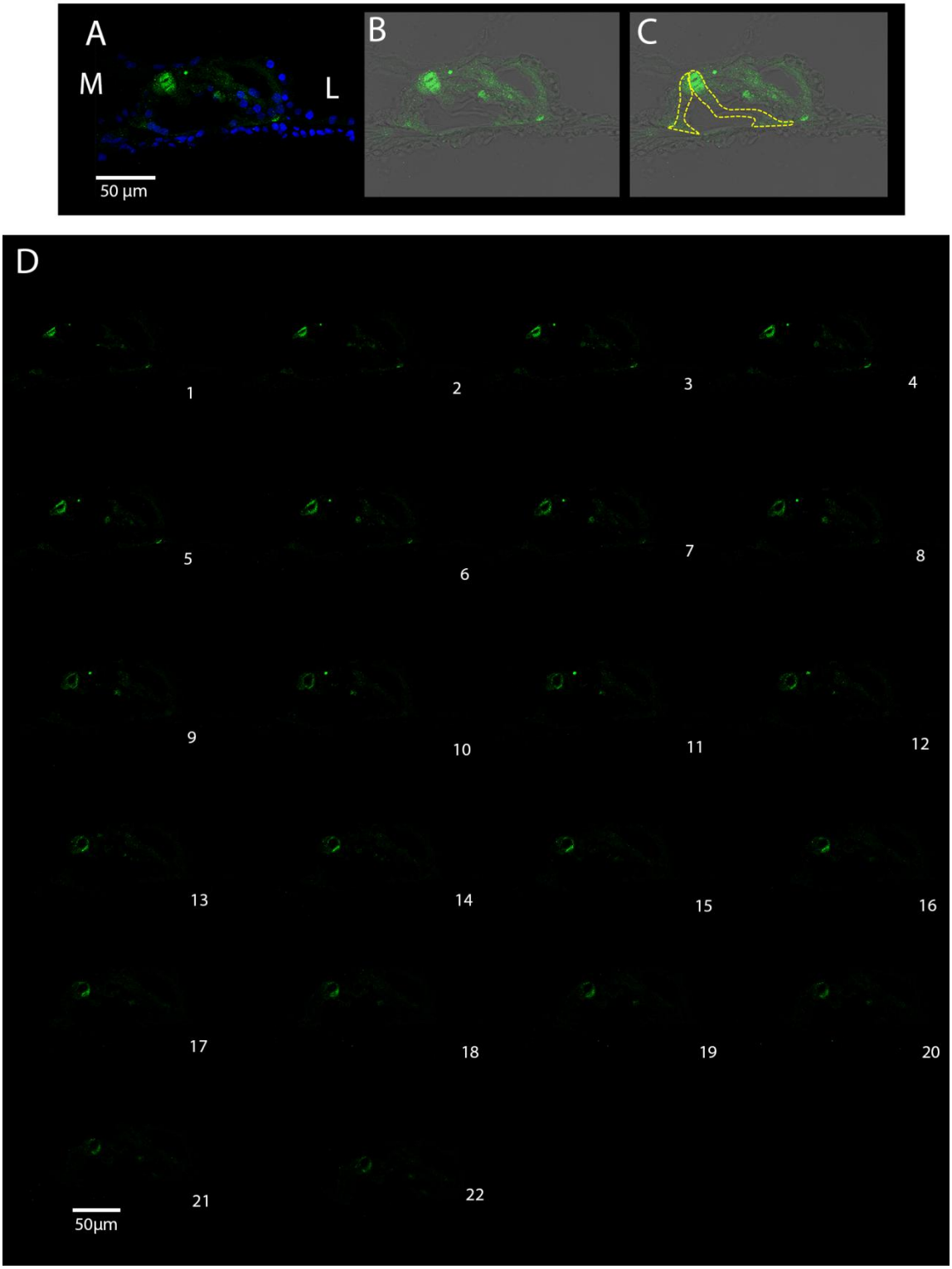

Figure 5. pAKT immunolocalization in Pillar cells. (A) Representative confocal image of a NH organ of Corti (A1 location) immunolabeled with anti-pAKT (blue) and counterstained with bisbenzimide nuclear dye (blue) (L: lateral, M: medial); (B) the same image was acquired with anti-pAKT signal (green) on a bright-field background to show the structure of the organ of Corti, and (C) the Pillar cells were delineated in yellow. (D) Serial confocal microscopy images of figure A, showing pAKT signal (green) every 0.5 µm. Scale bars: 50 µm.

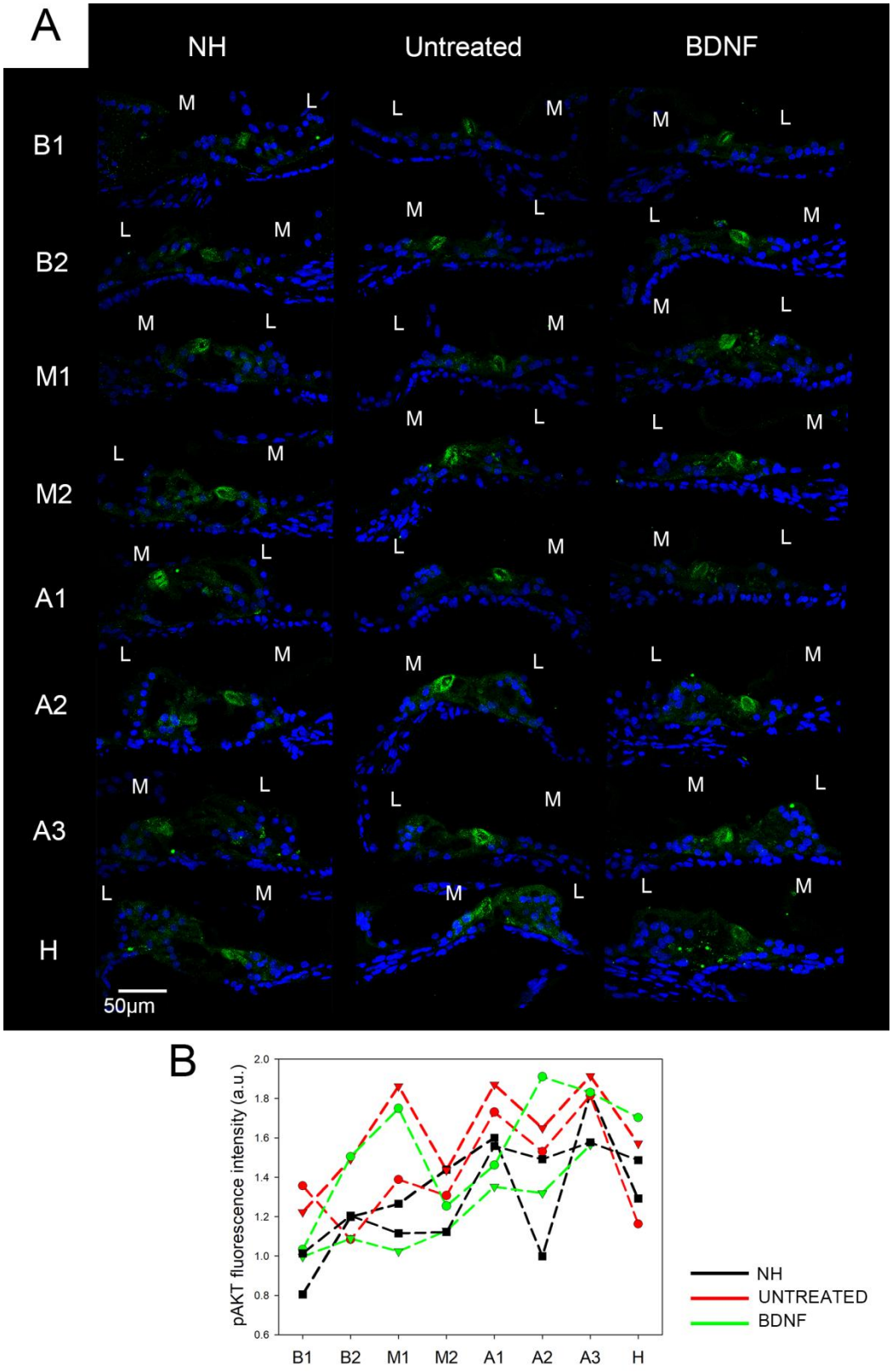

Figure 6. Immunostaining and fluorescence intensity of pAKT. (A) Representative confocal images showing the Organ of Corti immunolabelled with anti-pAKT (green) and counterstained with bisbenzimide nuclear dye (blue) of all experimental groups and for each cochlear location (from B1 to H). Scale bar: 50 µm. L: lateral, M: medial. (B) Fluorescence intensity analysis of pAKT immunostaining. The graph shows the signal intensity of each sample for all cochlear locations (black: NH, red: untreated, green: BDNF-treated). The same symbol was used to identify the BDNF-treated and untreated ears of individual animals.

4.2. mTOR and pmTOR analysis

Subsequently, we quantified the protein amount of pmTOR and mTOR proteins (Figure 7). We did not find any statistically significant differences between the experimental groups in all the conditions considered: pmTOR/mTOR (Figure 7 A) ($p=0.228$), mTOR/GAPDH (Figure 7 B) ($p=0.748$) and pmTOR/GAPDH (Figure 7 C) ($p=0.336$). Nevertheless, the deaf Organs of Corti of both treated and untreated ears showed an increasing trend of pmTOR levels compared to the NH group (Figure 7A, C), suggesting a higher activation of the signaling. Figure 7D shows representative western blot bands of pmTOR and mTOR from the three experimental groups.

Anti-mTOR immunostaining revealed that mTOR was localized in the whole organ of Corti, and a higher expression was observed in phalangeal, pillar and Deiters' cells than other supporting cells or hair cells (Figure 8). The same localization was observed in all the experimental groups at all the cochlear locations (Figure 9A). In addition, the BDNF-treated group showed a general increase of the mTOR signal across all cochlear turns, and this was particularly evident in the apex and helicotrema, where also the Hensen's cells displayed a high intensity signal. This observation was confirmed by fluorescence intensity quantification, which showed increased mTOR levels in the BDNF-treated samples compared to the untreated and NH ones (Figure 9B). In addition, the fluorescence intensity showed an increasing trend in the cochlea from base to apex.

Anti-pmTOR immunostaining showed a different localization (Figure 10 A). In addition to a diffuse signal in the whole organ of Corti, pmTOR was highly expressed in outer HCs (OHCs) and inner HCs (IHCs) (Figure 10 A). In deaf animals, the signal from HCs was fainter. However, the overall fluorescence intensity of the organ of Corti did not differ between the three groups for any of the cochlear locations (Figure 10B).

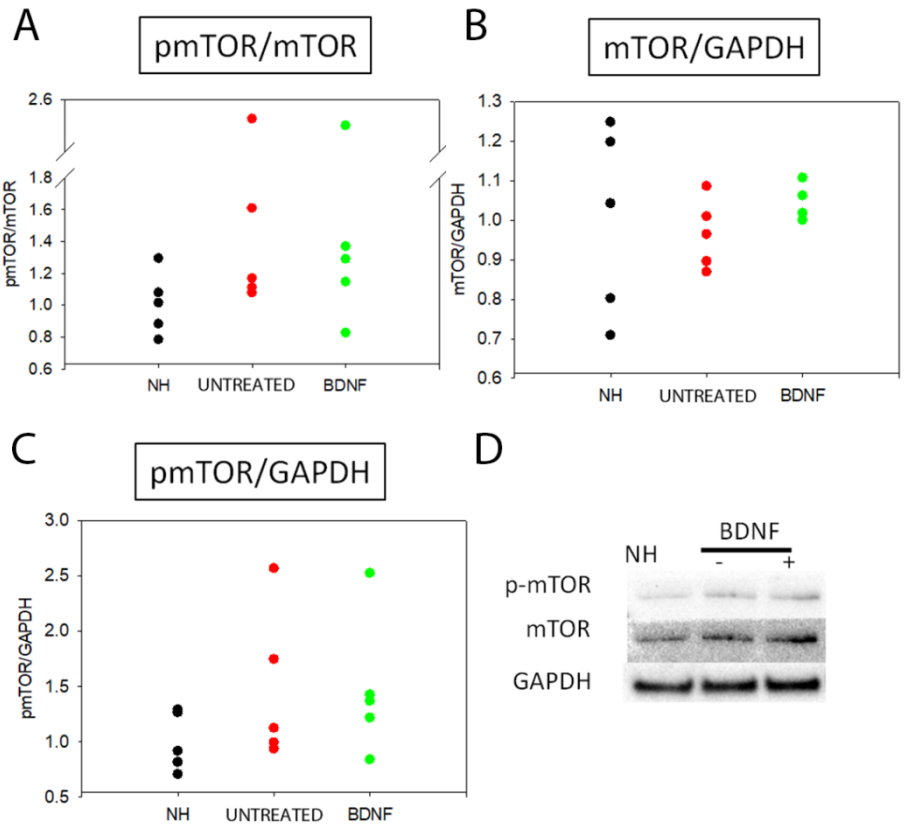

Figure 7. Protein quantification of pmTOR and mTOR. Western blot analysis of pmTOR/mTOR (A), mTOR/GAPDH (B) and pmTOR/GAPDH (C) on organ of Corti samples of all the experimental groups**.** Graphs show the densitometric values for individual samples; each sample is a pool of two organs of Corti (n=5). (D) Representative western blot bands.

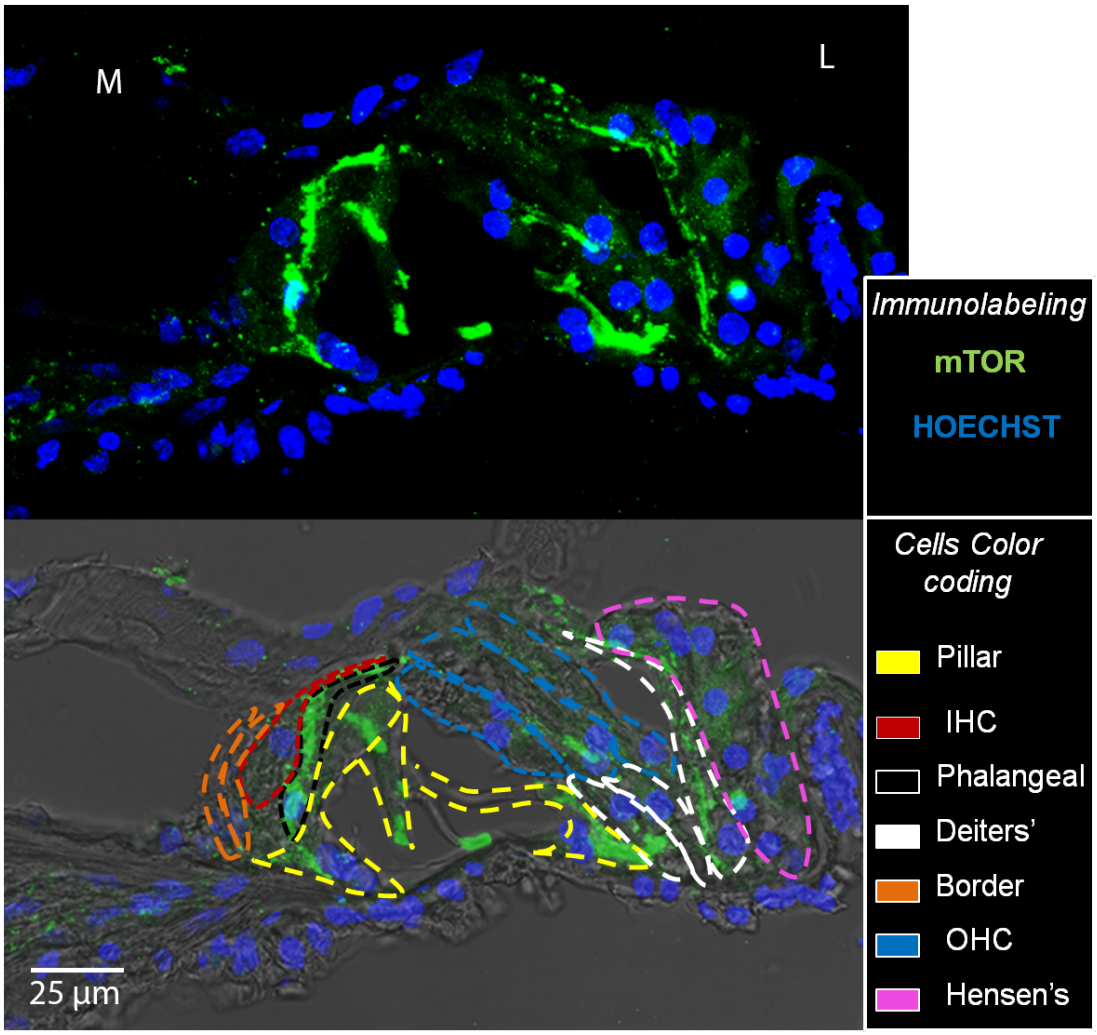

Figure 8. Immunolocalization of mTOR protein. Top: The figure shows a representative confocal image of the Organ of Corti of a NH cochlea (A1 location) immunolabelled with anti-mTOR (green) and counterstained with bisbenzimide nuclear dye (blue). Bottom: The same image was acquired with bright-field background to visualize the structure of the Organ of Corti; the different cell types were signed with a color coding (pillar: yellow, IHC: red, phalangeal: black, deiters': white, border: orange, OHC: blue, Hensen's: pink). L: lateral, M: medial.

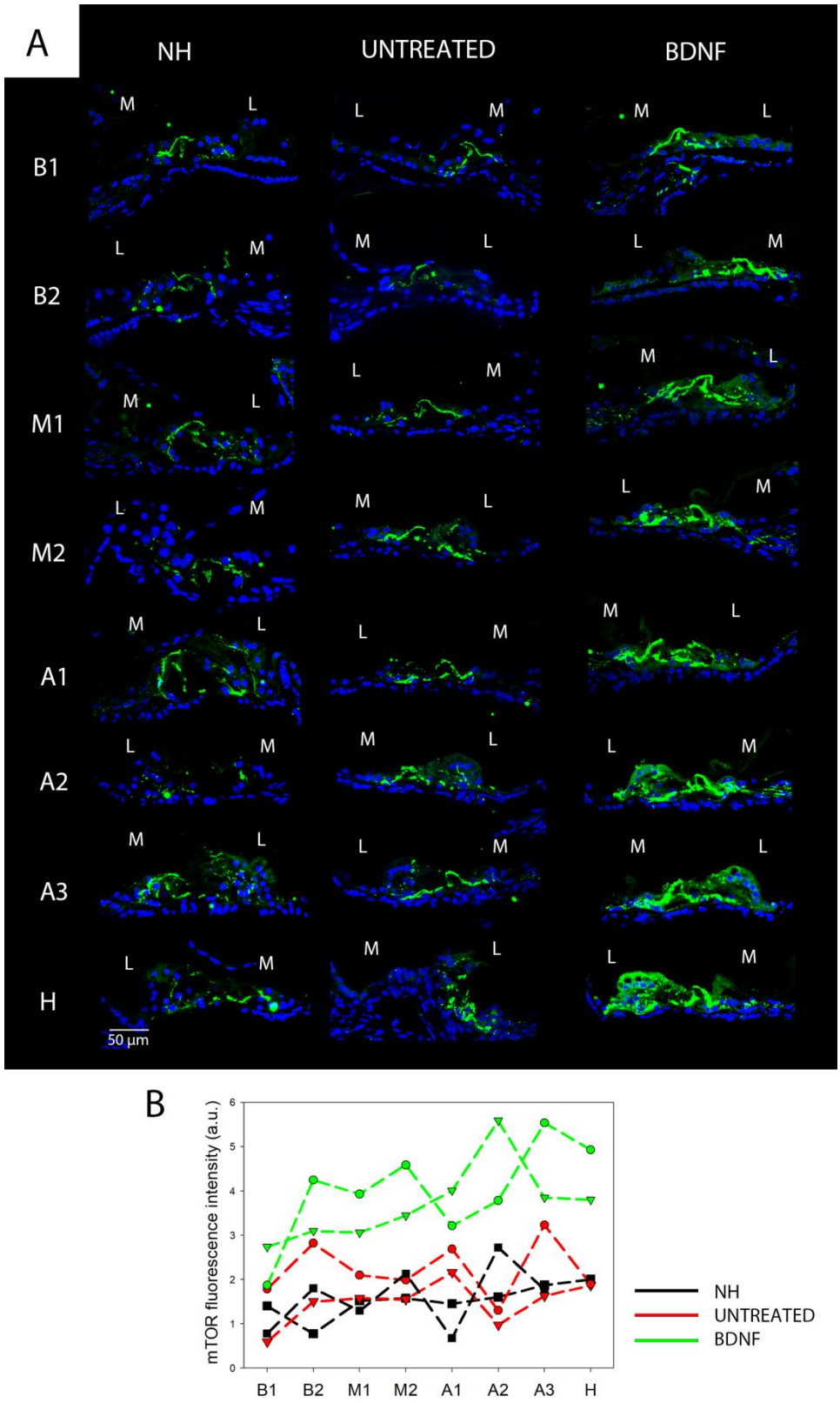

Figure 9. Immunolocalization and fluorescence intensity of mTOR. (A) Representative confocal images showing the organ of Corti immunolabelled with anti-mTOR (green) and counterstained with bisbenzimide nuclear dye (blue) of all experimental groups and for each cochlear location (from B1 to H). Scale bar: 50 µm. L: lateral, M: medial. (B) Fluorescence intensity analysis of mTOR immunostaining. The graph shows the signal intensity of each sample for all cochlear locations (black: NH, red: untreated, green: BDNF-treated). The same symbol was used to identify the BDNF-treated and untreated ears of individual animals.

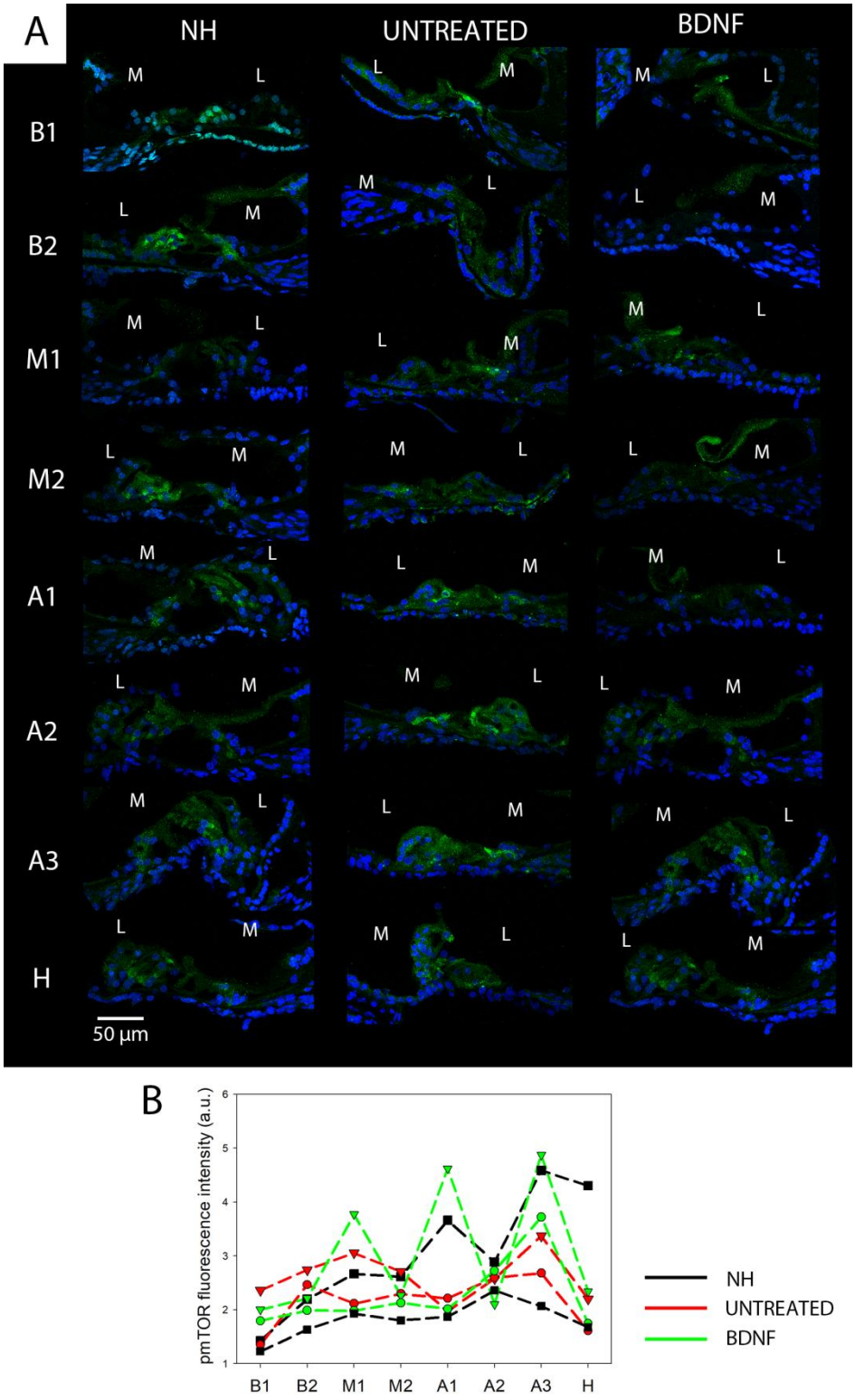

Figure 10. Immunolocalization and fluorescence intensity of pmTOR. (A) Representative confocal images showing the organ of Corti immunolabelled with anti-pmTOR (green) and counterstained with bisbenzimide nuclear dye (blue) of all experimental groups and for each cochlear location (from B1 to H). Scale bar: 50 µm. L: lateral, M: medial. (B) Fluorescence intensity analysis of pmTOR immunostaining. The graph shows the signal intensity of each sample for all cochlear locations (black: NH, red: untreated, green: BDNF-treated). The same symbol was used to identify the BDNF-treated and untreated ears of individual animals.

4.3. PTEN analysis

Finally, we investigated the expression of PTEN (Figure 11), which acts as an inhibitor of the mTOR signaling. PTEN protein levels were not different between the groups, and a high variability was found between the NH samples (Figure 11A). Figure 11B shows representative western blot bands of PTEN from the three experimental groups.

Anti-PTEN immunofluorescence staining showed a clear signal in the form of green puncta (Figure 12A). The signal was present in the whole organ of Corti in each of the cochlear locations of all three groups. Moreover, the fluorescence intensity of the immunostaining was not different between groups, as shown in Figure 12B.

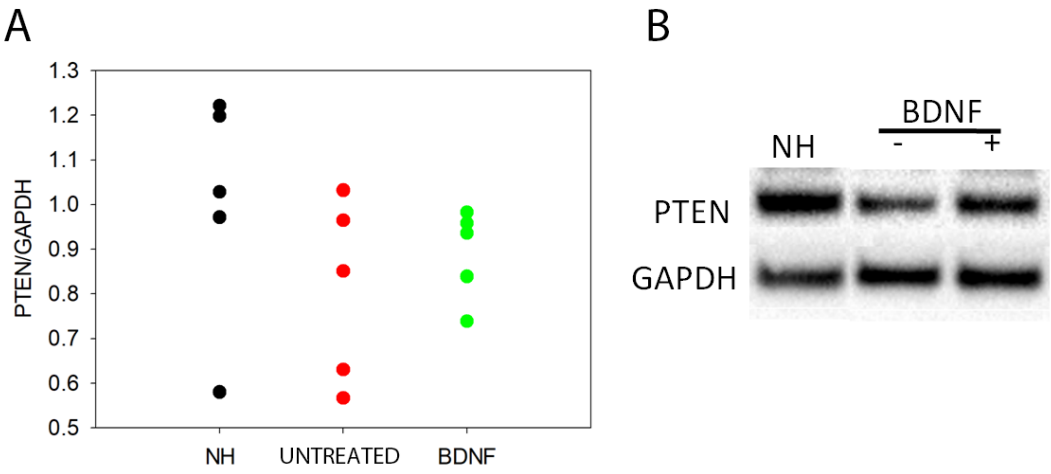

Figure 11. Protein quantification of PTEN. (A) Western blot analysis of PTEN/GAPDH on organ of Corti samples of all the experimental groups**.** Graph shows the densitometric values for individual samples; each sample is a pool of two organs of Corti (n=5). (B) Representative western blot bands.

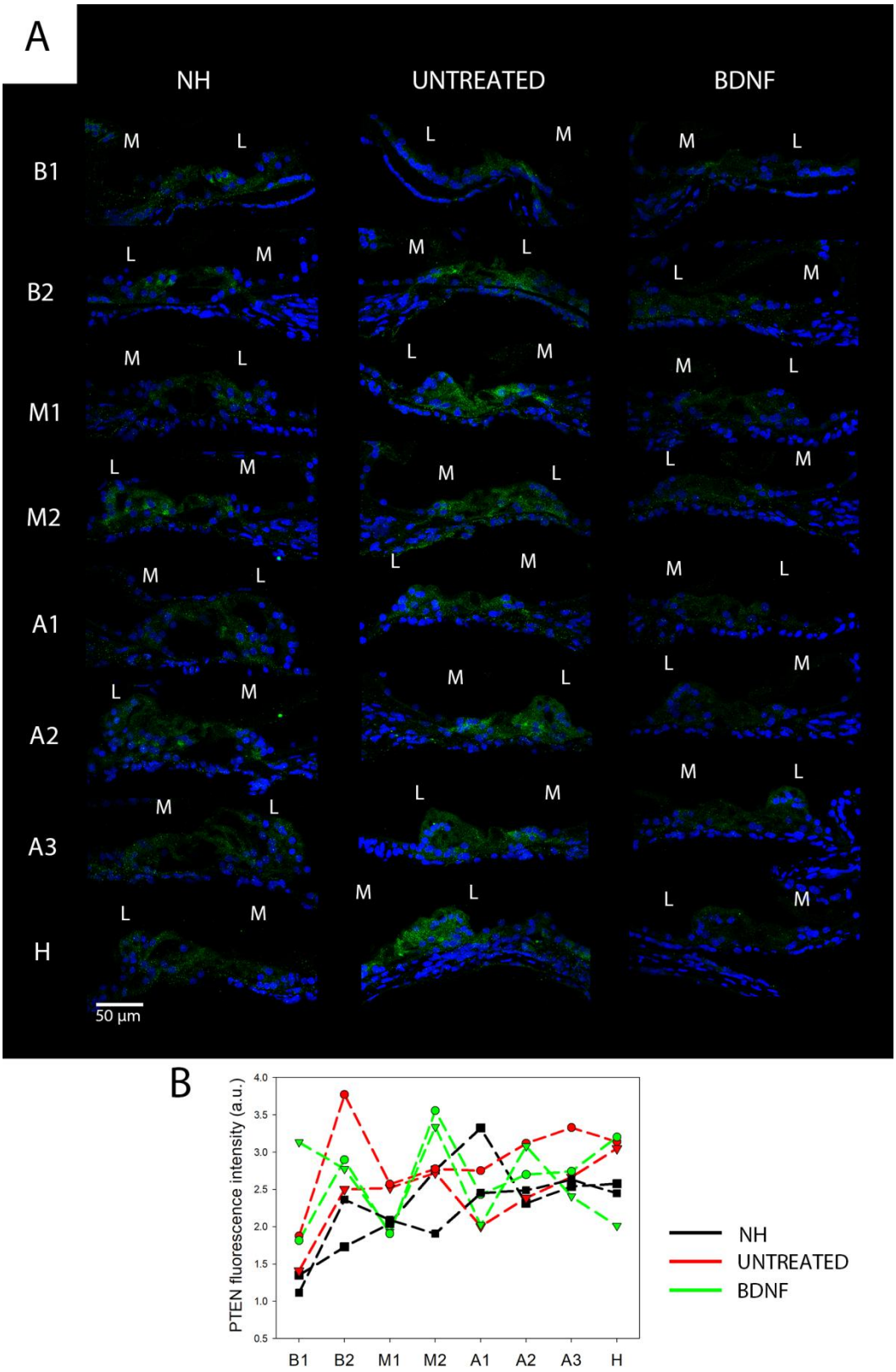

Figure 12. Immunolocalization and fluorescence intensity of PTEN. (A) Representative confocal images showing the Organ of Corti immunolabelled with anti-PTEN (green) and counterstained with bisbenzimide nuclear dye (blue) of all experimental groups and for each cochlear location (from B1 to H). Scale bar: 50 µm. L: lateral, M: medial. (B) Fluorescence intensity analysis of PTEN immunostaining. The graph shows the signal intensity of each sample for all cochlear locations (black: NH, red: untreated, green: BDNF-treated). The same symbol was used to identify the BDNF-treated and untreated ears of individual animals.

5. Discussion

In the present study we investigated the protein levels of AKT and mTOR (and their phosphorylated forms), and PTEN through a molecular approach based on western blot technique. We found no statistically significant differences in the protein levels, although an increasing trend of pmTOR was observed in the deaf animals, both treated and untreated, suggesting the activation of the signaling. We also took into account the localization of those proteins through immunofluorescence and confocal microscopy, which allowed us to identify an increased fluorescence intensity of mTOR in the organ of Corti of BDNF-treated cochleas. Below, we discuss the results obtained for all the markers in detail.

Taken together, the western blot analysis and immunofluorescence staining demonstrated that the protein levels and localization of AKT and pAKT were modulated neither by the deafening procedure nor by the treatment in our experimental conditions. This finding suggests that the PI3K/AKT cascade was not activated [20]. Indeed, we analyzed AKT phosphorylation at Thr 308, that is the one involved in the upstream cascade of the mTORC1 complex activation [20]. Interestingly, through the immunofluorescence staining, we identified for the first time the localization of those proteins in the Organ of Corti. Particularly interesting was the peculiar localization of pAKT in the apical region of pillar cells and marginally to the cell body. According to pillar cell structure, the apical region contains dense actin meshes [27], that could probably prevent the localization of pAKT in that region. Also, we did not observe any differences in the PTEN protein levels between the three groups. This is in agreement with the AKT and pAKT results, since PTEN is an upstream protein, the modulation of which affects the phosphorylation of AKT [20].

A more interesting result is related to the analysis of mTOR and pmTOR. The western blot technique showed an increasing trend of pmTOR protein levels in deaf animals, both treated and untreated, compared to the NH (Figure 7), suggesting the activation of mTOR signaling. Instead, no differences were found in the total mTOR content. Conversely, the immunofluorescence analysis revealed that pmTOR was similarly expressed in the three groups in the organ of Corti, while mTOR was markedly increased in the BDNF-treated samples. To explain the discrepancy between western blot (Figure 7) and immunofluorescence data (Figure 9), it is important to consider the following. (1) The western blot technique was performed on samples of Organ of Corti containing also other cochlear tissues like the basilar membrane, the tectorial membrane, stria vascularis, the bone. This probably could create a dilution of the proteins contained exclusively in the organ of Corti, and could hide any small modulation of the studied proteins. Complete isolation of the

organ of Corti was not possible due to technical problems related to the dimension and accessibility of the tissue, which make it very difficult to be studied. (2) The anti-mTOR antibody used in this study identifies all mTOR forms, including the phosphorylated mTOR. The result derived from cryosections analysis shows that there is an increase in the mTOR content, that is not observed when looking at pmTOR selectively. It is possible that the modulation of the mTOR signal therefore occurs at the transcriptional level, and BDNF could induce a higher expression of the mTOR protein. Alternatively, the pmTOR modulation observed in the western blot technique possibly did not occur in the organ of Corti itself but in the neighboring tissues and cells.

Taken together, the findings of our study suggest that BDNF induces a modulation of the mTOR protein in the organ of Corti of ototoxically deafened guinea pigs. This modulation is probably not associated with the activation of the mTORC1 complex, since we did not find any differences in the pAKT and PTEN protein levels [20]. Further studies would be needed to confirm the higher expression of mTOR also at the transcriptional level, and additional studies on the mTORC2 and mTORC1 complex proteins could allow to clarify the functional effects of this modulation. Nevertheless, this is the first evidence of mTOR modulation by BDNF in the (degenerating)organ of Corti. Given the relevant role of mTOR signaling in cell survival and synaptic plasticity [28,29], BDNF could potentially lead to a protective effect of the organ of Corti through the modulation of the mTOR signaling.

6. References

1. Johnson Chacko, L.; Blumer, M.J.F.; Pechriggl, E.; Rask-Andersen, H.; Dietl, W.; Haim, A.; Fritsch, H.; Glueckert, R.; Dudas, J.; Schrott-Fischer, A. Role of BDNF and neurotrophic receptors in human inner ear development. *Cell Tissue Res.* **2017**, *370*, 347–363, doi:10.1007/s00441-017-2686-9.
2. Singer, W.; Panford-Walsh, R.; Knipper, M. The function of BDNF in the adult auditory system. *Neuropharmacology* 2014, *76*, 719–728.
3. Barbacid, M. The Trk family of neurotrophin receptors. *J. Neurobiol.* **1994**, *25*, 1386–1403, doi:10.1002/neu.480251107.
4. Ramekers, D.; Versnel, H.; Grolman, W.; Klis, S.F.L. Neurotrophins and their role in the cochlea. *Hear. Res.* 2012, *288*, 19–33.
5. Schulze, J.; Staecker, H.; Wedekind, D.; Lenarz, T.; Warnecke, A. Expression pattern of brain-derived neurotrophic factor and its associated receptors: Implications for exogenous neurotrophin application. *Hear. Res.* **2020**, doi:10.1016/j.heares.2020.108098.
6. Vink, H.A.; Versnel, H.; Kroon, S.; Klis, S.F.L.; Ramekers, D. BDNF-mediated preservation of spiral ganglion cell peripheral processes and axons in comparison to that of their cell bodies. *Hear. Res.* **2021**, *400*, 108114, doi:10.1016/j.heares.2020.108114.
7. Ramekers, D.; Versnel, H.; Strahl, S.B.; Klis, S.F.L.; Grolman, W. Temporary neurotrophin treatment prevents deafness- induced auditory nerve degeneration and preserves function. *J. Neurosci.* **2015**, *35*, 12331–12345, doi:10.1523/JNEUROSCI.0096-15.2015.
8. Miller, J.M.; Chi, D.H.; O'Keeffe, L.J.; Kruszka, P.; Raphael, Y.; Altschuler, R.A. Neurotrophins can enhance spiral ganglion cell survival after inner hair cell loss. *Int. J. Dev. Neurosci.* **1997**, *15*, 631–643, doi:10.1016/S0736-5748(96)00117-7.
9. Gillespie, L.N.; Clark, G.M.; Marzella, P.L. Delayed neurotrophin treatment supports auditory neuron survival in deaf guinea pigs. *Neuroreport* **2004**, *15*, 1121–1125, doi:10.1097/00001756-200405190-00008.
10. Agterberg, M.J.H.; Versnel, H.; de Groot, J.C.M.J.; Smoorenburg, G.F.; Albers, F.W.J.; Klis, S.F.L. Morphological changes in spiral ganglion cells after intracochlear application of brain-derived neurotrophic factor in deafened guinea pigs. *Hear. Res.* **2008**, *244*, 25–34, doi:10.1016/j.heares.2008.07.004.
11. McGuinness, S.L.; Shepherd, R.K. Exogenous BDNF rescues rat spiral ganglion neurons in vivo. *Otol. Neurotol.* **2005**, *26*, 1064–1072, doi:10.1097/01.mao.0000185063.20081.50.

12. Ruan, R.S.; Leong, S.K.; Mark, I.; Yeoh, K.H. Effects of BDNF and NT-3 on hair cell survival in guinea pig cochlea damaged by kanamycin treatment. *Neuroreport* **1999**, *10*, 2067–2071, doi:10.1097/00001756-199907130-00014.
13. Shoji, F.; Miller, A.L.; Mitchell, A.; Yamasoba, T.; Altschuler, R.A.; Miller, J.M. Differential protective effects of neurotrophins in the attenuation of noise-induced hair cell loss. *Hear. Res.* **2000**, *146*, 134–142, doi:10.1016/S0378-5955(00)00106-4.
14. Ranum, P.T.; Goodwin, A.T.; Yoshimura, H.; Kolbe, D.L.; Walls, W.D.; Koh, J.Y.; He, D.Z.Z.; Smith, R.J.H. Insights into the Biology of Hearing and Deafness Revealed by Single-Cell RNA Sequencing. *Cell Rep.* **2019**, *26*, 3160-3171.e3, doi:10.1016/j.celrep.2019.02.053.
15. Shu, Y.; Li, W.; Huang, M.; Quan, Y.Z.; Scheffer, D.; Tian, C.; Tao, Y.; Liu, X.; Hochedlinger, K.; Indzhykulian, A.A.; et al. Renewed proliferation in adult mouse cochlea and regeneration of hair cells. *Nat. Commun.* **2019**, *10*, doi:10.1038/s41467-019-13157-7.
16. Waldhaus, J.; Durruthy-Durruthy, R.; Heller, S. Quantitative High-Resolution Cellular Map of the Organ of Corti. *Cell Rep.* **2015**, *11*, 1385–1399, doi:10.1016/j.celrep.2015.04.062.
17. Chen, S. Der; Wu, C.L.; Hwang, W.C.; Yang, D.I. More insight into BDNF against neurodegeneration: Anti-apoptosis, anti-oxidation, and suppression of autophagy. *Int. J. Mol. Sci.* 2017, *18*, 545.
18. Bockaert, J.; Marin, P. mTOR in Brain Physiology and Pathologies. *Physiol. Rev.* **2015**, *95*, 1157–1187, doi:10.1152/physrev.00038.2014.
19. Oh, W.J.; Jacinto, E. mTOR complex 2 signaling and functions. *Cell Cycle* 2011, *10*, 2305–2316.
20. Melick, C.H.; Jewell, J.L. Regulation of mtorc1 by upstream stimuli. *Genes (Basel).* 2020, *11*, 1–28.
21. Rabanal-Ruiz, Y.; Otten, E.G.; Korolchuk, V.I. MTORC1 as the main gateway to autophagy. *Essays Biochem.* 2017, *61*, 565–584.
22. Fu, X.; Sun, X.; Zhang, L.; Jin, Y.; Chai, R.; Yang, L.; Zhang, A.; Liu, X.; Bai, X.; Li, J.; et al. Tuberous sclerosis complex-mediated mTORC1 overactivation promotes age-related hearing loss. *J. Clin. Invest.* **2018**, *128*, 4938–4955, doi:10.1172/JCI98058.
23. Ye, B.; Wang, Q.; Hu, H.; Shen, Y.; Fan, C.; Chen, P.; Ma, Y.; Wu, H.; Xiang, M. Restoring autophagic flux attenuates cochlear spiral ganglion neuron degeneration by promoting TFEB nuclear translocation via inhibiting MTOR. *Autophagy* **2019**, *15*, 998–1016, doi:10.1080/15548627.2019.1569926.
24. Li, X.J.; Doetzlhofer, A. LIN28B/let-7 control the ability of neonatal murine auditory

supporting cells to generate hair cells through mTOR signaling. *Proc. Natl. Acad. Sci. U. S. A.* **2020**, *117*, 22225–22236, doi:10.1073/pnas.2000417117.

25. Shu, Y.; Li, W.; Huang, M.; Quan, Y.Z.; Scheffer, D.; Tian, C.; Tao, Y.; Liu, X.; Hochedlinger, K.; Indzhykulian, A.A.; et al. Renewed proliferation in adult mouse cochlea and regeneration of hair cells. *Nat. Commun.* **2019**, *10*, doi:10.1038/s41467-019-13157-7.
26. Vink, H.A.; van Dorp, W.C.; Thomeer, H.G.X.M.; Versnel, H.; Ramekers, D. Bdnf outperforms trkb agonist 7,8,3′-thf in preserving the auditory nerve in deafened guinea pigs. *Brain Sci.* **2020**, *10*, 1–20, doi:10.3390/brainsci10110787.
27. Zetes, D.E.; Tolomeo, J.A.; Holley, M.C. Structure and Mechanics of Supporting Cells in the Guinea Pig Organ of Corti. *PLoS One* **2012**, *7*, e49338, doi:10.1371/journal.pone.0049338.
28. Hoeffer, C.A.; Klann, E. mTOR signaling: At the crossroads of plasticity, memory and disease. *Trends Neurosci.* 2010, *33*, 67–75.
29. Hung, C.M.; Garcia-Haro, L.; Sparks, C.A.; Guertin, D.A. mTOR-dependent cell survival mechanisms. *Cold Spring Harb. Perspect. Biol.* **2012**, *4*, doi:10.1101/cshperspect.a008771.

CHAPTER 5

Concluding remarks

Concluding remarks

The organ of Corti is a complex sensory epithelium, that can be subjected to damaging stimuli and therefore degenerate leading to irreversible hearing loss. To date, there are no effective treatments to prevent its degeneration or to induce its regeneration. Moreover, spiral ganglion cells (SGCs) degenerate as a consequence of damage to the organ of Corti, resulting in reduced performance of cochlear implants. All these issues call for an urgent need of new therapeutic approaches. Moreover, due to its cellular heterogeneity and difficult accessibility, the few studies on the organ of Corti have been challenging and many efforts are needed to make improvements in the field. Neurotrophic factors have been shown to have a protective effect on cochlear cells, and represent an interesting research field for the development of new therapies.

On this basis, in this dissertation, we investigated the effects of recombinant human nerve growth factor (rhNGF) and recombinant human brain derived neurotrophic factor (rhBDNF) on sensory and non-sensory cells of the organ of Corti with multiple experimental approaches.

As a first step of the project, an *in vitro* study based on immortalized cells derived from the organ of Corti of mice was performed in order to analyze the miRNome induced by rhNGF and rhBDNF at different time points. Data are reported in **Chapter 2**. For the first time, it was demonstrated that both neurotrophins are able to induce substantial changes in the miRNome of cochlear cells. Interestingly, many of the modulated miRNAs were shared between rhNGF and rhBDNF, while others were different. This result suggests that the two neurotrophins follow a similar miRNAs expression pattern, although maintaining peculiar differences. The subsequent *in silico* analysis allowed us to identify a wide spectrum of target genes and signallings by the modulated miRNAs. Importantly, many of the target pathways by both neurotrophins involved cell survival, proliferation, neuronal differentiation and metabolic pathways. On one side, this data confirms the literature about the modulation of selected pathways by rhNGF or rhBDNF in cochlear cells, showing for the first time that they are modulated through a specific miRNA expression pattern, and paving the way for new miRNA-based therapeutic targets. For instance, once clarified the implications of selected miRNAs and their target genes and pathways, the miRNAs themselves could be used as potential new therapies, or could be the target of other compounds. On the other side the *in silico* analysis allowed the identification of new molecular signallings, that were never investigated until now in the cochlea, and that are potentially modulated by the neurotrophins. The results of the *in vitro* and *in silico* studies represented the basis for the following experiments. In fact,

the main limitation of the *in silico* study is that it is a bioinformatics prediction. It is therefore a first step necessary to identify potential genes and design focused experiments. Nonetheless, the *in silico* approach allows one to analyze all the identified miRNAs as a group, providing a wide overview of the biological pathways involved and an integrated representation of the possible function of those miRNAs. From this analysis, it is not possible to determine whether a treatment could be better than another due to the lack of information about the specific mechanism of action over the determined signaling (i.e. inhibition or activation). Nonetheless, from a translational point of view, a better knowledge of NGF and BDNF mechanisms of action, will allow one to improve the development of NGF- and BDNF-based therapies for the treatment of sensorineural hearing loss.

The next step of the project involved *in vivo* studies and the details of the experiments and the results obtained are reported in **Chapter 3** and **Chapter 4**.

First, we investigated the effects of rhNGF and rhBDNF on cell survival of the organ of Corti of ototoxically deafened guinea pigs (**Chapter 3**). The number of sensory and non-sensory cells were counted through a histological approach. We found limited effects by both neurotrophins, that could be explained by several considerations: (1) the treatment was administered when a high degree of damage had already occurred in the organ of Corti (i.e., severe hair cell loss), (2) we considered only one time point (treatment 2 weeks after deafening, analysis 4 weeks thereafter) and (3) one concentration for treatment, and (4) we used a gelfoam soaked in rhBDNF as drug delivery system. For instance, an earlier treatment administration after deafening, a higher dosage and a different route of administration (such as based on osmotic pumps) could result in a more effective protective outcome. In fact, although the gelfoam is a feasible and easy method to be applied also in clinics, some issues could affect the outcome of the treatment, such as the uncontrolled drug release. This could be overcome by other approaches, that however are less feasible from a translational point of view. Nevertheless, in our experimental conditions the rhBDNF treatment showed a great efficacy in preventing SGCs cell death without any correlation with the number of hair cells (HCs) and supporting cells (SCs) in the organ of Corti, suggesting that rhBDNF directly targets SGCs. It is important to note that we conducted only a morphological evaluation of the organ of Corti, and did not take into account any other aspects, such as the molecular events underlying the activity of those cells, that could affect their function. Crucially, although the number of cells did not differ between treated and untreated ears, the function and activity of those remaining cells may be different.

In **Chapter 4** we therefore performed molecular investigations in the organ of Corti of deafened guinea pigs undergoing rhBDNF treatment. Based on the results described in Chapter 2, we selected the mTOR signaling, which resulted to be modulated predominantly by rhBDNF. The mTOR signaling is particularly interesting because of its multiple functions involved especially in cell survival, synaptic plasticity and cell growth. However its precise role in the cochlea is still an issue of debate. Interestingly, we found that rhBDNF increased the expression of mTOR compared to normal hearing (NH) and untreated deafened cochleas; while the protein levels of pmTOR were higher in deafened ears, both treated and untreated, compared to NH. However, we did not find any differences in the amount of the proteins involved in the mTORC1 complex. We therefore hypothesize a different mTOR activation mechanism, that may be investigated in future studies, possibly involving the mTORC2 complex. Nevertheless, this was the first study to demonstrate an effect on the mTOR signaling by rhBDNF in the organ of Corti of deafened animals. Moreover, the higher expression of mTOR was detected in all the cell types, including the SCs of the organ of Corti of treated ears. This data suggests a different activity of the SCs and HCs of the treated cochleas compared to the untreated ones in deafened animals. Based on the absence of differences in the number of surviving cells between treated and untreated ears in the organ of Corti, as observed in Chapter 3, it is possible to speculate that rhBDNF may have a protective effect on the organ of Corti that is mainly associated with the molecular function of those cells and not appreciable in terms of cell number. This could imply the maintenance of healthier cells, which in turn would influence their secretory activity and cellular crosstalk. Further studies, involving mTOR inhibitors or inductors, together with additional studies on cell survival, growth and synaptic plasticity are needed. This would allow one to clarify the function of mTOR upregulation in the organ of Corti upon rhBDNF administration and to which extent those molecular modifications are implicated in the protection of the organ of Corti. Moreover, additional molecular studies would be useful to confirm the modulation of the mTOR signaling in our experimental conditions through a selective pool of miRNAs, as found in Chapter 2.

In conclusion, this dissertation provides a comprehensive overview over the effects of rhNGF and rhBDNF in the organ of Corti, and lies the foundation for the identification of new therapeutic targets. Particularly (1) it was described for the first time the miRNome induced by the two neurotrophins in the organ of Corti through in vitro assays; (2) it was performed a comprehensive *in silico* analysis, which enabled the identification of new potentially modulated molecular signalings by rhNGF and rhBDNF; (3) it was investigated for the first

time the cell survival in the organ of Corti of rhNGF- and rhBDNF-treated ears *in vivo*; and (4) it was confirmed the modulation of the mTOR signaling by rhBDNF, as resulted in the *in silico* analysis, in an animal model of sensorineural hearing loss.

Aknowledgments

Throughout the writing and exploitation of this dissertation, I have received a great deal of support and assistance. To all of them is addressed my gratitude.

University of L'Aquila

In primis, I would like to thank my esteemed supervisor, Prof. Rita Maccarone. Her expertise was invaluable in formulating the research questions, methodology and conclusion. I am deeply grateful to her because she mentored me patiently during all the PhD study, and helped me in improving myself as a professional, scientist and person day by day. Her plentiful experience and endless guidance have encouraged me in all the time of my academic research and daily life.

I would like to express my sincere gratitude to the research group by Prof. Edoardo Alesse, at the University of L'Aquila, who provided me with the expertise, support and tools necessary for the miRNAs and *in silico* experiments. I would particularly like to single out Prof. Alessandra Tessitore, who shared with me her plentiful experience and assisted me patiently during all the steps of those analyses. I would also like to thank Prof. Francesca Zazzeroni for her kind support during the project development. My gratitude extends to Dr. Chiara Compagnoni and Dr. Roberta Capelli, who gave me technical support to perform the molecular experiments.

I would like to extend my sincere thanks to Prof. Vincenzo Flati, from the University of L'Aquila, for his assistance and contribution to the western blot analysis.

I would also like to thank the PhD coordinator, Prof. Maria Grazia Perilli, for her kind support during the PhD study.

I am deeply grateful to all the members of the Retina Lab, at the University of L'Aquila, including past and present labmates, who have taken part in the research activities of the laboratory. A huge thank is reserved especially to Dr. Giulia Parete and Dr. Giulia Carozza, who helped me side by side most of the time.

Dompé Pharma Industry

I would like to thank Dr. Marcello Allegretti, from Dompé Pharma Industry, for the opportunity to conduct a research experience at his company. I would also like to thank Dr. Laura Brandolini and Dr. Anna Sirico for their assistance and support, and the R&D Technology - Biotech Proteins Formulation (BPF) group, especially Dr. Nicola Detta, for having hosted me and allowed me to perform some experiments.

University Medical Center (UMC) Utrecht

I would like to express my sincere gratitude to my supervisor from the University Medical Center (UMC) Utrecht, Prof. Huib Versnel, for his invaluable support and tutorship during the last months of the PhD research activity. His insight and knowledge into the subject matter steered me through this research and allowed me to complete the project with *in vivo* investigations. I would also like to thank Dr. Dyan Ramekers for his contribution to the *in vivo* experiments, and for his insightful comments and suggestions. Finally, I would like to thank Dr. Ferry Hendriksen for his technical support.

La borsa di dottorato è stata cofinanziata con risorse del Programma Operativo Nazionale 2014-2020 (CCI 2014IT16M2OP005), Fondo Sociale Europeo, Azione I.1 “Dottorati Innovativi con caratterizzazione industriale”.